

AALBORG UNIVERSITY

---

# Model Predictive Control of a Sewer System

---

Control and Automation:  
Master Thesis

Group:  
CA10-1030

7 June 2018





**Master thesis**  
Control and Automation  
Fredrik Bajers Vej 7  
DK-9220 Aalborg Ø, Danmark  
<http://www.es.aau.dk>

## **AALBORG UNIVERSITY**

### **STUDENT REPORT**

**Title:**

Model predictive control  
of a sewer system

**Abstract:**



**Project period:**

P10, Spring semester 2018

**Projectgroup:**

CA10-1030

**Participants:**

Jacob Naundrup Pedersen  
Thomas Holm Pilgaard

**Supervisors:**

Carsten Skovmose Kallesøe  
Palle Andersen  
Tom Søndergaard Pedersen

**Copies: TBD<sup>a</sup>**

**Pages: TBD**

**Completed: 07-06-2018**

---

<sup>a</sup>FiXme Note: Antal sider



# Preface

---

This report has been created by Thomas Holm Pilgaard and Jacob Naundrup Pedersen. The project is made on the master thesis of the master in Control and Automation at Aalborg University.

The report is intended for people with knowledge corresponding to a master student at Control and Automation. MATLAB is used as the programming language for this project. Figures are constructed by the group, otherwise a reference is included in the figure text to the source.

Units are indicated by square brackets after the parameter has been elaborated e.g.  $Q$  is the flow  $\left[\frac{m^3}{s}\right]$ .

Sources are indicated by [name,year], and can be found in the bibliography list at the given [name,year].

Noget med attachment mappe struktur

---

Jacob Naundrup Pedersen  
jnpe12@student.aau.dk

---

Thomas Holm Pilgaard  
tpilga12@student.aau.dk



# Contents

---

<b>Nomenclature</b>	<b>ix</b>
<b>1 Introduction</b>	<b>1</b>
1.1 General sewer construction . . . . .	1
1.2 Chemical and biological processes . . . . .	3
1.2.1 Chemical reactions in sewer lines . . . . .	4
1.2.2 Wastewater treatment plant . . . . .	4
1.3 Challenges of wastewater treatment . . . . .	6
1.4 Problem statement . . . . .	8
<b>2 System description</b>	<b>9</b>
<b>3 Simulation solutions &amp; limitations</b>	<b>17</b>
<b>4 Modeling</b>	<b>19</b>
4.1 Hydraulics of sewer line . . . . .	19
4.2 Transport of concentrate . . . . .	26
4.3 Sewer interconnection . . . . .	29
4.4 Tank . . . . .	30
<b>5 Simulation</b>	<b>33</b>
5.1 Structure . . . . .	33
5.2 Preissmann scheme . . . . .	37
5.2.1 Stability & Precision . . . . .	42
5.3 Concentrate . . . . .	45
5.4 Tank . . . . .	46
5.5 Implementation . . . . .	47
<b>6 Control</b>	<b>63</b>
6.1 Linearization . . . . .	63
6.2 Model predictive control . . . . .	66
6.2.1 Constraints . . . . .	71
6.2.2 Implementation of MPC . . . . .	72
<b>7 Results</b>	<b>79</b>
<b>8 Discussion</b>	<b>83</b>
<b>9 Conclusion</b>	<b>85</b>
<b>Bibliography</b>	<b>87</b>
<b>A Appendix</b>	<b>89</b>
A.1 Summary of company visits . . . . .	89
A.2 Pump information . . . . .	91
A.3 Flow profiles . . . . .	92
A.4 Formulas . . . . .	102





# Nomenclature

---

## Abbreviation

Abbreviation	Definition
GIS	Geographically Information System
WATS	Wastewater of Aerobic/Anaerobic Transformations in Sewers
WWTP	Wastewater Treatment Plant
OD	Openings degree
MPC	Model predictive control

## Symbols

Symbol	Description	Units
$A$	Area	$m^2$
$Q$	Water flow	$m^3/s$
$q$	Inflow of water	$m^2/s$
$q_c$	lateral flux input of concentrate	$g/(s \cdot m)$
$d$	Diameter meter	$m$
$r$	Radius	$m$
$F$	Force	$N$
$\theta$	Angle	$rad$
$v$	Velocity	$m/s$
$M$	Mass	$kg$
$V$	Volume	$m^3$
$\rho$	Density	$kg/m^3$
$l$	Length	$m$
$g$	Gravitational acceleration	$m/s^2$
$T$	Temperature	$^{\circ}C$
$m$	Mass flow	$kg/s$
$\phi$	Flux	$g/s$
$C$	Concentrate	$g/m^3$
$R$	Hydraulic radius = wetted area / wetted perimeter	$m$
$f$	Friction factor	$\cdot$
$b$	Channel width	$m$
$\omega$	Angular velocity	$rad/s$
$J$	Inertance	$kg/m^4$
$h_n$	Head loss	$\cdot$
$p$	Pressure	$Pa$
$h$	Height	$m$
$\mathcal{H}$	Cost function	$\cdot$



Sewers were created to solve the seemingly simple problem of removal of wastewater. The first sewers, registered, dates back to 7000 B.C. in urban settlements and were created to remove wastewater from houses and surface runoff created by precipitation. To avoid clogging and wear of the sewers grit chambers was constructed. They work by slowing the flow of sewage in long narrow channels making the solids, such as sand, end up as sediments in the channels due to gravity. The complexity of sewers increased in ancient Rome where large underground systems were created leading to the main sewer system called "Cloaca Maxima" making it possible to have latrines with running water within households, though mostly made available for the rich [Hvitved-Jacobsen et al., 2013].

During night time the population, without immediate access to a latrine in their household, still disposed waste onto the streets. The reason for this was that they simply did not want to put in the effort to properly dispose of the waste at night. Because of this, the ancient Rome suffered from illnesses related to waste lying in the streets. The hygienic aspect of proper disposal of wastewater in relation to drinking water was not considered until the 19th century, where several European cities saw a large outbreak of cholera causing the deaths of millions [Hvitved-Jacobsen et al., 2013].

The growth in waste furthermore caused the expansion of 26 km sewer network in Paris to 600 km during the 19th century. But it is not until the start of the 20th century that the chemical and microbial processes in sewers are considered. The microbial cause of cholera was identified by the German doctor Robert Koch in 1883, a discovery for which he in 1905 received the Nobel Prize in physiology and medicine. The growing industries and technological progress in the 20th century meant that more chemicals were disposed into the sewers having severe consequences for the organic life downstream of the receiving waters. Wastewater treatment plants were introduced to reduce the pollution, but several countries did not have any wastewater treatment plants before after World War II. Today disposal of sewage and setup of wastewater treatment plants is a given part of a construction of new settlements, even in poor regions of the world [Hvitved-Jacobsen et al., 2013].

## 1.1 General sewer construction

This section will elaborate on the general construction of sewers. Furthermore, a brief explanation, of the flow into the sewer to the output from the wastewater treatment plant (WWTP), is given.

Generally, sewer construction can be put into two categories which are gravity and pressurized sewers. Gravity sewers utilize the topographic advantages of the area in which they are constructed. But in places where the level of the surface area does not accommodate a slope of the sewer pipe, such that wastewater flow in the desired direction,

wells with pumps are used to transport the wastewater to an elevated level. An illustration of gravity and pressurized sewer lines can be seen in figure 1.1.

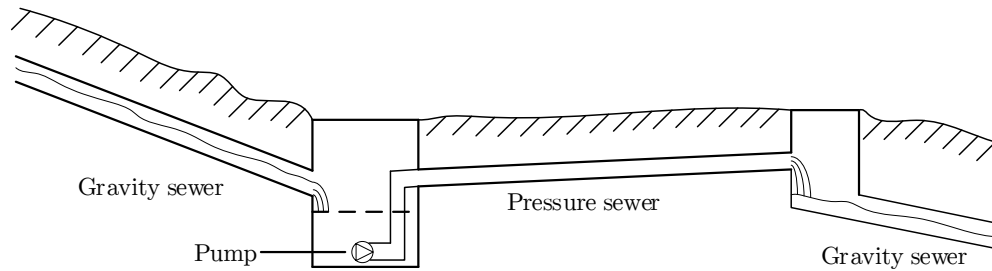


Figure 1.1: Illustration of flow in gravity and pressurized sewer lines.

Design of sewer systems involves careful considerations, such that as much of the network utilize gravity for transport of wastewater, to minimize the energy consumption. Therefore, the WWTP is typically located in a low topographic area near a river, fjord or the sea. Other design parameters involve dimensioning of the pipes to avoid overflow and to compensate for groundwater ingress into the sewer lines. Also, the depth should be sufficient, such that subzero temperatures does not prevent the flow in the sewers at any time. Furthermore, the slope of the pipes must be chosen such that sufficient flow is obtained and clogging is avoided. Different materials used to create the pipes gives different amount of friction e.g. a concrete surface will be rougher than polyethylene and thereby have a higher friction. This means that a larger slope of a concrete pipe is needed to avoid clogging. Typically, gravity sewer pipes are made of concrete and pressurized sewer pipes of polyethylene [Hvitved-Jacobsen et al., 2013].

In figure 1.2 a block diagram of the flow of wastewater is seen.

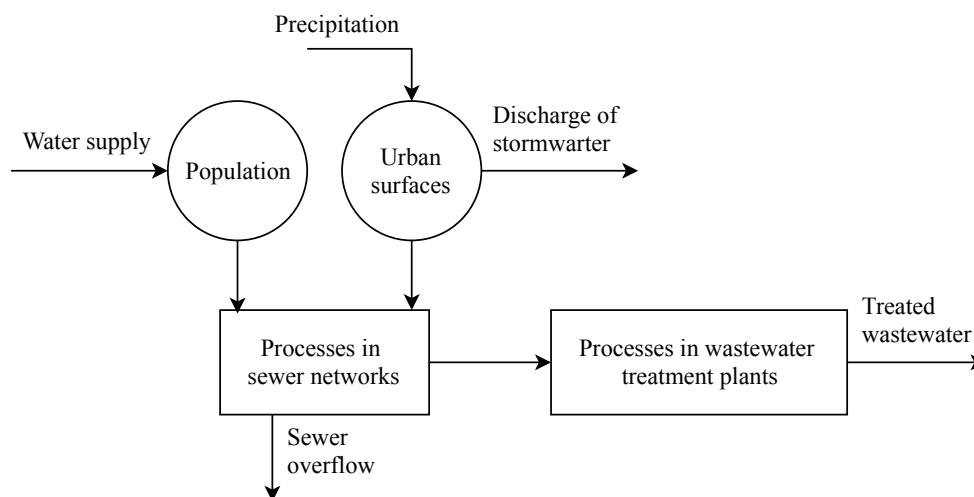


Figure 1.2: General overview of wastewater processes from inputs to treated output [Hvitved-Jacobsen et al., 2013].

Starting at the left side in the figure, precipitation from urban surfaces and roads are let into the sewer by inlets placed at the gutter. In recent times separate sewer systems for

surface runoff are constructed, which are also called storm water sewers. The water in these sewers is typically led into stormwater basins, rivers or the sea. In areas with older sewer constructions, storm water is let into sewers where it is mixed with wastewater. The wastewater comes from households or industry disposing of substances of varying consistency. Heavy precipitation can cause the sewers to be filled, and to avoid overflow, into a household or on roads, the wastewater is let into rivers or the sea during such events. The reason for designing storm water sewers is partly to avoid letting untreated sewage into nature, but also to better be able to control the cleansing process at the WWTP. When wastewater is received at the treatment plant it undergoes several processes to separate the unwanted substances from the received wastewater. The cleansed water is then released into nearby rivers or the sea. Due to the sizes of sewer networks, which can have inlets several kilometers from the WWTP, chemical reactions also occur in the sewer pipes [Hvitved-Jacobsen et al., 2013]. The chemical and microbial reactions happening in the sewer lines is discussed in subsection 1.2.1. The processes which the wastewater undergoes at the treatment plant is discussed in subsection 1.2.2.

## 1.2 Chemical and biological processes

This section will give an overview of the chemical and biological processes that wastewater undergoes from it is led into the sewer till it is cleansed at the WWTP. The various processes occurring at the WWTP is described, to clarify the problems that may arise during operation.

Within wastewater, there is a large number of living organisms. It contains somewhere between 100.000 to 1.000.000 microorganisms per milliliter. These organisms originate from sanitary waste and soil. They are a natural living part of the organic matter and they are an important part of the cleansing at the WWTP. To be able to obtain a high water quality at the output of the WWTP it is necessary to have a thorough understanding of these microorganisms [College, 2018].

Nearly all microorganisms found in wastewater are not harmful and do not cause illness in humans. However, a small group of the microorganisms can cause illness, and these are of great concern in wastewater treatment. The most known diseases to occur are typhoid fever, dysentery, cholera, and hepatitis [College, 2018].

The microorganisms in the WWTP have a specific role in the decomposition of the waste. The three most notable microorganisms in the biological treatment process are bacteria, fungi, and protozoa. The bacteria have the primary role of degrading the wastewater compounds. Bacteria is a single cell organism and is capable of reproducing rapidly when in contact with water. They feed off the waste by absorbing it through the cell wall turning it into sediment solids [College, 2018]. Fungi like bacteria decompose the organic waste, however, they also pose a significant problem for the treatment process as the fungi can proliferate to an extent where it affects the quality of the output from the WWTP [AquaEnviro, 2010]. Lastly, protozoa act as a predator toward the present bacterial population such that it can be controlled [College, 2018]. Reactions in sewer lines is discussed in subsection 1.2.1 and the processes at the treatment plant in subsection 1.2.2.

### 1.2.1 Chemical reactions in sewer lines

Wastewater is subject to a variety of mass changes in sewers. This is caused by free electrons in the wastewater, which causes chemical reactions and thereby leading to new compounds being created. The chemical reactions occurring is called redox reactions. A Redox reaction is the transfer of electrons between two compounds at an atomic scale. Chemical reactions are determined by the electron acceptors that are present in the wastewater. The electron acceptor is the compound that receives electrons in a redox reaction. Examples of dissolved acceptors are oxygen ( $O_2$ ), nitrate ( $NO_3^-$ ) and sulfate ( $SO_4^{2-}$ ). These acceptors are present, respectively, when aerobic, anoxic or anaerobic conditions exist in the sewer. The redox reaction converts these three compounds in the wastewater to new compounds such as water ( $H_2O$ ), molecular nitrogen ( $N_2$ ) and hydrogen sulfide ( $H_2S$ ) [Hvitved-Jacobsen et al., 2013].

Where redox reactions occur in a sewer line is, to a great extent, determined by the design of the sewer. The aerobic, anaerobic and anoxic conditions do not exist in the same part of the sewer, and the last only occurs if nitrate is artificially added to the wastewater. If the sewer is in an aerobic state then the typical characteristics of the sewer are either partly filled gravity sewer or an aerated pressure sewer. This means that there are free oxygen ( $O^+$ ) molecules, and these will bind to hydrogen molecules to create water. If the sewer is in an anoxic state, which occurs in pressure sewers, then the addition of nitrate to the wastewater results in molecular nitrogen. If the sewer is in an anaerobic state the characteristic of the sewer is either a pressure line or a full flowing gravity line. Reactions which occurs will result in hydrogen sulfide as the sulfate will bind with the hydrogen molecules. With the knowledge of these condition, sewers can actively be designed to achieve a specific state [Hvitved-Jacobsen et al., 2013]. The two desired states in sewers are aerobic in gravity lines and anoxic in pressure lines to avoid malodorous dissipation into the urban atmosphere.

To model, the chemical and biological reactions in sewer lines a model concept, Wastewater Aerobic/Anaerobic Transformation in Sewers (WATS), is used. The WATS model is expressed as differential mass balance equations which are suitable for numerical computation. It can, therefore, be included in simulations for a specific objective e.g. model of water and gas phase transformations. The WATS model can be applied to a sewer as long as a fundamental understanding of the sewer is available. Whether it is aerobic, anoxic or anaerobic conditions that dominate the sewer, furthermore the soil composition and the pH concentration of the wastewater must also be known and included in the WATS model [Hvitved-Jacobsen et al., 2013].

### 1.2.2 Wastewater treatment plant

Wastewater from households and industry contains organic and inorganic matter and if it is released into the environment it will result in a polluted environment. This can cause oxygen depletion and thereby affect the wildlife in the water environment negatively. In the following section, the process that wastewater undergoes in a WWTP is elaborated.

In figure 1.3 the various treatments wastewater undergoes is illustrated.

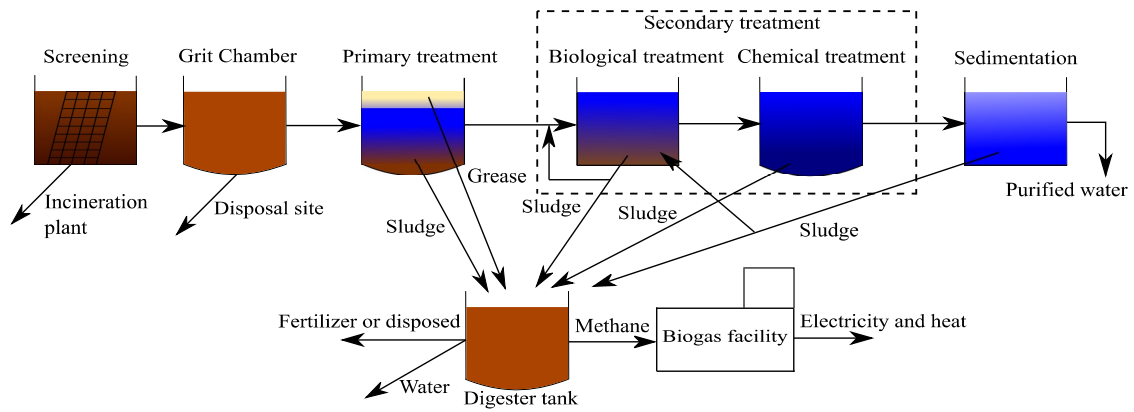


Figure 1.3: General overview of a wastewater treatment plant.

The first stage of cleansing the wastewater is screening, where larger objects are removed from the wastewater which either could cause congestion or damage the equipment. Examples of objects that are filtered from the wastewater are bottles, plastic bags, and diapers [Eschooltoday, 2017]. The wastewater is then lead to the primary treatment, where it first will enter a grit chamber, where objects as sand and stones will settle to the bottom of the tank. These grit chambers are crucial in WWTP that are connected with combined sewer systems. As storm-water may wash sand, stones, and gravel into the sewer these objects will be extracted in this process [EPA, 1994]. The collected objects are disposed at a disposal site. After the screening process the wastewater, still containing organic and inorganic matter, is lead into the primary treatment tank where flow and turbulence are reduced. The organic matter will sediment in the tank, while grease will accumulate at the surface. The grease is scrapped from the surface and lead into the digester tank. The matter that has sedimented is now called sludge or raw primary bio-solids. At the bottom of the tank, large scrappers are moving the sludge to the center of the tank where it is pumped into the digester tank [EPA, 1994].

In the secondary treatment, the wastewater is lead into an aeration tank where the air is pumped in at the bottom. This is called the biological treatment. By aeration of the wastewater, the bacteria gain optimal conditions for respiration. This will speed up the process of decomposing the remaining organic matter from the primary treatment process. In the process of decomposing the organic matter, the bacteria will produce  $CO_2$  that will dissipate into the atmosphere. Furthermore, when the bacteria have consumed the organic matter they will start to produce heavier particles that will sediment in the tank [Rinkesh, 2009]. In figure 1.4 this process is illustrated.

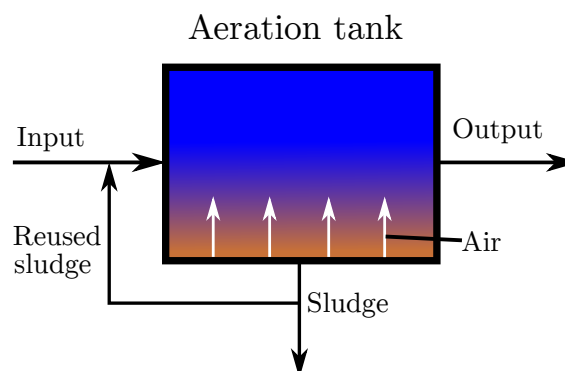


Figure 1.4: Illustration of the aeratation tank in the biological treatment process.

This is called the activated sludge process, because some of the sludge is reused in the aeration phase to retain a high bacteria population. The reused sludge contains millions of microorganisms which increase the efficiency of cleansing the wastewater. After some time the aeration is stopped which causes anaerobic conditions. Other bacteria is then activated in a process called denitrification, where it absorbs oxygen molecules from the nitrate converting it to nitrite. The nitrite flow to the surface in the tank and dissipates into the atmosphere. The remaining sludge that has sedimented is pumped to the digester tank [EPA, 1994, Rossi et al., 2014]. Hereafter a chemical treatment is performed to remove the inorganic matter that is left in the wastewater. Chemicals which is non-damaging to the environment is added to the wastewater. This will create chemical reactions and thereby create new compounds, that will sediment in the tank, which is pumped into the digester tank [Sjøholm, 2016].

After these treatment processes, there are still some particles left in the wastewater. It is therefore lead to a sedimentation tank where the remaining bacteria and sludge will settle before the wastewater is released into receiving waters. The sedimented particles or sludge will either be pumped to the digester tank for further processing or reused in the activated sludge process.

The sludge collected in the digester tank also undergoes further treatment, as the remaining water in the sludge is separated. The water is lead back to the wastewater treatment process where it will undergo the same process again. The sludge then undergoes anaerobic digestion for about a month, where the resulting bio-solids can be used as fertilizer. The methane gas created in the process can be used at a bio-gas facility to produce electricity and heat [Rinkesh, 2009].

### 1.3 Challenges of wastewater treatment

In the following section various challenges, such as flow and concentrate variations, which affects the treatment efficiency of the WWTP is discussed. Furthermore, this section will mostly be based on information obtained from a meeting with a WWTP, namely Fredericia Spildevand og Energi A/S. A summary of this meeting can be found in appendix A.1. A general daily intake of wastewater from a small town is illustrated in figure 1.5

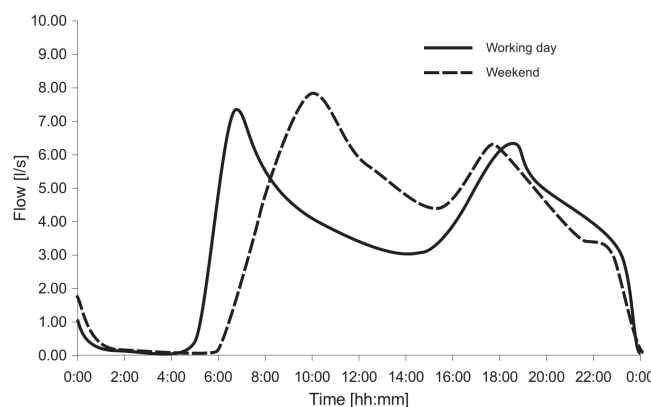


Figure 1.5: Typical daily flow pattern from the town Frejlev, with approximately 2000 residents [Schlütter, 1999].

At approximately 06:00 there is a steep increase in flow, which is due to people preparing



for work. During the day the flow lessens, until 16:00 where people start returning home from work. The flow increases due to typical household activity such as cooking, bathing, toilets flushing. During night time the flow is at a minimum as most people are at sleep. During weekends the flow patterns change slightly, which could be because of a different sleep pattern than during weekdays.

The flow variations created by human routines is challenging for the treatment process. As mentioned in subsection 1.2.2 sludge is reused to accommodate a sufficient amount of microorganisms to be able to cleanse the wastewater. When a sudden peak in flow occurs, there might not be enough microorganisms available to achieve a satisfying result from the cleansing process. Furthermore, it is not possible to store sludge, with the purpose of using the microorganisms at a later time, as they have a short span of life if the right conditions are not in place.

In Fredericia e.g. there are multiple large companies, which disposes large amounts of wastewater into the sewer. At day to day operation the wastewater flow into the WWTP is not a problem. But random occurrences of sudden large outlets of wastewater from the industry is seen. This could, for example, be from the dairy where a failed batch of cream is let into the sewer such that the tanks can be used to produce a new product. In some cases, the companies contact the WWTP to warn on the incoming amount of wastewater or to agree on the discharge flow of the discarded product. This is not something that the companies are required to do, and does not always happen. This means that the WWTP soonest discovers the added load at the inlet, and therefore has limited possibilities to react on the sudden change of flow. These outlets pose a problem for the WWTP. Not only because of the change in flow, but also because the concentrate of the various compounds in the wastewater is usually higher from the larger companies. Typically, the industry is efficient in letting out wastewater within certain pH levels at reasonable flow levels. The only countermeasure, for these incidents of sudden discharge, is to prevent overflow. This is done by letting some of the wastewater, in the later unfinished stages of the cleansing process, through into the fjord. Furthermore, changes in chloride concentration, from either industry outlets or back-flow from the fjord due to heavy precipitation, is problematic for the bacteria. Meaning that changes in concentrate cause a drop in efficiency until the bacteria have acclimated. Contrary, a static level of chloride does not pose a problem for the bacteria.

To sum up, the typical problems which a WWTP encounters. Flow variations are problematic as the cleansing process reuse sludge. The random changes are either caused by larger industry or as a result of heavy precipitation. Outlets by the industry are more of a concern when considering the concentration of the wastewater. Changes in concentration can cause inefficiency at the WWTP as the bacteria need time to acclimate to changes. Precipitation is a problem as a result of the large increase in flow it causes, which can lead to capacity problems at the WWTP.

## 1.4 Problem statement

Based on the information in the previous sections, which states that several problems occur during wastewater treatment, the problems can be summed to the following points:

1. Flow variations due to large industries and natural phenomenons
2. Concentration variations due to large industries and natural phenomenons
  - a) Chloride variations
  - b) Phosphor variations
  - c) Nitrogen variations
  - d) Organic matter variations

To be able to implement countermeasures towards these problems information is needed about the flow of wastewater in the sewer lines. As measurements is rarely available for entire sewer networks or even parts of it, an ideal solution would be to construct a simulation environment where different scenarios can easily be setup [Fredericia-Spildevand, 2018b]. Furthermore, a control scheme is needed to be able to implement an efficient countermeasure. It has been decided to utilize model predictive control (MPC) as the control scheme for this project. This control scheme excels in obtaining optimal control action when operating systems close to limitations, as constraints can be applied, making it ideal for this project. From this a problem statement can be formulated:

*How can a simulation environment be constructed, which mimic the behavior of a real sewer system, where MPC is utilized as the control scheme to obtain stable sewage output such that optimal performance can be obtained from a WWTP.*

# System description 2

---

This section will go into details of the structure of the sewer network for which the further work of this project will be based upon.

As mentioned in section 1.3 a steady flow of sewage with a fixed level of contaminants is desired such that an optimal utilization of the wastewater treatment plant can be obtained. An area of interest is Fredericia with a sizable population of approximately 40.000 people and industries where some of the largest consists of a brewery, bottling plant, refinery and a dairy plant [Statistics-Denmark, 2018]. All of these industries are placed at the outskirts of the city, meaning that the wastewater discharged into the sewer goes through populated areas creating an uneven flow of wastewater to the WWTP. Two main sewer lines separate the northern and southern part of the city. To limit the scope of the project only the northern main sewer line is considered. This line covers the largest part of the households and the industry, located in the city. In figure 2.1, a simplified overview is given of the northern main sewer line in Fredericia. The placement of the sewers shown in the figure is obtained from a Geographically Information System (GIS) map, which is made publicly available by the municipal of Fredericia [Fredericia-Spildevand, 2018a]. The red and green lines indicate sewers with flows of wastewater only and combined sewers with flows of wastewater and surface runoff, respectively. The populated areas are indicated by blue and green transparent colors, to easier be able to distinguish between the different parts of the sewer network. The red transparent areas indicate small to medium sized industry. Only the sewer lines out of or between the separate areas are shown. Furthermore, the areas connected by a red line has a separate sewer system for surface runoff, which is lead into various ponds or the sea, minimizing the load on the wastewater treatment plant. The bottling plant, refinery and the brewery are marked by the purple, brown and black rings, respectively. Furthermore, several inlets for surface runoff connected directly to the main sewer line exists.

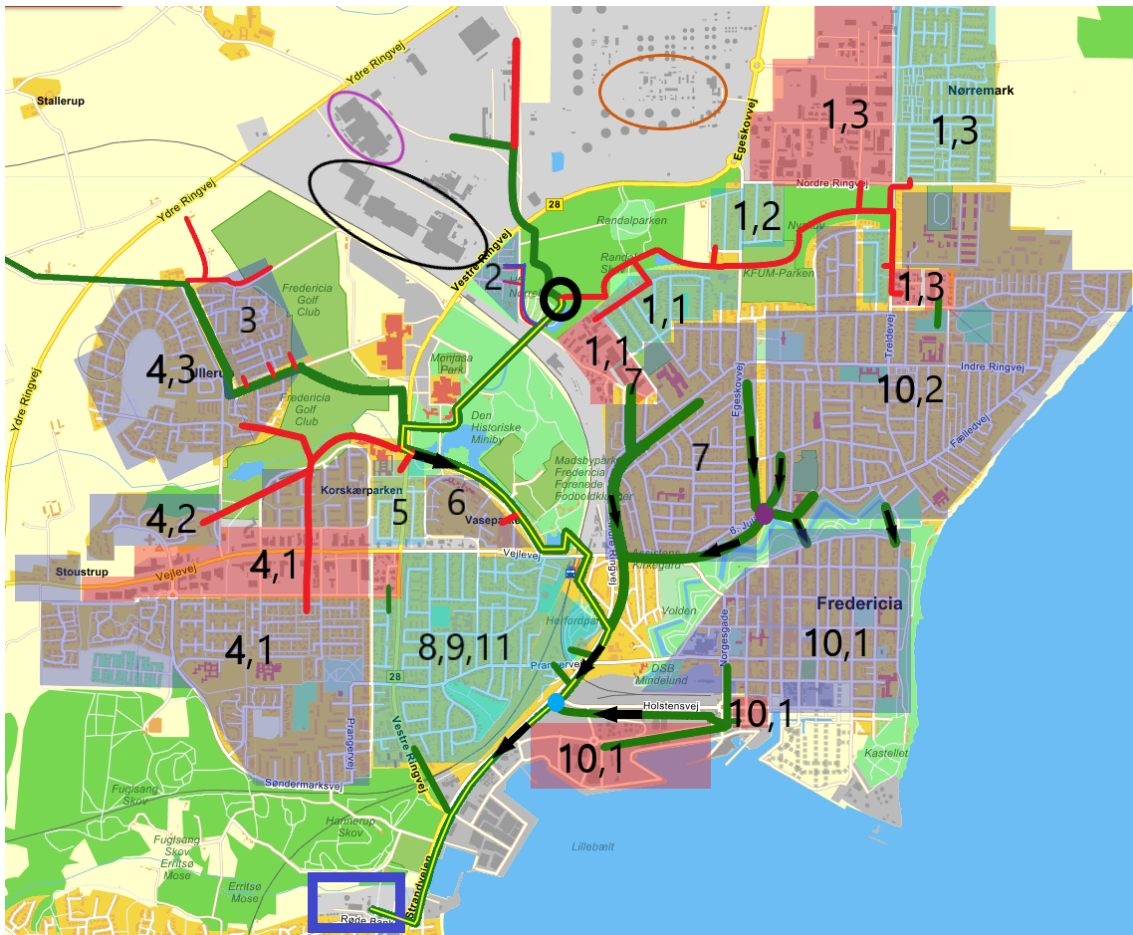


Figure 2.1: Simplified mapping of the northern part of the sewer network in Fredericia. The blue and green transparent colors indicate populated areas and the red transparent area indicate industry. Red and green lines are sewers with flows of wastewater and combined wastewater and surface runoff respectively. The bottling plant, refinery, and brewery are marked by purple, brown and black circles respectively. The black circle denotes the starting point of the main sewer line. The green line with a yellow stripe within represents the main sewer line. The purple dot is a connecting point with two incoming and two outgoing sewer lines. The blue dot is a wastewater pumping station which elevates sewage such that gravity can be utilized for the remaining transport into the treatment plant. Blue rectangle marks the location of the wastewater treatment plant. [Eniro, 2018] [Fredericia-Spildevand, 2018a]

The various enumerated parts in figure 2.1 is shown by order of attachment to the main sewer line, together with distance between each attachment, in figure 2.2.

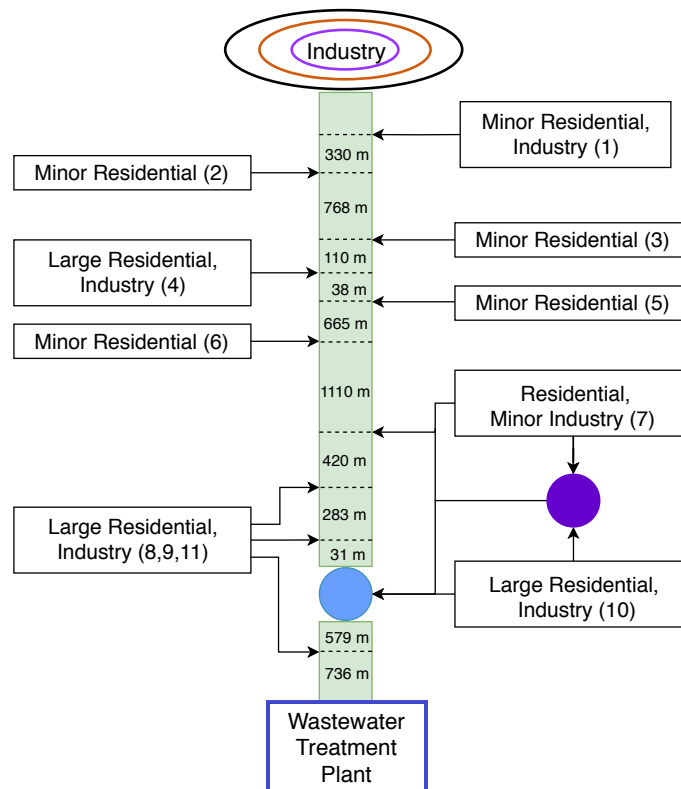


Figure 2.2: Simplification of the attachments to the main sewer line shown in figure 2.1. The numbers correspond to which area is connected to the main sewer line farthest from the wastewater treatment plant, with the distance between them [Fredericia-Spildevand, 2018a].

Furthermore, the different sections consist of pipes with varying diameters which can be seen in table 2.1.

Pipe section	Pipe length (meter)	Inner pipe diameter (mm)	Bed datum in (m)	Bed datum out (m)	Bed slope (‰)
1 → 2	303	900	11,56	10,65	3,00
	27	1000	10,65	10,57	3,00
2 → 3	155	1000	10,57	9,94	4,10
	295	800	9,94	6,33	12,20
	318	900	6,33	4,71	5,30
3 → 4	110	900	4,71	4,31	3,60
4 → 5	38	1000	4,31	4,40	-2,40
5 → 6	665	1000	4,40	2,43	3,00
6 → 7	155	1000	2,43	2,31	0,80
	955	1200	2,31	-0,48	2,90
7 → 8	293	1200	-0,48	unknown	
	11	1300	unknown	-1,38	
	116	1200	-1,38	-1,62	2,10
8 → 9	283	1400	-1,62	-2,09	1,70
9 → 10	31	1400	-2,09	-2,15	1,90
10 → 11	125	1600	0,31	0,05	2,10
	94	1500	0,05	-0,07	1,30
	360	1600	-0,07	-1,72	4,60
11 → WWTP	736	1600	-1,72	-2,60	1,20
Total length 1 → WWTP	5070				

Table 2.1: Table of the various lengths and the approximate inner diameter of pipe, appearing in order, in the main sewer line. Pipe section indicate the length of pipe between the attachment of the various areas to the main sewer line [Fredericia-Spildevand, 2018a].

Some assumptions are made to avoid possible complications during simulation. The negative slope of the section between connection point four and five is flipped such that no permanent storage of sewage happens. The reason for this assumption is that it will ease the computation, of the free flow in that section, if storage in the pipe sections could be disregarded during simulation. Furthermore, the new slope is deemed acceptable based on the obtained slopes of the remaining pipe sections. The two pipe sections between point seven and eight, where out- and input datum is unknown, are gathered into a single pipe section. This section will be designated an inner diameter of 1200 mm as the section with the larger diameter, because of its short length, is assumed insignificant when considering the free flow at the end point of the combined section.

Pipe section	Pipe length (meter)	Inner pipe diameter (mm)	Bed slope (‰)
4 → 5	38	1000	2,40
7 → 8	304	1200	3,00
	116	1200	2,10

Table 2.2: New slope values for sections with negative slope and unknown values.

To be able to simulate how the wastewater propagates throughout the main line the flows in each residential and industrial area is needed. However, Fredericia Spildevand og Energi A/S does not have measurements of the flow or concentration from the specific areas. Only at a limited amount of pumping stations, at various positions in the city, are there flow

measurements available. Therefore flow profiles for the various inputs shown in figure 2.2 needs to be designed. For this purpose, the flow profile, seen in figure 1.5, is utilized, for the residential and minor industry areas, as an estimate of the flow during 24 hours. The flow profiles are scaled to fit the size of each area and delayed approximately with the distances to the main line seen in figure 2.1.

From figure 2.2 it can be seen that 11 different flow profiles are to be constructed to cover each residential and industrial area wastewater contribution to the main line. By knowing the area and density of the population a flow profile can be scaled to each of the residential and industrial areas. On average there are 2,6 residents per house in Denmark which will henceforth be the foundation for obtaining population for the various areas [Nykredit, 2018]. Furthermore, it is assumed that the urban areas one to six together with eight, nine and eleven are single-family houses and zone seven and ten are apartments in buildings with several floors, meaning that area seven and ten have a higher density of population per square kilometers. As the northern part of Fredericia consists of the largest part of the city, the assumption is that around 30.000 of the approximately 40.000 people resides there. The residential area 1,1 is used to obtain an approximate density of people per square kilometer within the urban areas. The number of houses located in this area is found to be 199 which gives an average urban population density of 3098,2 per square kilometer. The approximated size of the various areas is found and from that the population by multiplying with the average population density. The remaining of the population is divided between area seven and ten. As area seven is approximately a third of the combined area it is given a third of the remaining population leaving the remaining to area ten. In table 2.3 the approximated size of the residential and industrial areas, together with the population of the residential areas, are shown.

Zone	Residential area [ $km^2$ ]	Industrial area [ $km^2$ ]	Population per area
1,1	0,167	0,0083	517
1,2	0,111	-	344
1,3	0,458	0,543	1418
2	0,056	-	173
3	0,167	-	517
4,1	1,125	0,375	3485
4,2	0,167	-	517
4,3	0,580	-	1797
5	0,104	-	322
6	0,115	-	356
7	0,771	0,014	5874
8 - 9	0,667	0,021	2067
10,1	0,903	0,333	3916
10,2	1,781	-	7832
11	0,278	-	865
<b>Total area</b>	<b>7,45</b>	<b>1,294</b>	<b>30000</b>

Table 2.3: Table of the sizes of the residential and industrial areas and the population in the residential areas [Nykredit, 2018].

In figure 2.3 a flow profile is shown for the residential area 1,1.

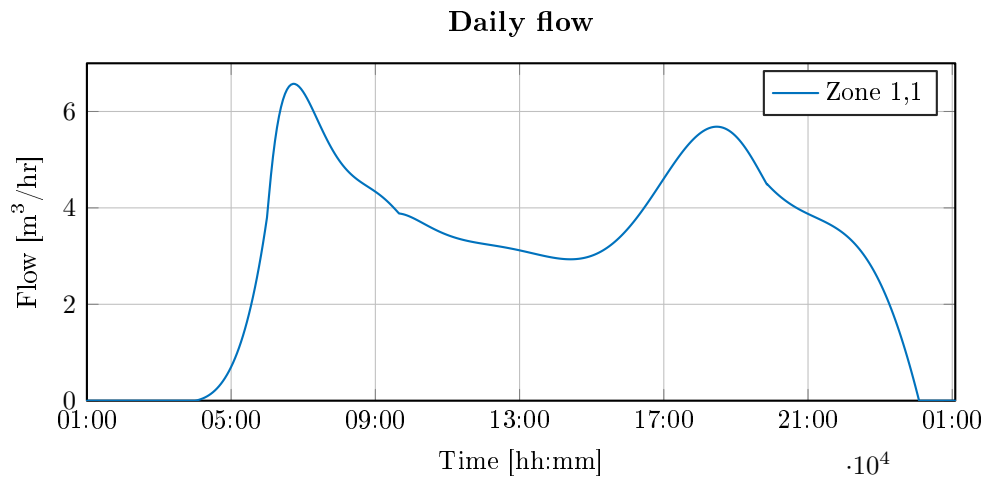


Figure 2.3: Flow profile for the residential area 1,1.

Flow profiles for the various residential and minor industry inputs to the main line and details on the creation of them can be found in appendix A.3.

Lastly, profiles are needed from the industry which counts the brewery, bottling plant and the refinery. In figure 2.4 combined flow from the brewery and bottling plant during 24 hours is seen.

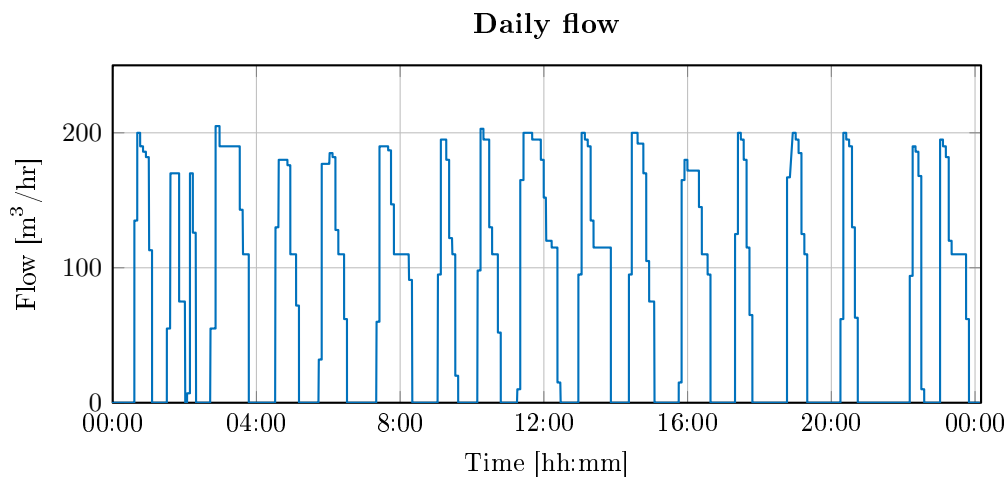


Figure 2.4: Flow profile from brewery and bottling plant combined during 24 hours.

From the figure, it can be seen that the flow from industry is in pulses of up to  $200 \text{ m}^3/\text{hr}$  where the longest pulse is around an hour and the shortest is around 10 minutes. Between the pulse the flow is limited and the duration of these zones are most often around 30 minutes. From the figure, it could indicate that there are two pumps pumping the wastewater away from the industry, as there are two levels in the plot. Around  $190\text{--}200 \text{ m}^3/\text{hr}$  and around  $110\text{--}120 \text{ m}^3/\text{hr}$ . This data will be used to create the input to the main sewer line from the industry.

In figure 2.5 the flow input into the WWTP can be seen.



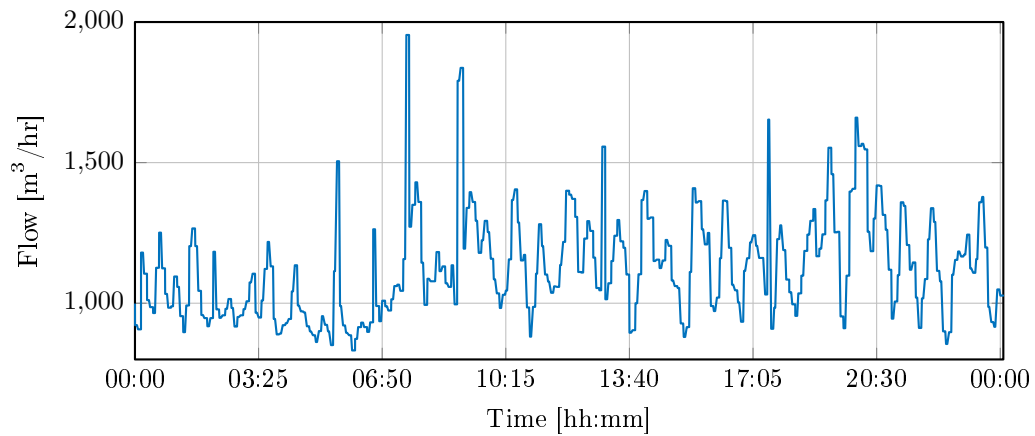


Figure 2.5: Flow input at Fredericia wastewater and treatment plant, from the fifth of February to the sixth of February.

From the figure, it can be seen how the flow into the WWTP fluctuates. From 00:00 to 03:25 the flow fluctuates between  $1000 \text{ m}^3/\text{hr}$  to  $1200 \text{ m}^3/\text{hr}$  and these huge shifts in flow rate is ongoing the entire day. Around 07:00 a large shift in flow occurs, it is unknown if this is a false measurement or it is due to a huge load change, as this peak seems to be only for one sample. However, it is very clear that the flow fluctuates across the entire day and it would be desirable to smooth the flow out.

In appendix A.3 figures A.13, A.13 and A.14 shows COD, phosphorus and nitrogen measurements respectively, from the input to the WWTP is shown. These figures show a similar pattern as the flow measurement, however, they do not vary as much as the flow. But a direct comparison cannot be done, as these measurements, the concentration measurements and the flow measurement, are measured at different dates, and therefore it can not be concluded if these concentrations are varying as much as the flow measurement. However, it can be concluded that these measurements also fluctuates across a day and therefore needs to be smoothed out to obtain a better cleansing process at the WWTP.



# Simulation solutions & limitations 3

---

In this chapter different solutions will be discussed to find the most optimal solution to implement in Fredericia to limit the flow and concentration variations into the WWTP.

To limit the variations into the WWTP a mechanism is needed to hold back the wastewater. This could either be done by placing valves within the pipes that would be able to limit the flow through a pipe. This is done by opening or closing the valve and thereby the flow into the WWTP could be controlled. Another possibility is to store the wastewater in tanks and thereby control the output of the tank with a pump.

Using a valve to hold back the flow corresponds to using the pipe as a tank. This could lead to overflow if not controlled properly and thereby cause wastewater to flow onto streets and into the surrounding environment. This issue were discussed with the wastewater department in Fredericia and they pointed out that storage is limited due to the size of the sewer pipes and constant flow.

In this project, it is therefore decided to use one or more tanks as a solution to limit flow and concentration variations into the WWTP. However, the tank must be controlled in a way where overflow in the tank is not permitted. In addition, from the meeting at Fredericia it was informed, that if tanks is used as a solution, it is necessary to keep retention time of the stored wastewater in mind. The reason for this is, that if the wastewater is kept in the tank for a longer period of time, it will start to produce malodorous gas. This is due to oxygen depletion, as the environment in the tank will go from an aerobic to an anaerobic state.

In Denmark sewers is made of concrete and the inner channel is constructed with a circular cross section area [Dansk-betonforening, 2013]. For this reason the simulation will be limited to work with sewer pipes of this form.



# Modeling 4

---

This chapter will in detail explain the modeling procedure of the various components comprising the sewer system seen in figure 2.1. In the following, methods to model the components such as flow in gravity and pressurized sewer lines (section 4.1), interconnections such that disturbances can be added to the main sewer line (section 4.3) and tanks in the sewer network (section 4.4). Furthermore transport of concentrate in the wastewater flowing in the main sewer line (section 4.2), is modeled.

## 4.1 Hydraulics of sewer line

A method to model the hydraulics of gravity sewer lines is explained in the following.

Modeling fluids is almost always done by considering it as a control volume. The reason is that it is rarely efficient, computational wise, or possible to consider the individual fluid particles. Henceforth the control volume will be denoted by the letter  $\Omega$  which will correspond to some amount of fluid in a length of sewer line.

The open channel flow in gravity sewer lines can be described by the Saint-Venant equations which gives an expression for conservation of mass and momentum. Some assumptions is made when deriving the Saint-Venant equations [Schütze et al., 2011]:

1. The flow in the channel is one dimensional, and prismatic, and as such any curvature or change in width of the sewer line is considered negligible.
2. Fluid in the sewer line is considered incompressible.
3. The pressure is assumed hydrostatic.
4. The only forces considered is friction, pressure and gravity.
5. The water height and velocity is uniform in the cross-section and only changes horizontally i.e. turbulence in the fluid is not considered.
6. The slope of the channel bed is small

**Continuity** equation for conservation of mass gives an expression for the amount of fluid flowing into and out of the control volume plus the fluid stored in it. In figure 4.1 a flow in a channel is shown.

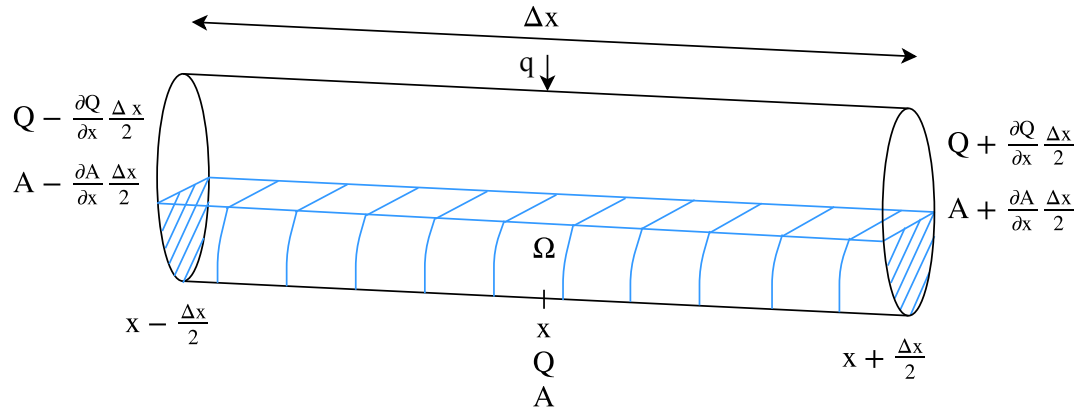


Figure 4.1: Illustration of a control volume,  $\Omega$ , of fluid in a sewer pipe, where  $Q$  is flow into the end of the channel,  $q$  is lateral flow into the channel and  $A$  is the cross section area of the flow.

The flows and the cross section area of the flow, seen in figure 4.1, is dependent on time and position. In the following a simpler notation is used for an easier outline.

Flow into the control volume, where  $Q$  is the flow considered from the middle of the control volume, is given as:

$$Q_{in} \cdot \Delta t = \left( Q - \frac{\partial Q}{\partial x} \cdot \frac{\Delta x}{2} \right) \cdot \Delta t + q \cdot \Delta x \cdot \Delta t \quad (4.1)$$

Where  $q$  is lateral inflow across the entire channel  $[\frac{m^2}{s}]$  and  $Q$  is the flow in the channel  $[\frac{m^3}{s}]$ . Lateral inflow could for example come from adjoint sewer pipes or road drain. The discharge flow of the channel is given as:

$$Q_{out} \cdot \Delta t = \left( Q + \frac{\partial Q}{\partial x} \cdot \frac{\Delta x}{2} \right) \cdot \Delta t \quad (4.2)$$

Average change in stored fluid in the channel is given as:

$$\begin{aligned} \frac{\partial}{\partial t} \left( \Delta x \cdot \frac{A - \frac{\partial A}{\partial x} \frac{\Delta x}{2} + A + \frac{\partial A}{\partial x} \frac{\Delta x}{2}}{2} \right) \Delta t &= \frac{\partial}{\partial t} \left( \Delta x \frac{2A}{2} \right) \Delta t \\ &= \frac{\partial A}{\partial t} \cdot \Delta x \Delta t \end{aligned} \quad (4.3)$$

As the flow into the channel minus the flow out is equal to the change in stored fluid in the channel, then due to the assumption of incompressible fluid and uniformity, the following can be written:

$$Q_{in} \cdot \Delta t - Q_{out} \cdot \Delta t = \frac{\partial A}{\partial t} \cdot \Delta x \cdot \Delta t \quad (4.4)$$

Inserting equations 4.1 and 4.2 in 4.4 the following is obtained:

$$\begin{aligned} \left( Q - \frac{\partial Q}{\partial x} \cdot \frac{\Delta x}{2} \right) \cdot \Delta t + q \cdot \Delta x \cdot \Delta t - \left( Q + \frac{\partial Q}{\partial x} \frac{\Delta x}{2} \right) \cdot \Delta t &= \frac{\partial A}{\partial t} \cdot \Delta t \cdot \Delta x \\ \Downarrow \\ q \cdot \Delta x \cdot \Delta t - \frac{\partial Q}{\partial x} \cdot \Delta x \cdot \Delta t &= \frac{\partial A}{\partial t} \cdot \Delta t \cdot \Delta x \end{aligned} \quad (4.5)$$

Equation 4.5 can be reduced to the following by isolating and dividing with  $\Delta x$  and  $\Delta t$ , on both sides, yielding the mass conservation part of the Saint-Venant equations.

$$\frac{\partial A(x, t)}{\partial t} + \frac{\partial Q(x, t)}{\partial x} = q(x, t) \quad (4.6)$$

For channel flows without lateral input the mass conservation is given as:

$$\boxed{\frac{\partial A(x, t)}{\partial t} + \frac{\partial Q(x, t)}{\partial x} = 0} \quad (4.7)$$

**Momentum** of the control volume  $\Omega$  shown in figure 4.2 can be found by utilizing Newtons second law which states that force is equal to mass times acceleration. Basically this means that the momentum of the control volume can be found by integrating the sum of forces in the following differential equation:

$$\frac{d\mathcal{M}(t)}{dt} = \sum_i F_i(t) \quad (4.8)$$

Where  $\mathcal{M}(t)$  is the momentum, given as mass times a velocity vector, of the control volume at time  $t$  and  $F_i(t)$  is the various external forces affecting the control volume. The forces are given by the various hydrodynamic and hydrostatic effects which affects the control volume.

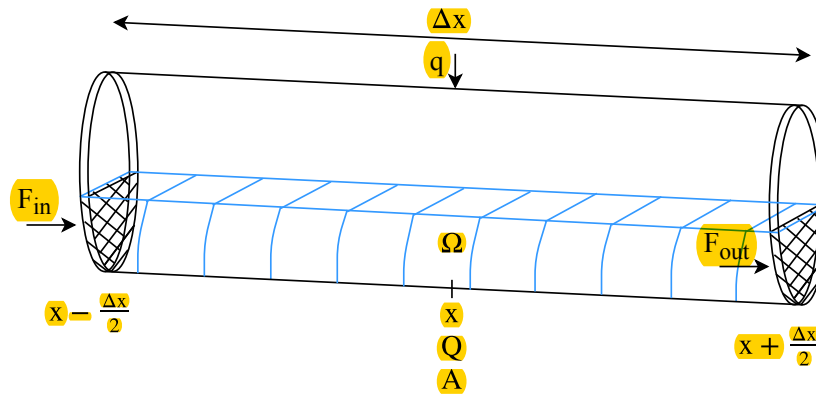


Figure 4.2: Illustration of the control volume  $\Omega$ , where the marked end pieces illustrates infinitely small slices.

If an infinite small slice of cross section in the control volume is considered, illustrated at the ends of the pipe in figure 4.2, and utilizing the product rule on the hydrodynamic force acting on the slice, the following is obtained:

$$F = M \cdot \frac{dv}{dt} + \frac{dM}{dt} \cdot v \quad (4.9)$$

Due to the assumption of incompressible fluid in the control volume the mass derivative term in equation 4.9 can be rewritten to:

$$\frac{dM}{dt} = \rho \frac{dV}{dt} = \rho \cdot Q \quad (4.10)$$

If assuming static speed then the acceleration term can be neglected. By inserting equation 4.10 into equation 4.9 the force, given by the slice of fluid particles, can be written as:

$$F = \rho \cdot Q \cdot v \quad (4.11)$$

The hydrodynamic force given by the in- and output of fluid particles in the control volume, when considering a slice of fluid particles at the center of the control volume, is given as:

$$F_{in} = \rho \cdot v \cdot Q - \frac{\partial}{\partial x}(\rho \cdot v \cdot Q) \cdot \frac{\Delta x}{2} \quad (4.12)$$

$$F_{out} = \rho \cdot v \cdot Q + \frac{\partial}{\partial x}(\rho \cdot v \cdot Q) \cdot \frac{\Delta x}{2} \quad (4.13)$$

Where subscript "in" denote the force going in through the left side of the channel in figure 4.2 and subscript "out" is the force going out to the right side. The change of particle momentum in the control volume is given as  $F_{in} - F_{out}$  and by replacing velocity with  $Q/A$  the following is obtained:

$$\begin{aligned} & \underbrace{\rho \cdot \frac{Q}{A} \cdot Q - \frac{\partial}{\partial x} \left( \rho \cdot \frac{Q}{A} \cdot Q \right) \cdot \frac{\Delta x}{2}}_{F_{in}} - \underbrace{\left( \rho \cdot \frac{Q}{A} \cdot Q + \frac{\partial}{\partial x} \left( \rho \cdot \frac{Q}{A} \cdot Q \right) \cdot \frac{\Delta x}{2} \right)}_{F_{out}} \\ &= -\rho \frac{\partial}{\partial x} \frac{Q^2}{A} \Delta x \end{aligned} \quad (4.14)$$

The remaining to be found are the forces imposed by gravity, friction and pressure. The force applied by gravity is given as:

$$F_g = \sin(\theta) \cdot g \cdot \rho \cdot \Delta x \cdot A \quad (4.15)$$

Where the slope of the pipe bed  $S_b = \tan(\theta) \approx \sin(\theta)$  for small values of  $\theta$  yields:

$$F_g = S_b \cdot g \cdot \rho \cdot \Delta x \cdot A \quad (4.16)$$

The friction force can be set up as:

$$F_f = S_f \cdot g \cdot \rho \cdot \Delta x \cdot A \quad (4.17)$$

Where  $S_f$  is a friction coefficient. This coefficient can be estimated by different formulas like Manning's or Darcy-Weishbach formula which is seen in equation 4.18 and 4.19 respectively.

$$S_f = \frac{n^2 Q^2}{A^2 R^{4/3}} = \frac{n^2 v^2}{R^{4/3}} \quad (4.18)$$



$$S_f = \frac{fQ^2}{8gRA^2} = \frac{fv^2}{8gR} \quad (4.19)$$

Where  $n$  is Manning's roughness factor [ $\frac{s}{m^{1/3}}$ ],  $f$  is the Weisbach resistance coefficient [ $\cdot$ ] and  $R$  is the hydraulic radius [ $m$ ] given as the wetted area divided by the wetted perimeter [Mays, 2001]. The Weisbach resistance coefficient is found by the Colebrook-White formula seen in equation 4.20.

$$\frac{1}{\sqrt{f}} = -2 \cdot \log \left( \frac{k}{14.84 \cdot R} + \frac{2.52}{4Re\sqrt{f}} \right) \quad (4.20)$$

Where  $k$  is a pipe roughness coefficient and  $Re$  is the Reynolds number.

Last the pressure forces on the  $x$  component of the control volume to be found is shown as  $F_{P1}$ - $F_{P3}$  in figure 4.3.

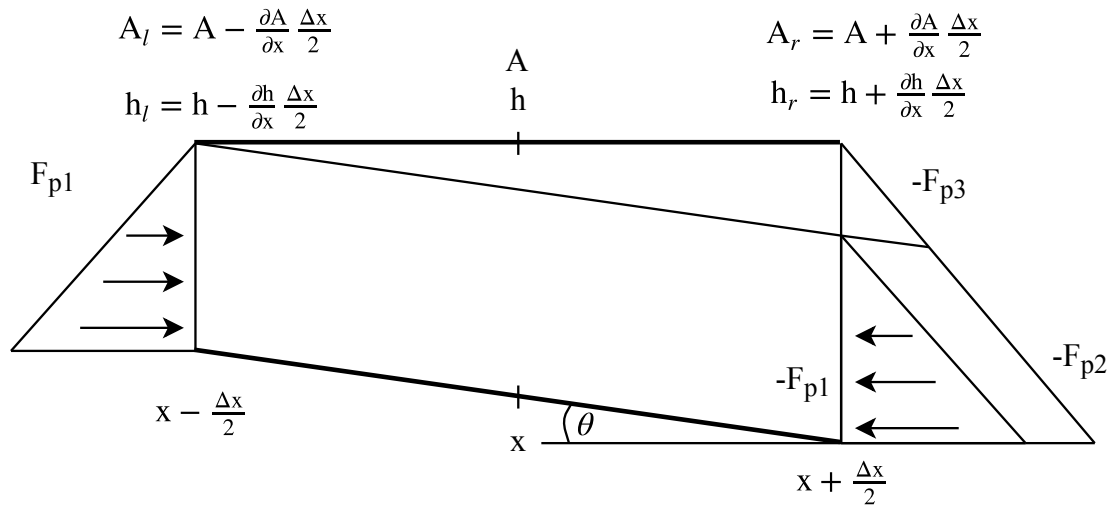


Figure 4.3: Pressure forces acting on a control volume.

1

By assuming hydrostatic pressure, the pressure in a height,  $z$ , above the bottom of the channel is given as  $g\rho(h - z)$ , where  $h$  is the height of the fluid. The pressure force acting on the left side of the control volume is given as:

$$F_{P1} = \int_0^{h_l} \rho \cdot g(h_l - z) \cdot b(z) dz \quad (4.21)$$

Where  $h_l$  is the fluid height at the left side of the control volume,  $b(z)$  is the width of the channel given the height  $z$ . The force acting on the right side of the control volume is

<sup>1</sup>Fixme Note: Ny tegning og sikkert også caption

given as:

$$\begin{aligned}
-\int_0^{h_r} \rho \cdot g \cdot (h_r - z) \cdot b(z) dz &= -\int_0^{h_l} \rho \cdot g \cdot (h_l - z) \cdot b(z) dz \\
&\quad - \int_0^{h_l} \rho \cdot g \cdot (h_r - h_l) \cdot b(z) dz \\
&\quad - \int_{h_l}^{h_r} \rho \cdot g \cdot (h_r - z) \cdot b(z) dz \\
&= -F_{P1} - F_{P2} - F_{P3}
\end{aligned} \tag{4.22}$$

The pressure force acting on the right side, at a height  $h_l$  from the channel bed, is given by  $F_{P1}$ ,  $F_{P2}$  and  $F_{P3}$  is the remaining force from  $h_l$  to  $h_r$ . The force  $F_{P2}$  is given as:

$$\begin{aligned}
F_{P2} &= \int_0^{h_l} \rho \cdot g \cdot (h_r - h_l) \cdot b(z) dz \\
&= \int_0^{h_l} \rho \cdot g \cdot \left( h + \frac{1}{2} \frac{\partial h}{\partial x} - \left( h - \frac{1}{2} \frac{\partial h}{\partial x} \right) \right) \cdot b(z) dz \\
&= \rho g \frac{\partial h}{\partial x} \Delta x A_l
\end{aligned} \tag{4.23}$$

The remaining pressure force, resulting from the height difference between  $h_l$  and  $h_r$ , is to be found. If, as a result of a small angle, it is assumed that the difference in height at each side is infinitely small. Then the force  $F_{P3}$  is given as:

$$\begin{aligned}
F_{P3} &= \int_{h_l}^{h_r} \rho \cdot g \cdot (h_r - z) \cdot b(z) dz \\
&\approx \rho \cdot g \cdot b(h) \cdot \left[ h_r \cdot z - \frac{z^2}{2} \right]_{h_l}^{h_r} \\
&= \rho \cdot g \cdot b(h) \cdot \left( h_r \cdot (h_r - h_l) + \frac{1}{2} \left( \frac{\partial h}{\partial x} \cdot \Delta x \right)^2 \right) \\
&\approx \rho \cdot g \cdot b(h) \cdot \frac{1}{2} \left( \frac{\partial h}{\partial x} \Delta x \right)^2
\end{aligned} \tag{4.24}$$

Taking the sum of forces from equations 4.21 and 4.22:

$$\begin{aligned}
F_{P1} - F_{P1} - F_{P2} - F_{P3} &= -\rho g \frac{\partial h}{\partial x} \Delta x A_l - \rho g b(h) \frac{1}{2} \left( \frac{\partial h}{\partial x} \Delta x \right)^2 \\
&= -\rho \cdot g \cdot \frac{\partial h}{\partial x} \cdot \Delta x \left( A_l + \frac{1}{2} b(h) \frac{\partial h}{\partial x} \Delta x \right) \\
&= -\rho \cdot g \cdot \frac{\partial h}{\partial x} \cdot \Delta x \left( A_l + \frac{1}{2} \frac{\partial A}{\partial x} \Delta x \right) \\
&= -\rho \cdot g \cdot \frac{\partial h}{\partial x} \cdot \Delta x \cdot A
\end{aligned} \tag{4.25}$$

By summing all the forces from equation 4.14, 4.15, 4.17 and 4.25 and inserting them into

equation 4.8 the following is obtained:

$$\begin{aligned}
 -\sum_i F_i = & -\frac{\partial}{\partial x} \rho \frac{Q^2}{A} \Delta x \\
 & -S_b \cdot g \cdot \rho \cdot \Delta x \cdot A \\
 & -S_f \cdot g \cdot \rho \cdot \Delta x \cdot A \\
 & -\rho \cdot g \cdot \frac{\partial h}{\partial x} \cdot \Delta x \cdot A
 \end{aligned} \tag{4.26}$$

Lastly the time derivative expression of the momentum, which is given by mass times velocity, are:

$$\frac{d\mathcal{M}(t)}{dt} = \frac{\partial}{\partial t} \left( \rho \cdot A \cdot \Delta x \cdot \frac{Q}{A} \right) \tag{4.27}$$

Where mass is given by  $\rho \cdot A \cdot \Delta x$  and velocity by  $Q/A$ .

Having obtained expressions for equation 4.27 and equation 4.26 they can be inserted into equation 4.8 yielding the following expression:

$$\begin{aligned}
 \frac{\partial}{\partial t} \left( \rho \frac{Q}{A} A \cdot \Delta x \right) = & -\frac{\partial}{\partial x} \rho \frac{Q^2}{A} \Delta x \\
 & -S_b \cdot g \cdot \rho \cdot \Delta x \cdot A \\
 & -S_f \cdot g \cdot \rho \cdot \Delta x \cdot A \\
 & -\rho \cdot g \cdot \frac{\partial h}{\partial x} \cdot \Delta x \cdot A
 \end{aligned} \tag{4.28}$$

Dividing with  $g \cdot \rho \cdot \Delta x \cdot A$  and isolating, then the following definition of the equation is obtained:

$$\boxed{\frac{1}{gA} \frac{\partial Q}{\partial t} + \frac{1}{gA} \frac{\partial}{\partial x} \left( \frac{Q^2}{A} \right) + \frac{\partial h}{\partial x} + S_f - S_b = 0} \tag{4.29}$$

Some or all of the terms in equation 4.29 can be utilized when simulating free channel flow. An overview of the limitations when excluding parts of the momentum equation is given in table 4.1.

Approximation	Kinematic wave (1)	Noninertia (2)	Quasi-steady dynamic wave (3)	Dynamic wave (4)
momentum equation	$S_b = S_f$	$\frac{\partial h}{\partial x} = S_b - S_f$	$\frac{1}{gA} \frac{\partial}{\partial x} \left( \frac{Q^2}{A} \right) + \frac{\partial h}{\partial x} = S_b - S_f$	equation 4.29
Boundary conditions required	1	2	2	2
Account for downstream backwater effect and flow reversal	No	Yes	Yes	Yes
Damping of flood peak	No	Yes	Yes	Yes
Account for flow acceleration	No	No	only convective acceleration	Yes

Table 4.1: Limitations when excluding, 1.(inertia and pressure terms), 2.(inertia terms), 3.(pressure term relating to local acceleration) and 4.(none), from the momentum equation [Mays, 2001].

The kinematic wave is the simplest approximation and ignores the terms representing changes in inertia and pressure by assuming that the slope of the water surface is identical to that of the channel bed. Furthermore only one boundary condition is needed, meaning that only the upper boundary of the channel is needed to solve the Saint-Venant equations. Some considerations is needed when utilizing this approximation. Due to the simplicity of the kinematic wave approximation, attenuation, which occurs in a real free flowing channel, should not be present. But due to numerical damping, which is induced because of the nature of discretization, it occurs. Some, wrongfully attempts to mitigate it by choosing smaller steps of  $\Delta x$  and  $\Delta t$ . Instead they should be chosen such that the simulated channel flow mimics that of the real channel. Due to its simplicity the kinematic wave approximation has been used and researched extensively. If the back water effect is not an issue the kinematic wave approximation is often used when dealing with simulation of flows in sewer lines. To limit the complexity of the further work of the project, the kinematic wave approximation, of the momentum equation, is chosen [Mays, 2001]. Furthermore it is decided to disregard lateral input, i.e. not take gutter drains into consideration. This means that side input to the main sewer line is assumed attached at the end of the pipe section as shown in table 2.1. Further details can be found in section 4.3.

## 4.2 Transport of concentrate

A model for transport of concentrate in sewer pipes is obtained in the following. The following assumptions is made obtaining the transport equation.

1. The flow of concentrate is assumed to be steady and uniform in the cross section.
2. The anoxic, anaerobic or aerobic processes occurring in the sewer line is neglected

In figure 4.4 a control volume is seen.

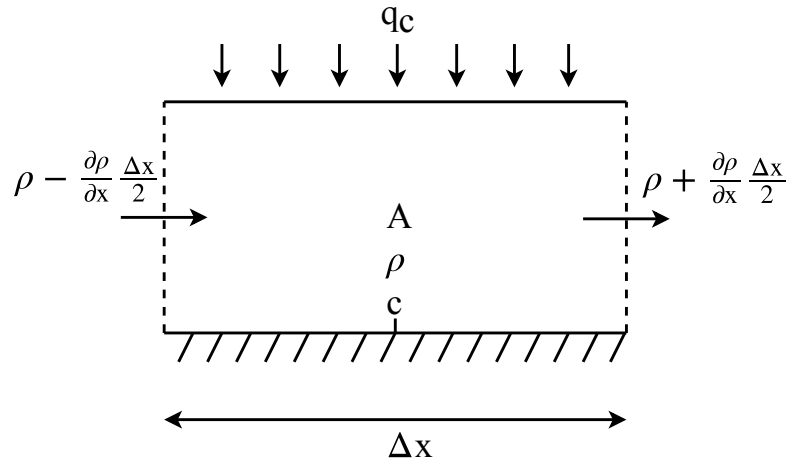


Figure 4.4: Illustration of a control volume containing concentrate.

The conservation of concentrate in the control volume is as in section 4.1 dependent on the change in stored mass and change in flow. This means that the equation for conservation of mass given by equation 4.6, which is shown below, can be utilized.

$$\frac{\partial A}{\partial t} + \frac{\partial Q}{\partial x} = q \quad (4.30)$$

Assuming average concentrate,  $C$ , across the control volume, and multiplying it with the terms of the continuity equation, the following is obtained:

$$\frac{\partial A \cdot C}{\partial t} + \frac{\partial \phi}{\partial x} = q \cdot C_{lat} \quad (4.31)$$

Where  $\phi$  is a flux  $[\frac{g}{s}]$  term replacing the flow term,  $Q$  and  $C_{lat}$  is lateral concentrate input into the control volume  $[\frac{g}{m^3}]$  [Vestergaard, 1989].

Depending on the desired approximation the flux and lateral inflow terms can be expanded. The expanded lateral term describes a dead zone at the bottom of the channel, which can be useful to model if dealing with rugged channel bed. Due to the prismatic assumption in 4.1 of the sewer channel the dead zone in the channel is not investigated further. Flux terms describing convective flow and dispersion can be seen in table 4.2.

Approximation	Convective flow	Convective + (dispersion)
Flux term	$\phi = Q \cdot C$	$\phi = Q \cdot C + (-\epsilon \cdot A \frac{\partial C}{\partial x})$
boundary conditions required	1	2

Table 4.2: Table of convective flux term without and with dispersion where  $Q$  is flow,  $C$  is concentrate,  $A$  is area and  $\epsilon$  is a dispersion coefficient  $[\frac{m^2}{s}]$  [Vestergaard, 1989] .

The dispersion term shown in the above table, also known as Fickian diffusion, gives an expression for how the molecules of the concentrate spreads. On a molecular level the the concentrate will to some degree disperse upstream and downstream as shown in figure 4.5.

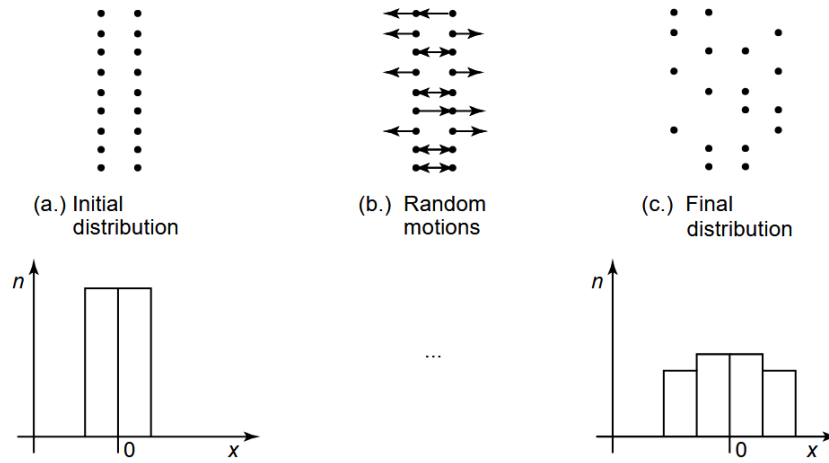


Figure 4.5: Illustration of distribution of convective flow without dispersion (a) and with (c), where dots illustrate molecules of the concentrate within a control volume [Institute of hydromechanics, ].

For various concentrates the dispersion coefficient  $\epsilon$  which varies with temperature can be found in lookup tables [Institute of hydromechanics, ].

Inserting the terms in table 4.2 into equation 4.31 then the following expressions of the continuity equation is obtained:

$$\frac{\partial(A \cdot C)}{\partial t} + \frac{\partial(Q \cdot C)}{\partial x} - \epsilon \cdot \frac{\partial^2(A \cdot C)}{\partial x^2} = q \cdot C_{lat} \quad (4.32)$$

$$\frac{\partial(A \cdot C)}{\partial t} + \frac{\partial(Q \cdot C)}{\partial x} = q \cdot C_{lat} \quad (4.33)$$

In closed environments such as sewers longitudinal dispersion can often be neglected [Vestergaard, 1989]. For this reason and to reduce complexity of the simulation, equation 4.33 is utilized further on. As the change in flow and area in the channel is solved by the Saint-Venant equations, an expression which only considers change in concentrate suffices. The terms in equation 4.33 can be rewritten to the following:

$$C \cdot \frac{\partial A}{\partial t} + A \cdot \frac{\partial C}{\partial t} + C \cdot \frac{\partial Q}{\partial x} + Q \cdot \frac{\partial C}{\partial x} = q \cdot C_{lat} \quad (4.34)$$

Multiplying equation 4.30 with C yields:

$$C \cdot \frac{\partial A}{\partial t} + C \cdot \frac{\partial Q}{\partial x} = q \cdot C \quad (4.35)$$

Subtracting equation 4.35 from 4.34 then results in the following:

$$A \cdot \frac{\partial C}{\partial t} + Q \cdot \frac{\partial C}{\partial x} = q \cdot (C_{lat} - C) \quad (4.36)$$

Neglecting lateral flow and concentration inputs the following expression is obtained:

$$\boxed{A \cdot \frac{\partial C}{\partial t} + Q \cdot \frac{\partial C}{\partial x} = 0} \quad (4.37)$$

Equation 4.37 can thereby be solved with the solutions of  $Q$  and  $A$  obtained from the Saint-Venant equations.

### 4.3 Sewer interconnection

This section will explain how pipes are interconnected and how the concentration for two joint pipes are calculated.

In figure 4.6 an illustration of two pipes that are connected to the same point.

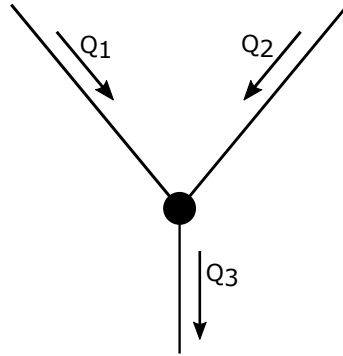


Figure 4.6: Illustration of an interconnection between two flow inputs and one output.

The two pipes leading into the point are connected, where the wastewater from the two pipes will be added up and transferred to the following pipe. The flow  $Q_3$  is calculated as:

$$\boxed{Q_3 = Q_1 + Q_2} \quad (4.38)$$

Which is a sum of the flows going into the point. This assumes that there are no turbulence in the joint wastewater from the the pipes. However, this is not the case in a real sewer, but it is deemed sufficient for this model.

To calculate the concentration in a interconnection the following equation is used:

$$\boxed{C_3 = \frac{C_1 Q_1 + C_2 Q_2}{Q_3}} \quad (4.39)$$

Where  $C_1$  and  $C_2$  are the concentration in the respective pipe  $[g/m^3]$ . <sup>2</sup>

---

<sup>2</sup>FiXme Note: Mangler antagelser

## 4.4 Tank

In this section a model for flow and concentrate is derived for a tank. The assumptions made deriving the tank model is:

1. Turbulence, caused by in- or output in the tank, is neglected.
2. Level of concentrate of the fluid in the tank is considered uniform, meaning mixing with the new inflow occurs instantly.

In figure 4.7 an illustration of a tank is shown.

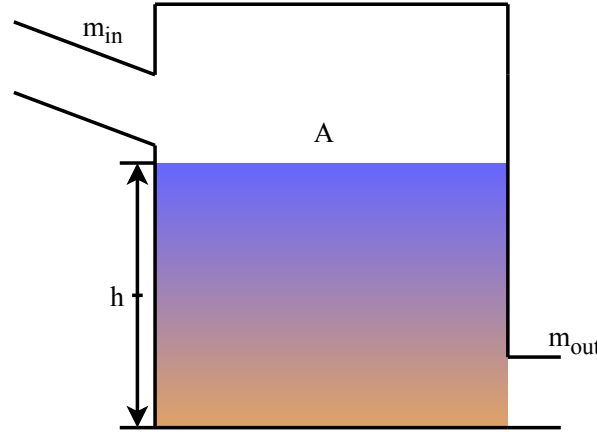


Figure 4.7: Illustration of a tank.

The illustration will be used to derive the model for the tank. From the left, a pipe that discharges fluid into the tank is shown. The fluid going into the tank has a mass flow rate  $m_{in}$  [kg/s]. At the bottom right, the fluid is discharged from the tank with a mass flow rate,  $m_{out}$ . Within the tank the height of the stored fluid is dependent on horizontal cross-section area and the mass in- and outflow. The mass balance equation is derived in [Vojtesek et al., ] and is given as:

$$\frac{dM_{cv}(t)}{dt} = m_{in}(t) - m_{out}(t) \quad (4.40)$$

Where  $M_{cv}$  is the total mass within the control volume [kg], and  $m_{in}$  and  $m_{out}$  is the mass in and outflow rate of the tank [kg/s]. The mass balance can be written as  $M_{cv} = \rho Ah$  where  $\rho$  is the density [kg/m<sup>3</sup>],  $A$  is the area [m<sup>2</sup>] and  $h$  is the height [m]. The mass flow rate can be written as  $m = \rho Q$ , where  $Q$  is the flow [m<sup>3</sup>/s]. Inserting this into equation 4.40 the following is obtained:

$$\frac{d(\rho Ah(t))}{dt} = \rho Q_{in}(t) - \rho Q_{out}(t) \quad (4.41)$$

By assuming incompressible fluid such that density is constant then the in- and outflow



can be isolated.

$$\rho A \frac{dh(t)}{dt} = \rho (Q_{in}(t) - Q_{out}(t)) \quad (4.42)$$

Simplifying equation 4.42 by dividing with  $\rho A$ :

$$\frac{dh(t)}{dt} = \frac{1}{A} (Q_{in}(t) - Q_{out}(t)) \quad (4.43)$$

This equation describes the change in height according to in- and outflow. Due to the nature of a sewer system, it is typically not possible to implement a tank where the outflow is controlled by gravity and a valve. For this reason, it is decided to implement an actuator in the form of a pump within the tank, which control the output flow into the adjoining pipe. In figure 4.8 the chosen tank setup is seen.

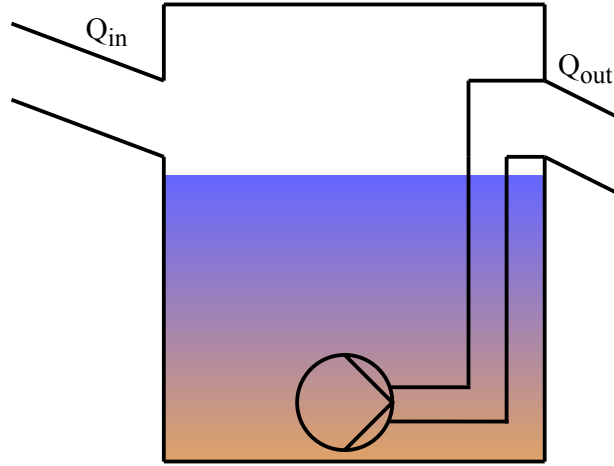


Figure 4.8: Illustration of a tank with a pump inserted to regulate the output flow.

Due to the nature of free flow in pipes, the dynamics of the pump will be mitigated for longer pipes. For this reason, it is decided to disregard pump dynamics and implement a simple linear term where an actuator input controls the output flow.

$$Q_{out}(t) = u(t) \cdot \overline{Q} \quad (4.44)$$

Where  $u$  is pump control input and  $\overline{Q}$  is a fixed operating point which for example could be the maximum flow of the adjoining pipe. By inserting equation 4.44 into equation 4.43 the following is obtained:

$$\boxed{\frac{dh(t)}{dt} = \frac{1}{A} (Q_{in}(t) - u(t) \cdot \overline{Q})} \quad (4.45)$$

Equation 4.45 then gives an expression where a change in height is given as a function of inflow and outflow.

For the concentration part of the tank, there is the ratio of concentrate to consider. At some point, the level of concentrate flowing into the tank might differ from the concentrate level already in the tank. Then as the stored fluid is pumped out of the tank the concentrate level should go towards the inflow concentration. When empty the concentration of the outflow should be equal to the inflow concentration. By the initial assumptions the change in concentration in the tank is given by equation 4.46.

$$\frac{dC_{tank}(t)}{dt} = C_{in}(t) \cdot \frac{\frac{Q_{in}(t)}{A}}{h(t)} - C_{out}(t) \cdot \frac{\frac{Q_{out}(t)}{A}}{h(t)} \quad (4.46)$$

As the output concentration is equal to what is in the tank at the current time the following is obtained.

$$\boxed{\frac{dC_{tank}(t)}{dt} = \frac{1}{A} \left( C_{in}(t) \cdot \frac{Q_{in}(t)}{h(t)} - C_{tank}(t) \cdot \frac{Q_{out}(t)}{h(t)} \right)} \quad (4.47)$$

The advantage of this scheme is that flow and height are already known. This keeps the computational power required at a minimum while some realism, in the level of concentrate flowing through the tank, is obtained.

In this chapter, an overview is given of the design process of the simulation environment. Furthermore, the schemes utilized to be able to simulate the nonlinear parts of the sewage flow, with its various concentrations, is explained. Lastly, the designed environment is implemented and verified. It is decided to utilize MATLAB as the platform to be used for this project. Furthermore, it is assumed that readers are familiar with basic terminology related to MATLAB, and therefore specifics will not be given hereof.

In the following, the basic structure of the simulation and the design of it is explained.

## 5.1 Structure

For the simulation environment to be useful, some basic functionality is needed. The simulation should be easy to setup and adjust if needed. Furthermore, an easy way to view the result of the simulation is needed such that necessary adjustments can easily be made based on the result.

The first overall thing to consider is the composition of components desired to simulate. To make the simulation environment useful it should be able to handle different compositions of pipes and tanks. Meaning that the simulation environment can simulate different setups than the one shown in figure 2.1. For this, a simple setup procedure, where different sizes of pipes with different parameters can be chosen, is needed. The second thing to consider is that the environment should be brought to a steady state before the simulation starts. The reason for this is that unintended results can arise when working with non-linear systems. Transients caused by the system not to be in a steady state, when starting simulating, can skew the initial data obtained, which is not ideal. Also if a linearized approach to the MPC scheme is chosen a linearized model is necessary, which requires a system in steady state to obtain. The simulation should be able to run for a predefined amount of iterations. Based on this the basic structure of the simulation environment can be split into three parts as shown in figure 5.1.

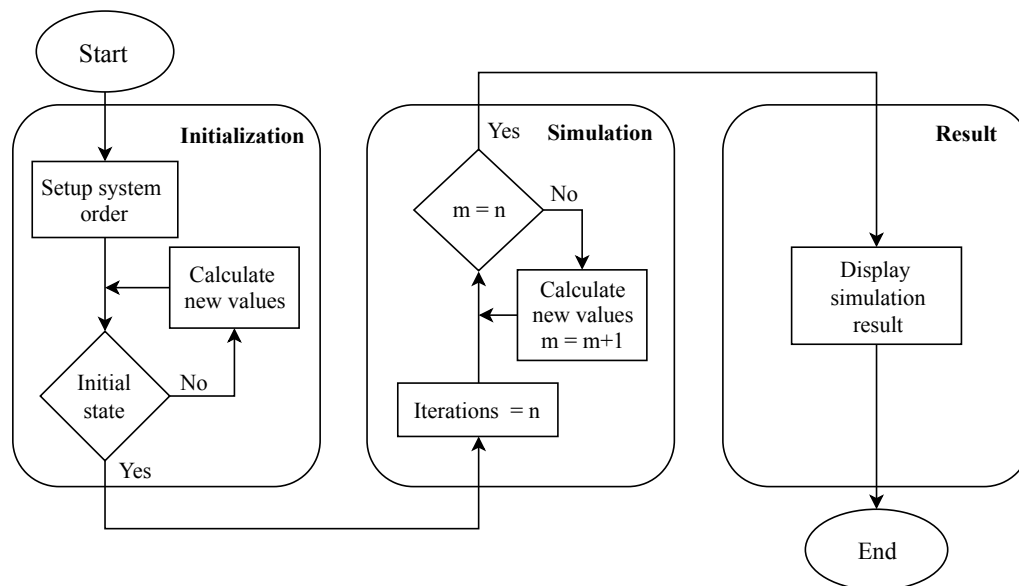


Figure 5.1: Basic overview of simulation environment

The following will go into details, on the thoughts and the considerations made during the design phase, of the three parts shown in the figure.

### Initialization

The initialization process is, as shown in figure 5.1, comprised of several parts. The first part is to set up the desired system of pipes and tanks such that the system is simulated with the chosen components in the right order. Secondly, the system should be brought in to a steady state from which the simulation can start. The reason for this is that the Saint-Venant equations utilized to simulate the flow in the sewer pipes is non-linear. Because of this, it can be difficult to find a steady state by hand, which do not produce an unintended result when starting simulating. Though it might be possible to find fitting initial values for small setup it is assumed that larger setup will increase the chance of unintended results when starting simulating.

For the first part, a simple system setup is decided upon, where the desired components are added to a list. The order of the list then decides how the components is connected when simulating. An example of this setup procedure is shown in figure 5.2.

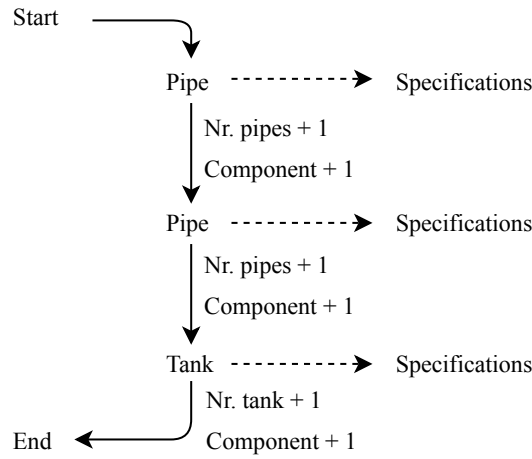


Figure 5.2: Setup scheme of system order initiation

The specifications for each part in figure 5.2 refers to the parameters needed to run the simulation. The necessary specifications entered for pipe and tank should as a minimum be the required parameters needed to utilize the Preissmann scheme explained in section 5.2 and to simulate in- and outflow of one or more tanks, respectively. Furthermore, constants which are utilized during simulation should be calculated during initialization such that the computational load is kept as low as possible during simulation.

A simple solution to bring the desired system setup to an initial steady state is to give a fixed input flow and iterate. The iteration continues until a satisfactory error between the fixed input and the flow within the designated setup is deemed sufficiently low. For this to work, it is important to have side input or disturbance input in mind. In figure 5.3 a simple setup is shown of a possible setup to be simulated.

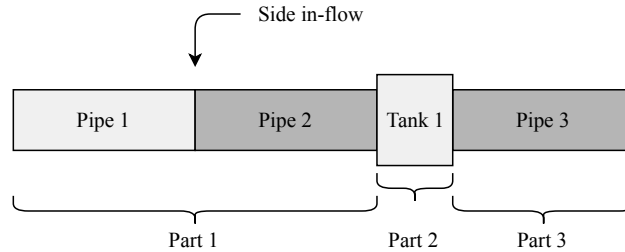


Figure 5.3: Simple setup with three pipes, a tank and a single side input

To make the steady state iteration scheme work on a dynamic level, the components can be separated into parts where adjoint pipes are seen as a single part. The system can then be brought in to steady state one part at a time. As the pipes are the only non-linear part of the system, they are the only parts needed to be iterated upon. Taking the first part in figure 5.3 as an example, there are two pipes and the second one has a side input. A general expression of the average flow in the parts containing pipes is given by the following equation:

$$\text{Part-m}_{\text{avg}} = \frac{\sum_{i=1}^n \text{Pipe-input}_i + \text{side inflow}_i}{n_{\text{pipes}}} \quad (5.1)$$

Equation 5.1 can then be used to obtain the desired steady state flow and a current one by utilizing values obtained by solving the Saint-Venant equations. The iteration can then be set to stop when the error between the desired and the measured average is sufficiently low. The next part in figure 5.3 is, in this case, a tank, set to have an in- and outflow equal to the output of the second pipe, which is the combined flow of the first pipe plus the side input. For the third part, the iteration process then starts over with the outflow of the tank as input. As the concentrate flow is depending on the solution of the Saint-Venant equations it is assumed that when the flow is in a steady state the concentrate will have reached steady state as well.

## Simulation

Having obtained a setup in steady state the next part is to simulate it for the predefined amount of iterations. An important part of the simulation is to store data in a way such that it is easily and intuitively obtainable for purposes such as debugging or customized plots. For this reason, it is decided to store the data, from simulating, into separate blocks. This means that data from individual pipes and tanks should be stored separately in the order given by the initial component setup shown in figure 5.2. In figure 5.4 a simple overview of the simulation procedure is given.

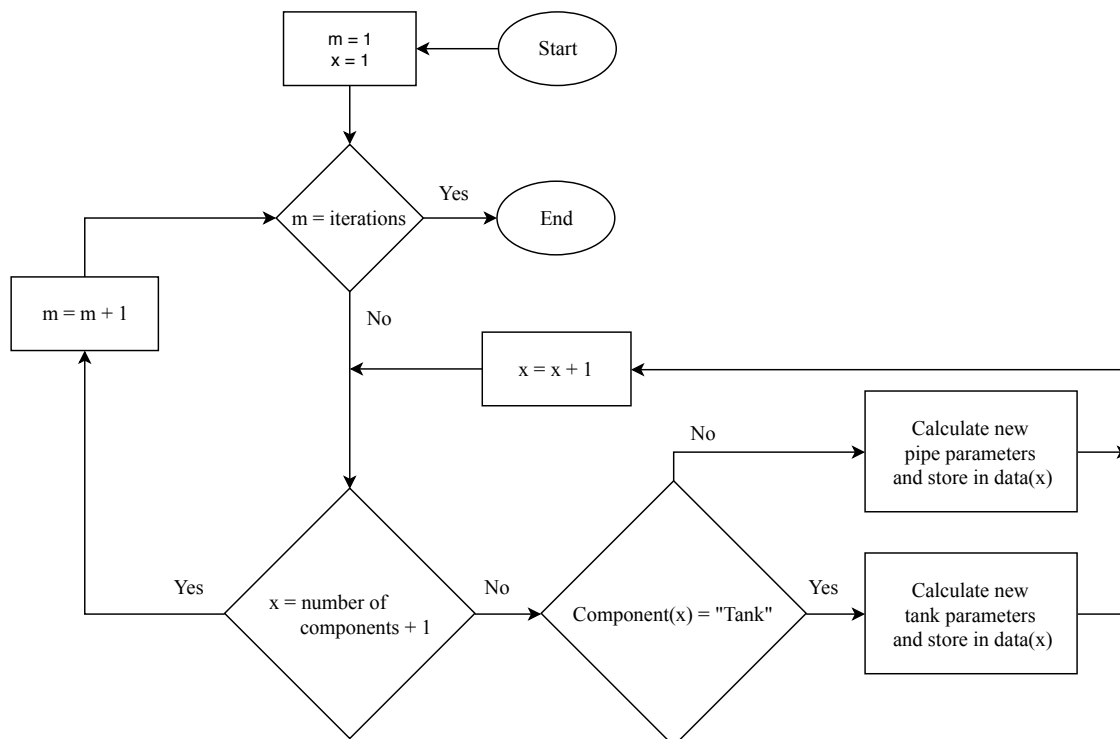


Figure 5.4: Basic overview of the simulation scheme.

## Result

Having obtained data from simulating the user-defined system an overview of the results is needed. Considerable time can be spent in designing a function which can display the data in various forms. As the data can consist of a large number of components as well as a considerable time span it can get quite time-consuming to pinpoint parts of interest in time and place. For this reason, it is decided that a simple solution which can give an overview, of the obtained data, is needed. The chosen solution is a function which can playback the simulated data at a user defined speed and intervals in the data. Furthermore, it should be possible to pause and start the playback at a user-defined iteration.

Having outlined the basic details of the construction of the simulation environment the scheme needed to solve the non-linear Saint-Venant equations is explained in detail in the next section.

## 5.2 Preissmann scheme

In this section, a numerical method for solving the Saint-Venant equations are chosen and elaborated on.

The numerical method chosen, for solving the Saint-Venant equations, is the Preissmann scheme which is based on the box scheme. Other methods exist such as Lax scheme, Abbot-Ionescu scheme, leap-frog scheme, Vasiliev scheme, however, the Preissmann scheme is commonly known as the most robust. Basically, by using the Preissmann scheme the Saint-Venant equations can be discretized, and thereby utilized to simulate the flow and height throughout a pipe.

In section 4.1 the Saint Venant equations for conservation of mass and momentum are derived, they are also shown below.

$$\frac{\partial A(x, t)}{\partial t} + \frac{\partial Q(x, t)}{\partial x} = 0 \quad (5.2)$$

$$\frac{1}{gA} \frac{\partial Q}{\partial t} + \frac{1}{gA} \frac{\partial}{\partial x} \left( \frac{Q^2}{A} \right) + \frac{\partial h}{\partial x} + S_f - S_b = 0 \quad (5.3)$$

In figure 5.5 a single mesh for the Preissmann scheme is illustrated.

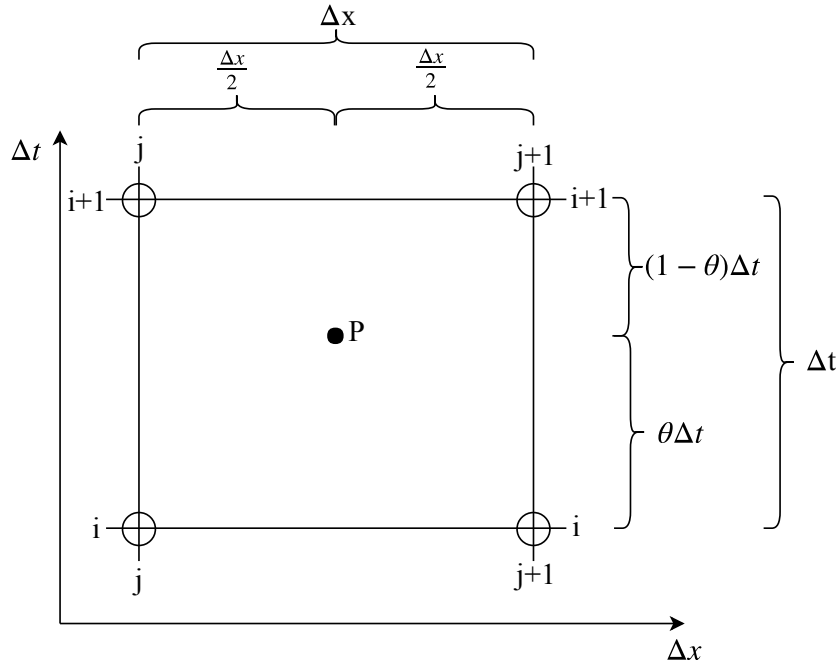


Figure 5.5: Preissmann non-staggered grid scheme.

Where  $\theta$  is a weighting parameter ranging between zero and one,  $j$  is an index of cross section and  $i$  is an index of time. The mesh contains four nodes,  $(j,i)$ ,  $(j+1,i)$ ,  $(j,i+1)$  and  $(j+1,i+1)$ , however in the implementation the dimension of the grid is  $\Delta t \times \Delta x$  for  $0 \leq x \leq L$  and  $0 \leq t$ . Where  $L$  defines the length of the pipe section. The derivatives in equations 5.2 and 5.3 are calculated as an approximation at the point  $P$ , which is in the middle of the interval of  $\Delta x$ . The difference between the box scheme and the Preissmann scheme is that the point  $P$  is always found at the middle of  $\Delta x$  and the point can only move along the time axis within this mesh by adjusting the weighting parameter  $\theta$ . An arbitrary function  $f_p(x,t)$  calculated at point  $P$  is approximated by [Szymkiewicz, 1998].

$$f_P \approx \frac{1}{2}(\theta \cdot f_j^{i+1} + (1-\theta)f_j^i) + \frac{1}{2}(\theta \cdot f_{j+1}^{i+1} + (1-\theta)f_{j+1}^i) \quad (5.4)$$

The numerical approximation for the derivatives in equations 5.2 and 5.3 for time and length are shown below [Szymkiewicz, 1998].

$$\left. \frac{\partial f}{\partial t} \right|_P \approx \frac{1}{2} \left( \frac{f_j^{i+1} - f_j^i}{\Delta t} + \frac{f_{j+1}^{i+1} - f_{j+1}^i}{\Delta t} \right) \quad (5.5)$$

$$\left. \frac{\partial f}{\partial x} \right|_P \approx (1-\theta) \frac{f_{j+1}^i - f_j^i}{\Delta x} + \theta \frac{f_{j+1}^{i+1} - f_j^{i+1}}{\Delta x} \quad (5.6)$$

These approximations from equations 5.5 and 5.6 can therefore be inserted for the derivatives in the Saint-Venant equations 5.2 and 5.3 and thereby achieve the following,

$$\theta \frac{Q_{j+1}^{i+1} - Q_j^{i+1}}{\Delta x} + (1-\theta) \frac{Q_{j+1}^i - Q_j^i}{\Delta x} + \frac{1}{2} \frac{A_{j+1}^{i+1} - A_{j+1}^i}{\Delta t} + \frac{1}{2} \frac{A_j^{i+1} - A_j^i}{\Delta t} = 0 \quad (5.7)$$



$$\begin{aligned}
& \frac{1}{gA_p} \left( \frac{1}{2} \left( \frac{Q_{j+1}^{i+1} - Q_{j+1}^i}{\Delta t} + \frac{Q_j^{i+1} - Q_j^i}{\Delta t} \right) \right) \\
& + \frac{1}{gA_p} \left( \frac{\theta}{\Delta x} \left( \left( \frac{Q^2}{A} \right)_{j+1}^{i+1} - \left( \frac{Q^2}{A} \right)_j^{i+1} \right) \right) \\
& + \frac{1-\theta}{\Delta x} \left( \left( \frac{Q^2}{A} \right)_{j+1}^i - \left( \frac{Q^2}{A} \right)_j^i \right) + \theta \left( \frac{h_{j+1}^{i+1} - h_j^{i+1}}{\Delta x} \right) + (1-\theta) \left( \frac{h_{j+1}^i - h_j^i}{\Delta x} \right) \\
& + S_f - S_b = 0
\end{aligned} \tag{5.8}$$

By discretizing the Saint-Venant equations they can be used in a simulation to calculate parameters for the pipe model. The mesh shown in figure 5.5 is used to calculate the node  $(j+1,i+1)$  by knowing the previous values in time and length  $(j,i)$ ,  $(j+1,i)$  and  $(j,i+1)$ . Therefore some initial condition must be known to calculate the parameters for the pipe in the first iteration. The boundary condition for the flow, at  $t=0$ , must be known throughout the pipe. Furthermore, the flow that will enter the pipe for  $t \leq 0$  must be known, as illustrated with the circles in figure 5.6.

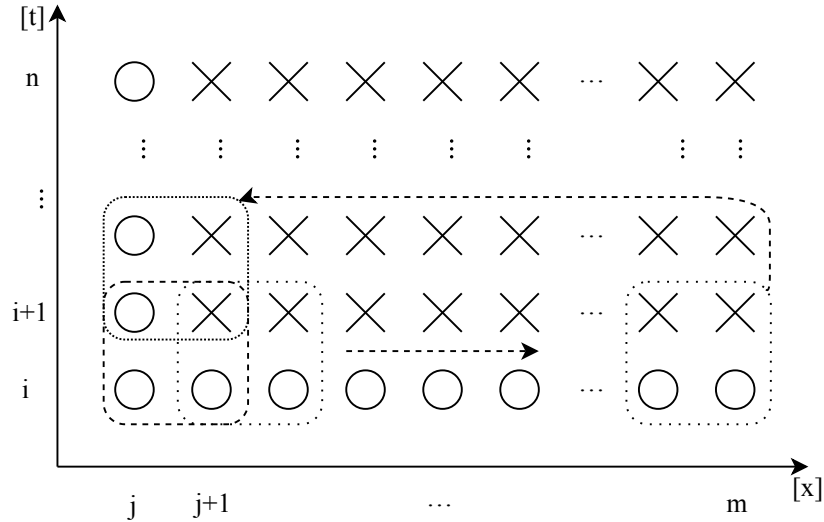


Figure 5.6: Preissmann non-staggered grid scheme example of calculation pattern.

By knowing the flow and parameters for the pipe, the height can be calculated in the initialization nodes, which will be elaborated on later. With equation 5.7, the flow  $(j+1,i+1)$  can be calculated by knowing the flow and height in the previous nodes  $(j,i)$ ,  $(j+1,i)$  and  $(j,i+1)$  as illustrated with the box in the left bottom corner in figure 5.6.

The discretized continuity equation 5.7, stated below, is solved for the desired flow in equation 5.10,

$$\theta \frac{Q_{j+1}^{i+1} - Q_j^{i+1}}{\Delta x} + (1 - \theta) \frac{Q_{j+1}^i - Q_j^i}{\Delta x} + \frac{1}{2} \frac{A_{j+1}^{i+1} - A_{j+1}^i}{\Delta t} + \frac{1}{2} \frac{A_j^{i+1} - A_j^i}{\Delta t} = 0 \quad (5.9)$$

$$Q_{j+1}^{i+1} = -\frac{1}{2\theta} \cdot (A_{j+1}^{i+1} - H) \cdot \frac{\Delta x}{\Delta t} \quad (5.10)$$

Where  $H$  is a parameter for the previous flows and areas in time and section, which are known, as these has been calculated, as shown in figure 5.6.

$$H = \left( 2 \cdot (1 - \theta) \cdot Q_j^i - 2 \cdot (1 - \theta) \cdot Q_{j+1}^i + 2\theta Q_j^{i+1} \right) \cdot \frac{\Delta t}{\Delta x} - A_j^{i+1} + A_j^i + A_{j+1}^i \quad (5.11)$$

It has been chosen to set the slope of the water surface identical to the pipe bed,  $I_e = I_b$ . By doing this the calculation of the flow throughout the pipe has been simplified, thus some limitation about the dynamics of the water flow are excluded, which is explained in section 4.1 and also shown in table 4.1. Therefore, instead of using the second discretized Saint-Venant equation 5.8 an equation for calculating the flow in a circular pipe will be used to find the flow and area used in the Preissmann scheme and can be seen in appendix A.4 [Michelsen, 1976]:<sup>1</sup>

$$Q = \left( 0.46 - 0.5 \cdot \cos \left( \pi \frac{h}{d} \right) + 0.04 \cdot \cos \left( 2\pi \frac{h}{d} \right) \right) \cdot Q_f \quad (5.12)$$

This equation describes the flow in a circular pipe by knowing the diameter,  $d$  height,  $h$  and the flow for a filled pipe  $Q_f$ .

$$Q_f = -72 \cdot \left( \frac{d}{4} \right)^{0.635} \pi \cdot \left( \frac{d}{2} \right)^2 \cdot I_e^{0.5} \quad (5.13)$$

$Q_f$  is calculated from Mannings equation and can be seen in appendix A.4.<sup>2 3</sup>

In equation 5.10 the flow  $Q_{j+1}^{i+1}$  is a function of the unknown area  $A_{j+1}^{i+1}$ , and by subtracting the flow on each side the following is achieved,

$$0 = -Q_{j+1}^{i+1} - \frac{1}{2\theta} \cdot (A_{j+1}^{i+1} - H) \cdot \frac{\Delta x}{\Delta t} \quad (5.14)$$

By naming the right hand side of equation 5.14 for  $V$  the following is obtained,

$$V = -Q_{j+1}^{i+1} - \frac{1}{2\theta} \cdot (A_{j+1}^{i+1} - H) \cdot \frac{\Delta x}{\Delta t} \quad (5.15)$$

There are still two unknowns in equation 5.15,  $Q_{j+1}^{i+1}$  and  $A_{j+1}^{i+1}$ .  $Q_{j+1}^{i+1}$  can be replaced with equation 5.12 for calculating the flow. Equation 5.12 is inserted into equation 5.15 and thereby the following is obtained,

$$V = -Q_f \cdot \left( 0.46 - 0.5 \cdot \cos \left( \pi \frac{h_{j+1}^{i+1}}{d} \right) + 0.04 \cdot \cos \left( 2\pi \frac{h_{j+1}^{i+1}}{d} \right) \right) \frac{\Delta t}{\Delta x} - \frac{1}{2\theta} (A_{j+1}^{i+1} - H) \quad (5.16)$$

<sup>1</sup>FiXme Note: Skal der står mere om valg af at sætte  $I_e = I_b$

<sup>2</sup>FiXme Note: skal der skrives her, at det er antaget at friction er lig med hældning?

<sup>3</sup>FiXme Note: lav hjælpeformeller

Furthermore  $Q_f$  from equation 5.13 is inserted into equation 5.16,

$$V = -72 \left( \frac{d}{4} \right)^{0.635} \pi \cdot \left( \frac{d}{2} \right)^2 I_e^{0.5} \cdot \left( 0,46 - 0,5 \cdot \cos \left( \pi \frac{h_{j+1}^{i+1}}{d} \right) + 0,04 \cdot \cos \left( 2\pi \frac{h_{j+1}^{i+1}}{d} \right) \right) \frac{\Delta t}{\Delta x} - \frac{1}{2\theta} \left( A_{j+1}^{i+1} - H \right) \quad (5.17)$$

V is now a function of the height  $h_{j+1}^{i+1}$  as the height is the only unknown parameter for finding the area  $A_{j+1}^{i+1}$  and the flow for the pipe, where the wetted area for a circular pipe is calculated with the following [Michelsen, 1976]:

$$A = \frac{d^2}{4} \cdot \arccos \left( \frac{\frac{d}{2} - h}{\frac{d}{2}} \right) - \sqrt{h \cdot (d - h)} \cdot \left( \frac{d}{2} - h \right) \quad (5.18)$$

To find a height in equation 5.17 Newton's method is used. Newton's method is a method used to find better approximations to the roots of a real-valued function. The method requires a real-valued function  $f$ , the derivate  $f'$ , and a initial guess  $x_0$ , of the root of the function. If the assumption is satisfied and the initial guess is close then a better approximation can be obtained by:

$$x_1 = x_0 - \frac{f(x_0)}{f'(x_0)} \quad (5.19)$$

Where  $x_1$  is the better approximation of the root, for the function  $f$ . Newtons method can be iterated until a satisfied root is obtained:

$$x_{n+1} = x_n - \frac{f(x_n)}{f'(x_n)} \quad (5.20)$$

By using the Newton method the roots of equation 5.17 can be found, which will be a approximation of the height in the pipe. The approximation for the height is:

$$(h_{j+1}^{i+1})_{k+1} = (h_{j+1}^{i+1})_k - \frac{V_k}{V'_k} \quad (5.21)$$

Where  $k$  is the number of iterations,  $V'$  is the differentiated of  $V$  with respect to height,  $(h_{j+1}^{i+1})_k$  is an initial guess of the root and  $(h_{j+1}^{i+1})_{k+1}$  is a better approximation of the height. This calculation is iterated until a satisfied approximation is achieved which fulfills the requirement,

$$\left( h_{j+1}^{i+1} \right)_k - (h_{j+1}^{i+1})_{k-1} < (\epsilon \cdot h_{j+1}^{i+1})_k \quad (5.22)$$

Where  $\epsilon$  is a small tolerance number, e.g. five-centimeter variation in water height. Equation 5.22 calculates if the difference between the previous and the current height, if it is smaller than the tolerance, the calculation stops and returns the height. If not, the iteration scheme will stop and return an error. Thereby the water height can be found and the area of the water can be calculated with equation 5.18<sup>4</sup> and thereafter equation 5.10 can be used to calculate the flow of the node.

This calculation is performed for each node in the Preissmann scheme, therefore it is an iterative method of solving the flow for a pipe and in figure 5.7 a flow chart of how these equations are iterated is shown.

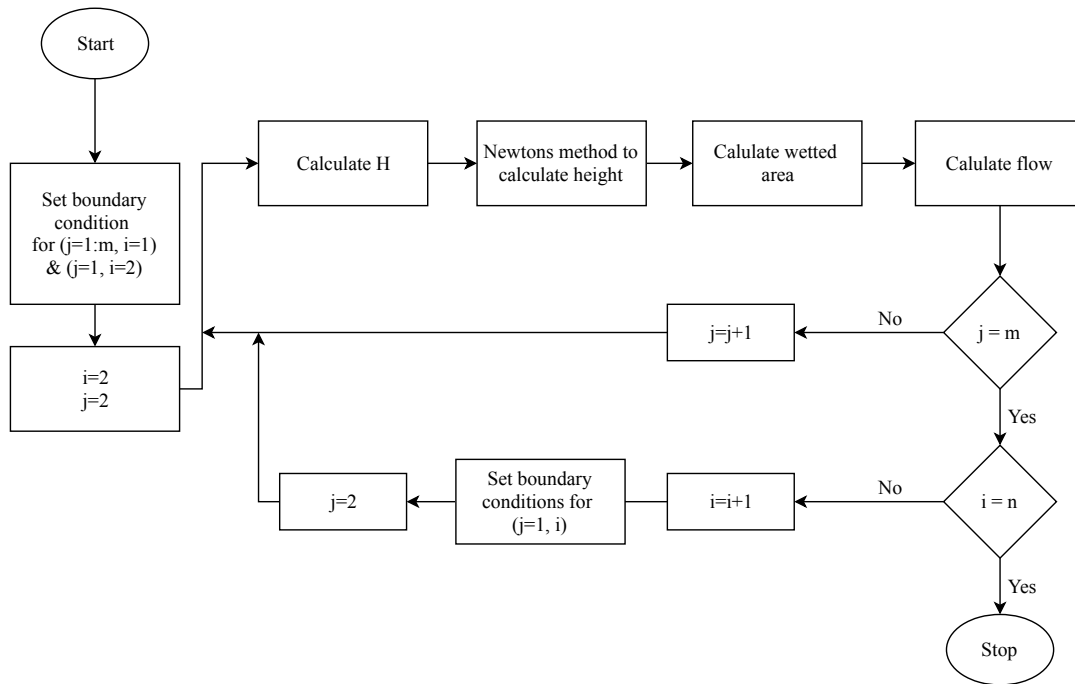


Figure 5.7: Flow chart of the iteration process to calculate the flow in each point.

The iteration scheme starts with setting the boundary conditions for the flow and height as seen in figure 5.6, thereafter  $i$  and  $j$  are countered one up before starting the iteration process. Hereafter the calculation for  $H$ ,  $h$ ,  $A$ , and  $Q$  are conducted iteratively throughout the pipe. Finally, a check is made to investigate if the iteration scheme has been through the whole pipe before it steps one up in time. This iteration process will go on until the  $i = n$ , which means that all the inputs to the pipe have been calculated throughout the pipe.

### 5.2.1 Stability & Precision

Stability is an important parameter to consider when trying to obtain a solution for nonlinear equations. An advantage of the Preissmann scheme is that if the parameter  $\theta$  is chosen  $0.5 \leq \theta \leq 1$ , then stability is unconditionally guaranteed [Cunge et al., 1980]. But guaranteed stability does not necessarily mean precision in the obtained solution. An accurate solution can be found when  $\theta$  is set to 0,5 and appropriate values of  $\Delta t$  and  $\Delta x$  are chosen. For some explicit schemes, utilized for solving the Saint-Venant equations,

<sup>4</sup>FiXme Note: afsnit om de forskellige ligninger til beregning af Areal, Ie,Ib,Qf,Q

the Courant number is often used as a stability criterion. It can also be utilized as an indication of precision of the Preissmann scheme. The Courant number can be obtained by the following equation [Cunge et al., 1980, Szymkiewicz, 2010].

$$C_r = \frac{\sqrt{g \cdot \bar{H}} \cdot \Delta t}{\Delta x} \quad (5.23)$$

Where  $g$  is the gravitational constant,  $\bar{H}$  is average flow height in the pipe,  $\Delta t$  is time step and  $\Delta x$  is distance step. A test clarifying the effect of various Courant numbers is performed on a pipe with the specifications shown in table 5.1.

Length	500 m
Sections	25
$\Delta x$	20 m
Diameter	1.2 m
Ib	3 ‰

Table 5.1: Pipe specifications



In the above pipe a step in inflow is given from 0,35 m<sup>3</sup>/s to 0,7 m<sup>3</sup>/s and for various Courant numbers,  $\Delta t$  is found by equation 5.23. The results can be seen in figure 5.8.

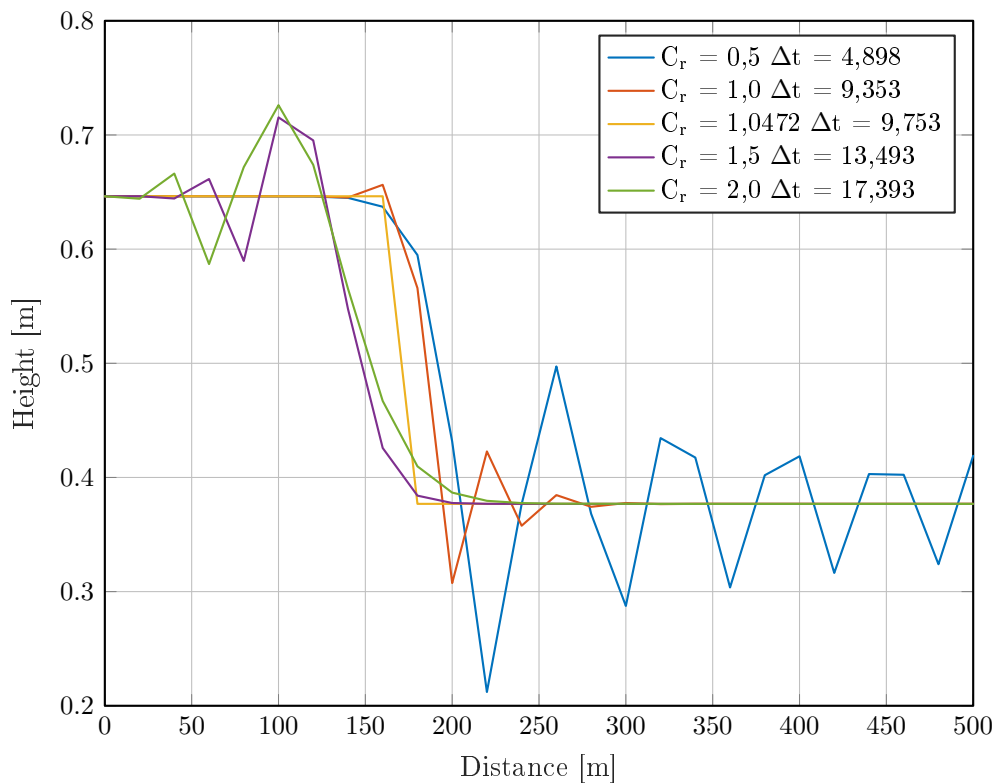


Figure 5.8: Step in inflow given from 0,35 m<sup>3</sup>/s to 0.7 m<sup>3</sup>/s at first iteration in pipe listed in table 5.1. Plot for all tests is made at approximately  $t = 100$  seconds.

It is clear from the results shown in figure 5.8 that considerations when choosing  $\Delta t$  and  $\Delta x$  should be made, as it can have an undesirable effect on the results. Another anomaly

discovered is that the Courant number has to be slightly more than one to obtain a perfect calculation, i.e. no oscillation occurring before or after the wave. An attempt to mitigate the error by minimizing the threshold of the approximation by Newton's method from  $10^{-6}$  to  $10^{-9}$  yielded no change in the obtained result. Further investigations were not made on the subject. The parameter  $\theta$  should not be left out of the equation, as higher values have a dampening effect on the wave. In figure 5.9 various values of  $\theta$  is tested with  $\Delta t$  set to 9,754.

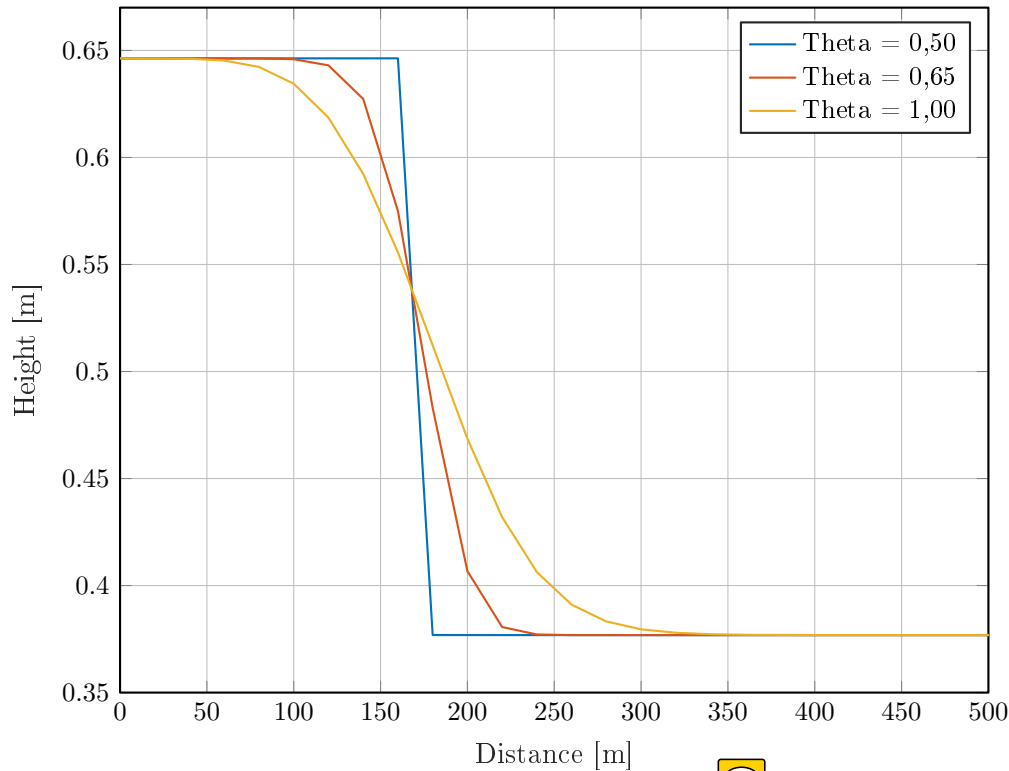


Figure 5.9: Step in inflow given from  $0,35 \text{ m}^3/\text{s}$  to  $0.7 \text{ m}^3/\text{s}$  at first iteration in pipe listed in table 5.1 and 9,753 chosen for  $\Delta t$ . Plot for all tests is made at approximately  $t = 97,5$  seconds.

Due to the choice of simplifying, any natural dampening effect has thereby been disregarded, but as seen in figure 5.9 artificial dampening due to numerical errors can be reintroduced. By choosing a proper value of  $\theta$  the simplification can be somewhat rectified, but at the same time, it can mitigate oscillations, which would be bound to happen when pipes of different diameters, slopes and  $\Delta x$  are adjoined. As a consequence of introducing numerical dampening, waves of low amplitude will be dampened out. But due to the lengths sewer pipes typically are it is assumed to be an insignificant consequence compared to the reduction in oscillation which can be obtained. According to [Cunge et al., 1980] a value of approximately 0.65 is a reasonable choice for  $\theta$ , and for that reason, it will be used for the remaining part of the project. For comparison the test in figure 5.8 is replicated with the chosen value of  $\theta$  and can be seen in figure 5.10.

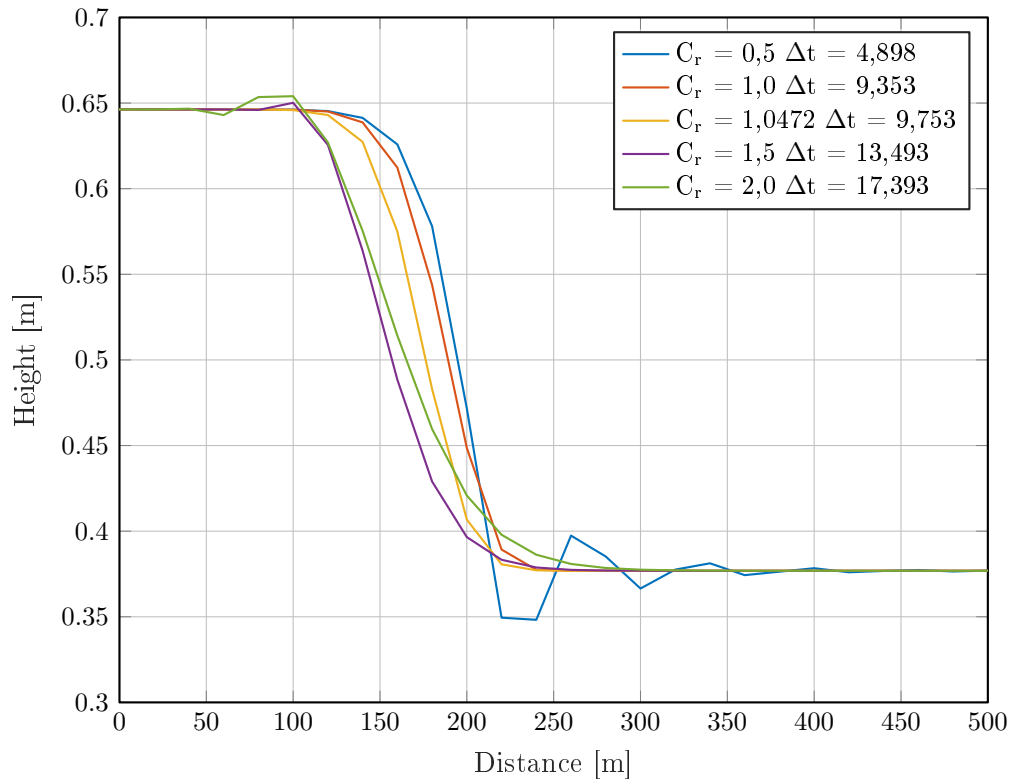


Figure 5.10: Step in inflow given from  $0,35 \text{ m}^3/\text{s}$  to  $0.7 \text{ m}^3/\text{s}$  at first iteration in pipe listed in table 5.1. Plot for all tests is made at approximately  $t = 100$  seconds.

The chosen value of  $\theta$  together with Courant's number as a tuning parameter could be a simple way to obtain values of  $\Delta t$  and  $\Delta x$  for which the simulated results are less affected by distortion caused by numerical errors. To be able to conclude on this as a feasible tuning parameter, further testing would be needed with different pipes with different specifications. Furthermore different steps in both directions of inflow at different initial heights would also be needed to conclude on the uniformity of the Courant number.

### 5.3 Concentrate

Various explicit and implicit schemes exists to solve the transport equation obtained in section 4.2 and shown below.

$$A \cdot \frac{\partial C}{\partial t} + Q \cdot \frac{\partial C}{\partial x} = 0 \quad (5.24)$$

As area and flow is already found by solving the Saint-Venant equations by the Preissmann scheme in section 5.2 a simple discretization of the transport equation suffices. The discretized transport equation is shown below:

$$A(x, t) \cdot \frac{C(x, t) - C(x, t - \Delta t)}{\Delta t} + Q(x, t) \cdot \frac{C(x, t) - C(x - \Delta x, t)}{\Delta x} = 0 \quad (5.25)$$

Isolating for  $C(x,t)$  in steps is shown in the following:

$$\begin{aligned}
A(x,t) \cdot \frac{C(x,t)}{\Delta t} + Q(x,t) \cdot \frac{C(x,t)}{\Delta x} &= A(x,t) \cdot \frac{C(x,t-\Delta t)}{\Delta t} + Q(x,t) \cdot \frac{C(x-\Delta x,t)}{\Delta x} \\
\Downarrow \\
C(x,t) \cdot \left( \frac{A(x,t)}{\Delta t} + \frac{Q(x,t)}{\Delta x} \right) &= A(x,t) \cdot \frac{C(x,t-\Delta t)}{\Delta t} + Q(x,t) \cdot \frac{C(x-\Delta x,t)}{\Delta x} \\
\Downarrow \\
C(x,t) &= \frac{A(x,t) \cdot \frac{C(x,t-\Delta t)}{\Delta t}}{\frac{A(x,t)}{\Delta t} + \frac{Q(x,t)}{\Delta x}} + \frac{Q(x,t) \cdot \frac{C(x-\Delta x,t)}{\Delta x}}{\frac{A(x,t)}{\Delta t} + \frac{Q(x,t)}{\Delta x}} \\
\Downarrow \\
C(x,t) &= \frac{A(x,t) \cdot C(x,t-\Delta t)}{A(x,t) + Q(x,t) \cdot \frac{\Delta t}{\Delta x}} + \frac{Q(x,t) \cdot C(x-\Delta x,t)}{Q(x,t) + A(x,t) \cdot \frac{\Delta x}{\Delta t}}
\end{aligned} \tag{5.26}$$

It can be seen that the concentration can be obtained at current time and place by known values and the solutions of the Saint-Venant equations.

## 5.4 Tank

This section will go through the discretization of equation 4.45 and 4.47. Discretizing the equation expressing change in height the following is obtained:

$$\begin{aligned}
\frac{h(t) - h(t-\Delta t)}{\Delta t} &= \frac{1}{A} (Q_{in}(t) - u(t) \cdot \bar{Q}) \\
\Downarrow \\
h(t) &= \frac{1}{A} (Q_{in}(t) - u(t) \cdot \bar{Q}) \cdot \Delta t + h(t - \Delta t)
\end{aligned} \tag{5.27}$$

Some limitations is needed to be considered during implementation such that outflow can never exceed what is currently in the tank. Solving the equation for change in level of concentrate in the tank explicit, and discretizing it the following is obtained:

$$\begin{aligned}
\frac{C_{tank}(t) - C_{tank}(t-\Delta t)}{\Delta t} &= \frac{1}{A} \left( C_{in}(t) \cdot \frac{Q_{in}(t)}{h(t)} - C_{tank}(t-\Delta t) \cdot \frac{Q_{out}(t)}{h(t)} \right) \\
\Downarrow \\
C_{tank}(t) &= \frac{1}{A} \left( C_{in}(t) \cdot \frac{Q_{in}(t)}{h(t)} - C_{tank}(t-\Delta t) \cdot \frac{Q_{out}(t)}{h(t)} \right) \cdot \Delta t + C_{tank}(t-\Delta t) \\
\Downarrow \\
C_{tank}(t) &= C_{in}(t) \cdot \frac{1}{A} \frac{Q_{in}(t)}{h(t)} \cdot \Delta t - C_{tank}(t-\Delta t) \cdot \frac{1}{A} \frac{Q_{out}(t)}{h(t)} \cdot \Delta t + C_{tank}(t-\Delta t) \\
\Downarrow \\
C_{tank}(t) &= C_{in}(t) \cdot \frac{1}{A} \frac{Q_{in}(t)}{h(t)} \cdot \Delta t - C_{tank}(t-\Delta t) \cdot \left( 1 - \frac{1}{A} \frac{Q_{out}(t)}{h(t)} \cdot \Delta t \right)
\end{aligned} \tag{5.28}$$

To avoid instability or oscillation when the condition  $h(t) < Q_{out} \cdot \Delta t / A$  occurs, the concentrate level in the tank should be set equal to the inflow level. The condition corresponds to the fluid being in the tank at one time step has been emptied out of the tank at the next, meaning that the fluid in the tank at the next time step is new inflow.



## 5.5 Implementation

In this section the implementation of the various parts, which the simulation environment consist of, is explained. The chosen structure, which is described in section 5.1, is seen in figure 5.11.

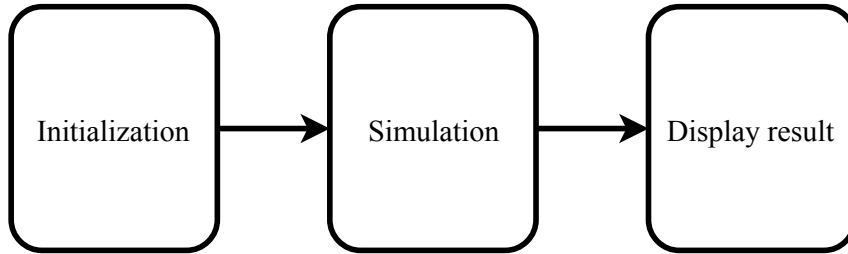


Figure 5.11: Chosen structure of simulation environment.

The first part to be elaborated upon is the initialization.

### Initialization

For the setup procedure of the simulation in list form, the specifications part shown in figure 5.2 needs to be defined. The necessary parameters in the list for both pipe and tank can be seen in table 5.5.

#### 1. Pipe

- Length [m]
- Sections (Number of sections the pipe should be split in to)
- $I_b$  (Slope) [‰]
- $\Delta x = \text{Length} / \text{Sections}$  [m]
- Diameter [meter]
- Theta (parameter used in Preissmann scheme)
- $Q_f$  (maximum flow found by Manning formula, see equation 5.13) [ $\text{m}^3/\text{s}$ ]
- Side/lateral inflow present
- Section location in data

#### 2. Tank

- Size [ $\text{m}^3$ ]
- Height [m]
- Area = Size / Height [ $\text{m}^2$ ]
- Maximum outflow [ $\text{m}^3/\text{s}$ ]
- Section location in data

Some parameters can be found from others and is set to be calculated automatically. Furthermore an item is added to the list which indicates, where the initial and simulated data, for the specific item can be found. To give an overview of the system to be simulated, and to easily be able to locate specific parameters needed during simulation, three structures is returned to the workspace. These are named “pipe\_spec”, “tank\_spec” and “sys\_setup”. The first two structures holds the information shown in table 5.5 respectively. The last one, “sys\_setup”, holds information of the various parts indexed in the order the system is setup and simulated. In figure 5.12 the content of “sys\_setup” is shown for a setup with two pipes and a tank.




Fields	 type	 component	 sections
1	'Pipe'	1	10
2	'Tank'	1	1
3	'Pipe'	1	10
4	'Total'	3	21

Figure 5.12: Display of structure holding system setup information in MATLAB.

An initialization scheme is constructed as per figure 5.3 where adjoint pipes is considered as one part of the system and each tank is an individual part, which means that tanks is used as a separator between parts consisting of pipes. The iterative scheme shown in figure 5.6 requires that boundary conditions is found before the iterative Preissmann scheme can be started. It has been decided by the project group that input should be given in flow, as input in height would be needed to be specific for the pipe inserted, to make the simulation universal. This means that from an initial input flow the corresponding height in the pipes needs to be found. By equation 5.12 flow can be obtained from height, but the equation is transcendental i.e. can not be solved analytically for height. This means that other means is necessary to obtain height from flow. A solution to the problem is that for each pipe, during initialization, a data set from zero to the diameter of the pipe in sufficient steps is created, and from which the corresponding flow is obtained by equation 5.12. From this data a curve fitted polynomial can be obtained by the MATLAB curve fitting toolbox or a lookup table can be constructed. Flow data is generated for 10.000 height steps for a pipe with the parameters shown in table 5.2.

Diameter	0,9 meter
Slope ( $I_b$ )	3 ‰
Length	200 meter
Sections	10

Table 5.2: List of parameters used to obtain data shown in figure 5.13

In figure 5.13 a comparison is shown of the generated data and a ninth order polynomial fitted to the data.

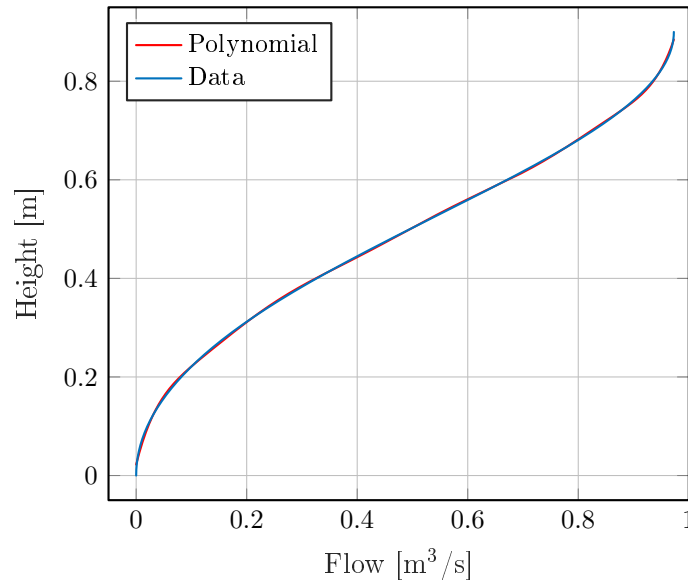


Figure 5.13: Comparison between data obtained by equation 5.12 and the same data curve fitted to a ninth order polynomial.

The two plots in the figure is seemingly identical, but if observed closer the curve fit has what could be described as a low frequency oscillation compared to the plotted data. Furthermore the curve fit does not reach the same end points. This will result in the height at the end points never to be zero or the diameter of the pipe, when no inflow or maximum inflow is present. In figure 5.14 the plot is separated into three for an easier overview.

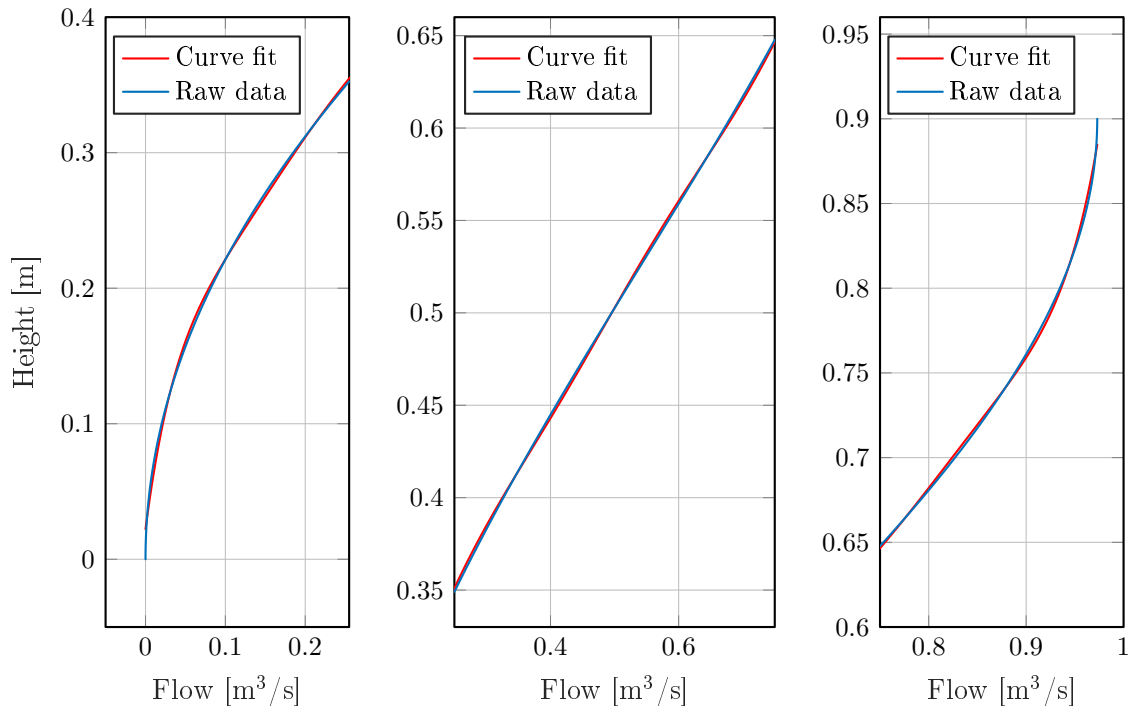


Figure 5.14: Comparison between data obtained by equation 5.12 and the same data curve fitted to a ninth order polynomial.

As discussed in section 5.1, a scheme which brings the system to an initial steady state

could be necessary due to the nonlinear nature of the Saint-Venant equations. A test is performed where two adjoint pipes, with the specifications given in table 5.2, is calculated for different amount of iterations. The boundary condition is found by the fitted polynomial for each pipe respectively. The result of this test is seen in figure 5.15.

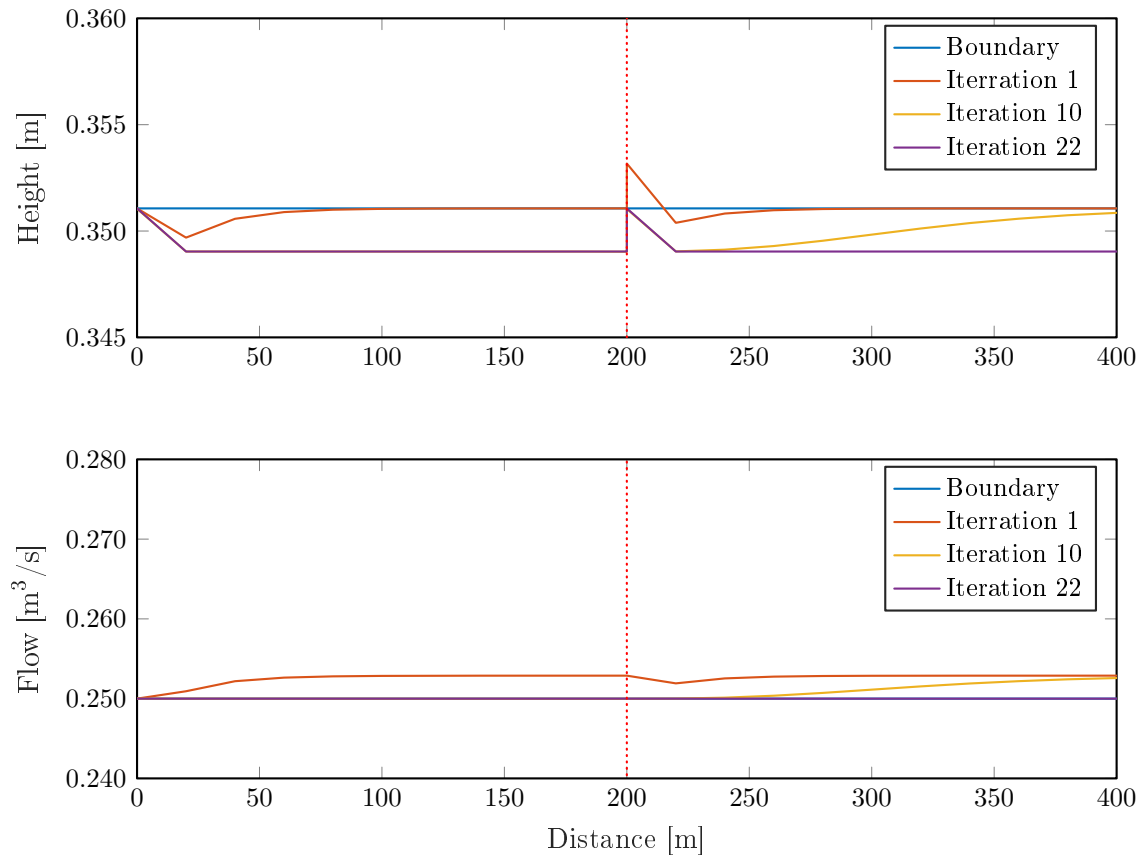


Figure 5.15: Height and flow in two adjoint pipes, with identical specifications given in table 5.2, given boundary conditions found by fitted polynomial, and calculated at various amount of iterations with constant flow input of  $0,25 \text{ m}^3/\text{s}$ . Dotted line indicate intersection between pipes.

In figure 5.15 a maximum of 22 iterations are performed, as the error between the input flow of  $0.25 \text{ m}^3/\text{s}$  desired to be in all sections and the calculated flow in all the sections of the two pipes is less than  $1 \cdot 10^{-7}$  which is a preset condition. Some discrepancy in heights can be seen at the start of both pipes. These two points are the boundary conditions that are found by the fitted polynomial. Even though the anomalies are small they could pose a problem when expanding the simulation with more pipes and different slopes.

In figure 5.16 the specifications of the main line of Fredericia mentioned in section 2, and given by table 2.1 with corrections from table 2.2, is seen.

Fields	length	sections	Dx	lb	d
1	303	15	20.2000	0.0030	0.9000
2	27	1	27	0.0030	1
3	155	8	19.3750	0.0041	1
4	295	14	21.0714	0.0122	0.8000
5	318	15	21.2000	0.0053	0.9000
6	110	5	22	0.0036	0.9000
7	38	2	19	0.0024	1
8	665	30	22.1667	0.0030	1
9	155	7	22.1429	8.0000e-04	1
10	955	40	23.8750	0.0029	1.2000
11	304	15	20.2667	0.0030	1.2000
12	116	5	23.2000	0.0021	1.2000
13	283	12	23.5833	0.0017	1.4000
14	31	1	31	0.0019	1.4000
15	125	6	20.8333	0.0021	1.6000
16	94	4	23.5000	0.0013	1.5000
17	360	15	24	0.0046	1.6000
18	736	30	24.5333	0.0012	1.6000

Figure 5.16: Setup in MATLAB of pipe system from section 2 of main line in Fredericia.

The amount of sections for each pipe is chosen such that each section is close to being 20 meters, with some sections deviating due to pipe length and others deviates on purpose to see if it affects the outcome. In figure 5.17 iterations of the pipe setup shown in figure 5.16 is seen.

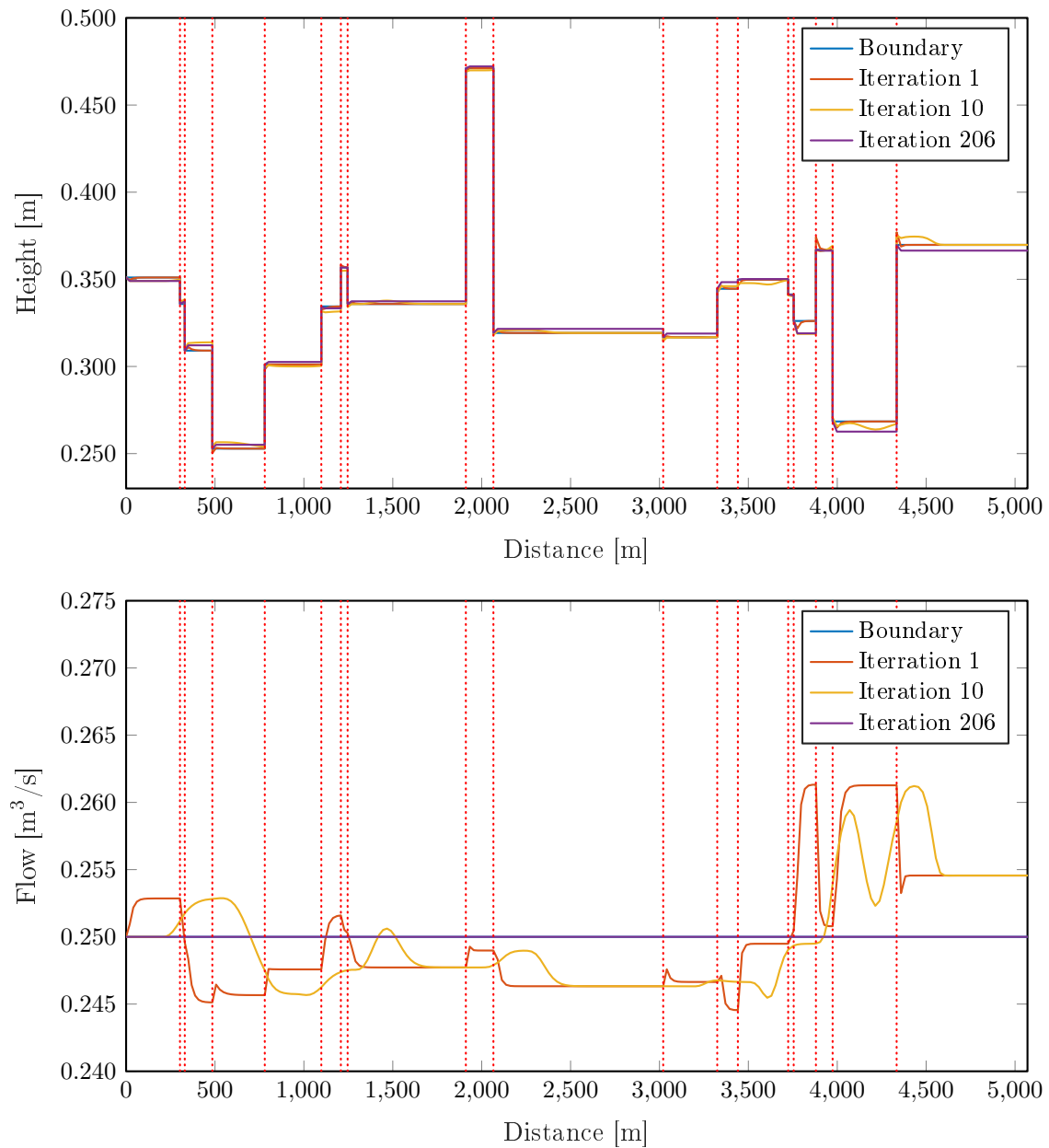


Figure 5.17: Height and flow in pipe setup, given by table 2.1 with corrections from table 2.2, of part of Fredericia where boundary conditions is found by fitted polynomial. Various amount of iterations, with constant flow input of  $0,25 \text{ m}^3/\text{s}$ , is performed. Dotted line indicates pipe intersections.

It is clear that the larger setup increases the undesired behavior seen in figure 5.15. But it can also be seen that the flow can be brought to an acceptable initial state from which the system can start simulating. In figure 5.18 a section of the height plot from figure 5.17 is seen.

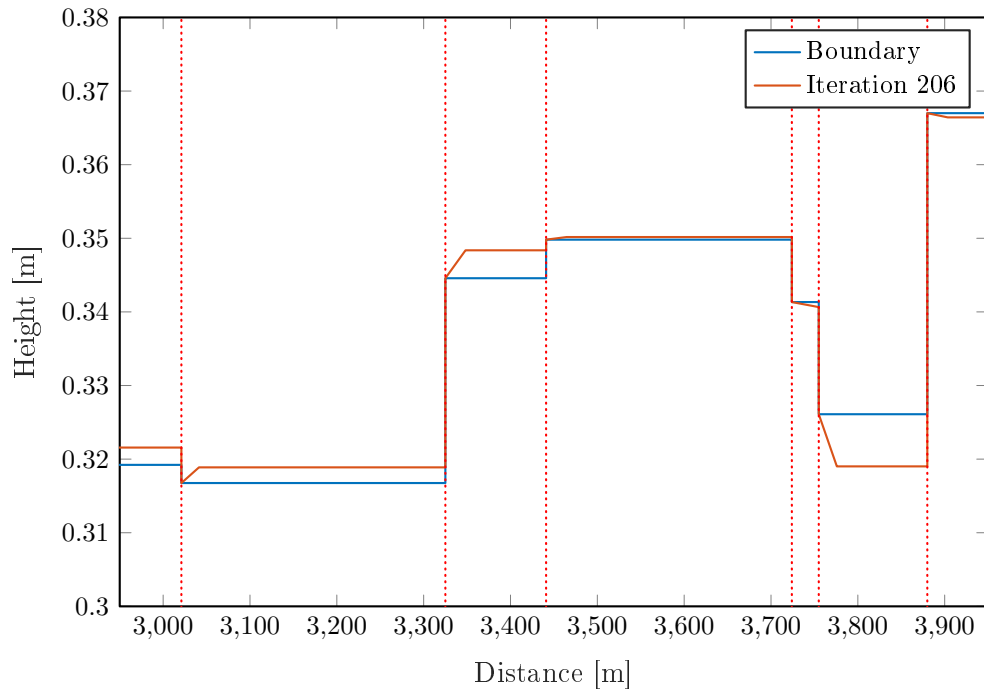


Figure 5.18: Segment of the height plot shown in figure 5.17. Pipe 10 and 16 is seen in part at the left and right side and 11 to 15 in between with a red stippled line separating pipes.

In the above figure, the obtained height from the fitted polynomial is at it worst off by almost a centimeter. But when simulating this offset will only occur in the first section of the pipe. This means that it will be a greater disturbance on short pipes with few sections than larger ones with more sections. An alternative method is attempted to conclude if the deviations of the curve fitted polynomial seen in figure 5.14 is the cause or if there is an unforeseen error in the Preissmann scheme. A lookup table, where the same data used to create the polynomial, is utilized. A simple implementation is made where the index in the vector of flow is found by subtracting the input flow from the vector. The desired index is then found by searching for the lowest absolute value. Finally the resulting height is given as the desired index of the height vector. The chosen scheme for creating the lookup table means that the height will in worst case be rounded to the nearest step. But indexing the flow and height into the chosen 10.000 steps, it is assumed to be an insignificant error, and in worst case the amount of steps can be increased. In figure 5.19 an identical test of the pipe setup of Fredericia is performed at various iterations.

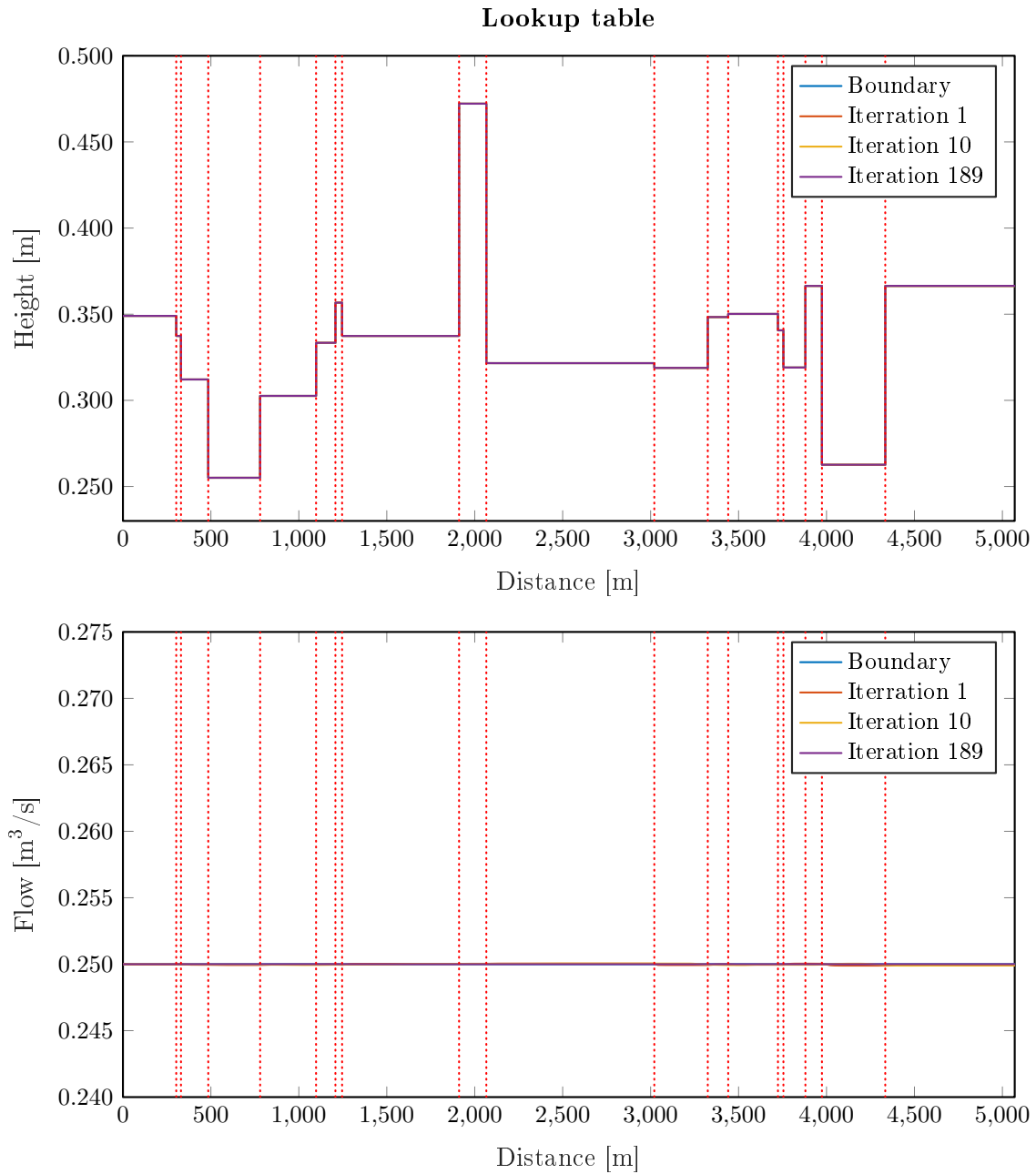


Figure 5.19: Height and flow in pipe setup, given by table 2.1 with corrections from table 2.2, of part of Fredericia where boundary conditions is found by lookup table. Various amount of iterations, with constant flow input of  $0,25 \text{ m}^3/\text{s}$ , is performed. Dotted line indicates pipe intersections.

It is clearly shown that the deviation between the boundary conditions found by the lookup table and the values found by the following iterations of the Preissmann scheme is significantly decreased. Something else to note is that even though the difference seem to be non existent it still required 189 iterations before the flow error were minimized to the same  $1 \cdot 10^{-7}$  as before. For this reason it is decided to implement the scheme which brings the adjoint pipe parts into steady state before simulation starts. A decisive choice is not made at this point whether the curve fitted polynomial or the lookup table should be implemented. The reason for this is that some imprecision can be accepted if reduction in simulation time can be obtained. A test will therefore be performed, in the simulation



part of the implementation, to decided which scheme should be utilized. A flow chart of the initialization scheme, where initial values for the entire setup is found, can be seen in figure 5.20.

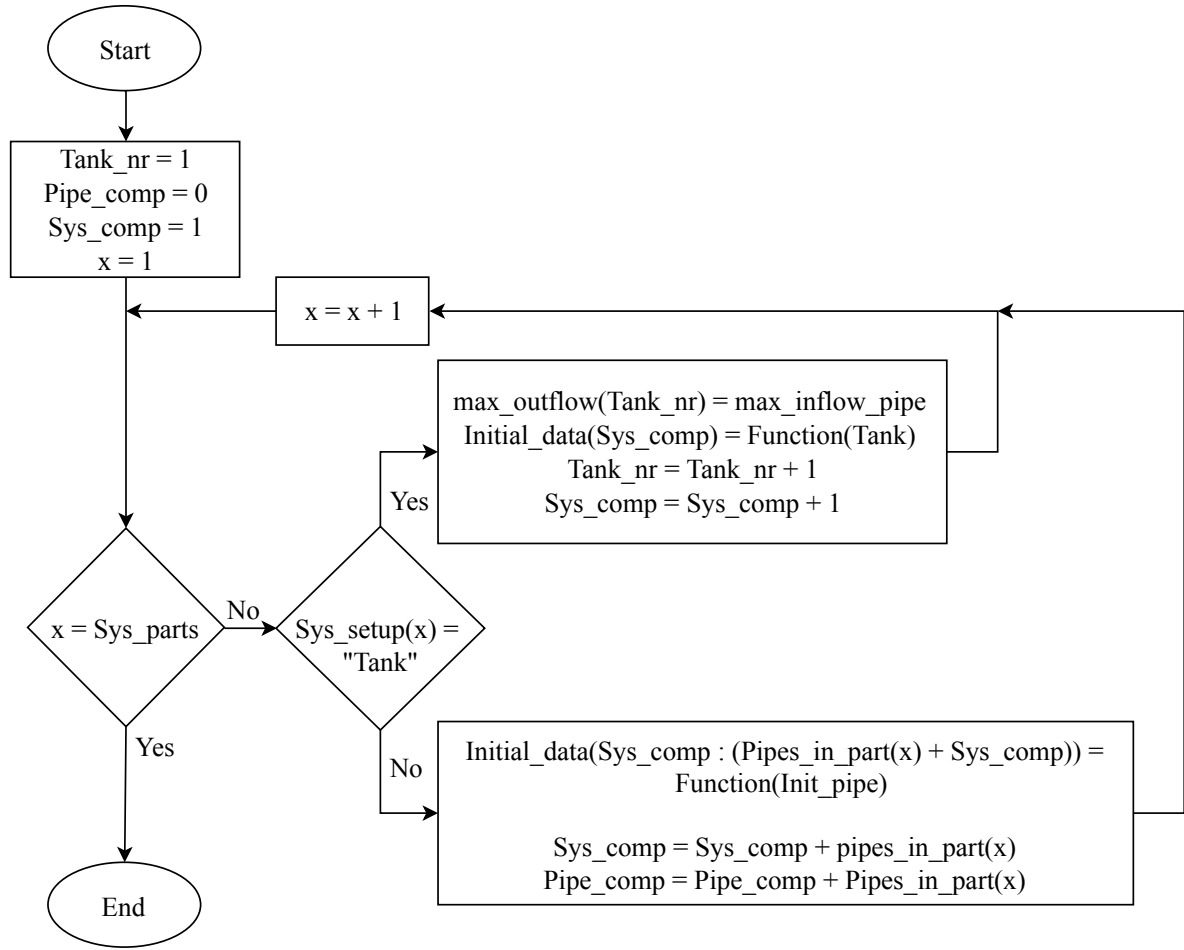


Figure 5.20

Two functions, namely “Tank” and “Init\_pipe”, is used to obtain the initial values for tanks and the boundary conditions, for the pipes, needed to start iterating with the Preissmann scheme. The tank function returns the initial flow, height and the input needed for the pump, such that inflow is equal to outflow in the tank. Due to MPC requiring constraints for the input to the pump in the tank and due to time constraint of the project, a limitation in the simulation is made. The limitation refers to tanks not being able to be the end point of the entire system setup. The reason for this is that a uniform control input of zero to one for all pumps, to ease constraint setup when utilizing MPC, is obtained. The following parameters is set in the tank function:

- $Q_{in} = Q_{initial} [m^3/s]$
- $Q_{out} = Q_{in} [m^3/s]$
- $u_{initial} = Q_{in}/Q_{max-outflow} [\cdot]$
- $h = h_{initial} [m]$
- $C = C_{initial} [g/m^3]$

Where  $Q$  is flow,  $u$  is pump input,  $h$  is height and  $C$  is concentrate. The pipe function is given initial flow, component number from the system setup list in figure 5.12, the corresponding pipe specifications to the amount of pipes indicated by the system setup

list and an error value. The error value is the accepted error between desired flow and the flow obtained by iterating with the Preissmann scheme, which means that when the error is less than the error value the system is in the desired steady state. A flowchart of the pipe function can be seen in figure 5.21.

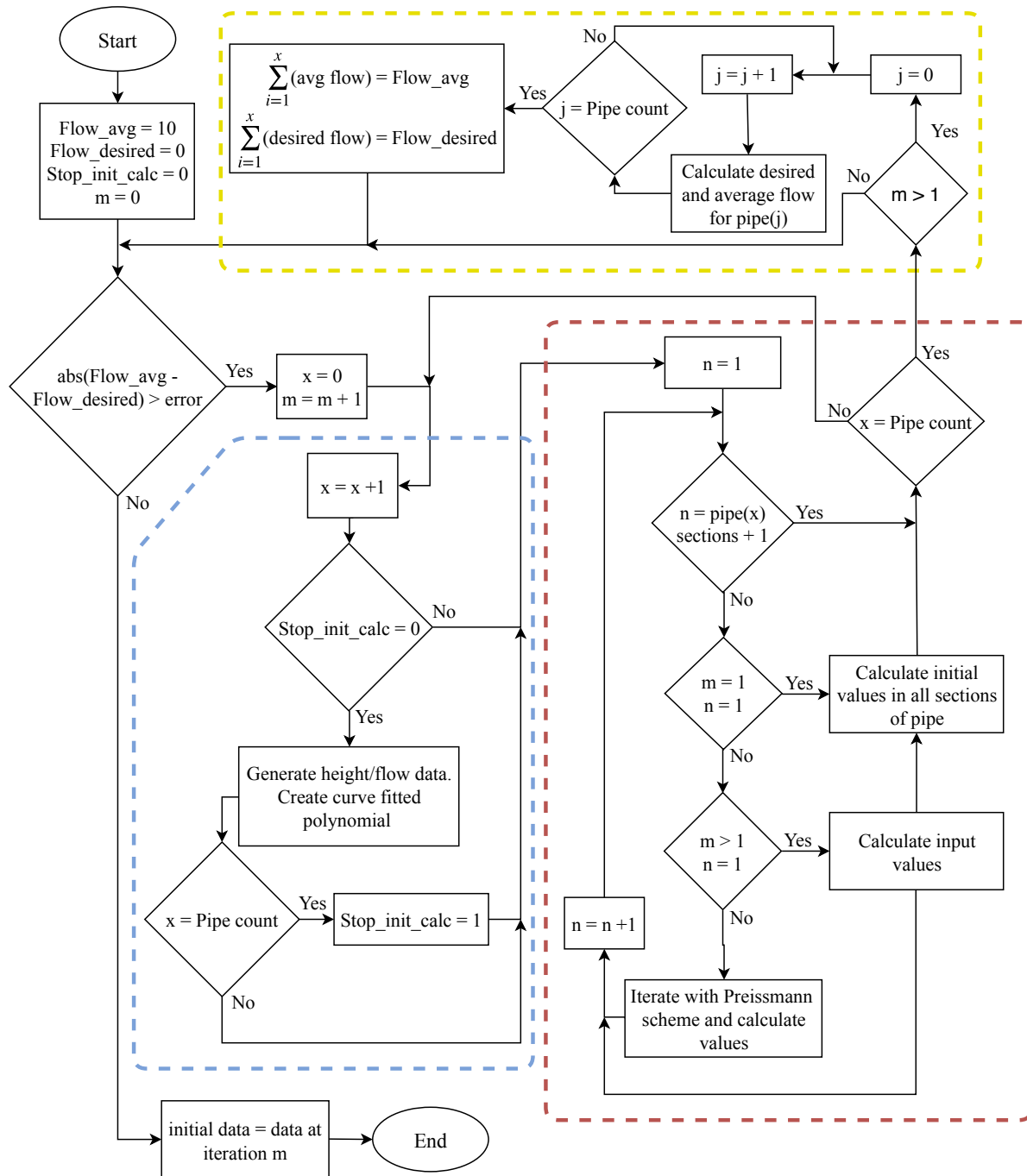


Figure 5.21: Flow chart of pipe initializing function where the blue box is setup of curve fitted polynomial for each pipe, red box is computation of data in pipes and the yellow box calculates desired and average flow for error stop condition. Furthermore “x” indicates a specific pipe, “m” is time step and “n” indicates section in pipe.

The pipe initialization function can be separated into three parts as indicated by the blue, red and yellow stippled boxes. In the blue stippled box the generated data, which can

also be used for a lookup table, is used to create the curve fitted polynomial. When data are generated for all the pipes given to the function, a flag is set such that unnecessary calculations is not performed further on. In the red stippled box the calculations of the height and concentrate is performed. In the first time iteration “ $m = 1$ ” the initial boundary condition is set for all sections of pipe number “ $x$ ”. This corresponds to the  $i$ -th row of circles shown in figure 5.6. Furthermore when iterating through the pipes the corresponding pipe specifications is checked to decide if the pipe has side inflow. If it is present then the inflow into the pipe is a simple summation of input flow and side inflow. The concentrate input in the case of side inflow is found by equation 4.39. For the next pipe the input is then set to be the output of the previous pipe plus eventual side inflow. At the following time iterations the input boundary condition is found at section “ $n = 1$ ”. The Preissmann scheme is then utilized to find the height, and the concentrate is calculated, for the remaining pipe sections. This is done for all the pipes given to the function. Lastly in the yellow stippled box the desired and average flow values in the pipe or pipes is calculated. At the first time iteration “ $m = 1$ ” the values of “Flow\_avg” and “Flow\_desired” are not updated. The reason is that the initial flow is inserted as the flow in all sections of all the pipes, which would give an error which are zero and stop the initialization loop. In the following iterations, disregarding the boundary condition which are still calculated, the flow is found from height which can vary for some iterations as seen in figure 5.17. When the flow in all sections of all the pipes has an error which is sufficiently small from the desired flow the iterations is stopped. The flow, height and concentrate data from the latest iteration is returned and the simulation has a steady state point from where it can start. The amount of iterations and the accuracy of the steady state of course depends on the chosen error value. In figure 5.22, the result of various tested error values can be seen.

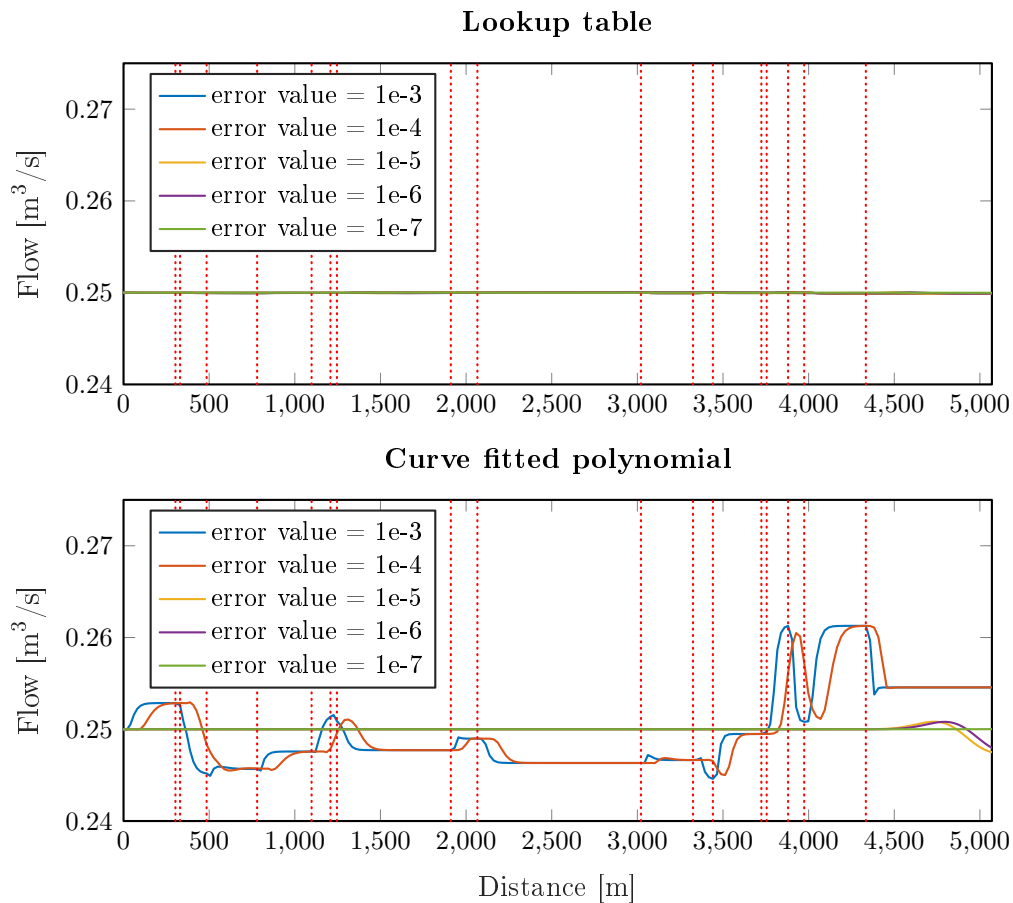


Figure 5.22: Various values of error value is tested with lookup table and curve fitted polynomial tested on pipe setup shown in figure 5.16 of Fredericia.

If the curve fitted polynomial is utilized to obtain boundary conditions then an error value below  $1 \cdot 10^{-6}$  is preferable. But for setup's with more pipes it can be necessary to lower this value even further. The lookup table on the other hand is due to its better precision not considerably affected in the first place, though some precision is obtained by lowering the error value. As the tested error value is performed on a simple test, and final decision has not been made on which scheme to utilize an error value of  $1 \cdot 10^{-9}$  has been decided upon. The reason being the results shown in figure 5.16, and that various setups where more pipes with different initial flows might yield a worse result.

## Simulation

Having obtained initial data, for which iterating with the Presissmann scheme can begin, the next part to be implemented is the simulation of the initialized setup. To ease eventual future expansion of the simulation a simple design, where individual parts is simulated one at a time, is chosen. This is realized by nesting functions in two steps from the main simulation module which is seen in figure 5.23.

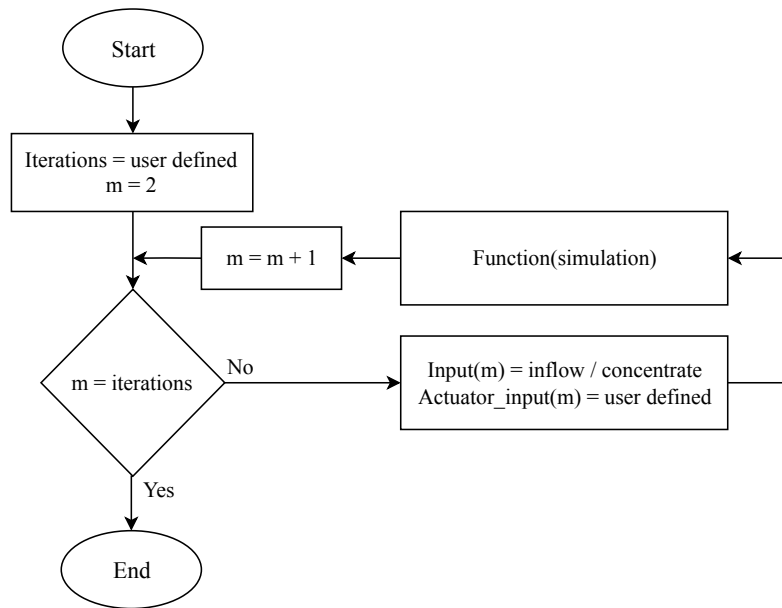


Figure 5.23: Main simulation loop.

The amount of iterations desired to simulate the system for is chosen. As the system is already initialized and MATLAB does not have zero indexing the system is initialized at  $m$  equal to one. Therefore the first iteration is performed at  $m$  equal to two and proceeds until the chosen amount of iterations is reached. The function “simulation” is given flow and concentrate input, system specification (Sys\_setup), pipe specification (pipe\_spec). If a tank is present, actuator input and tank specification (tank\_spec) is also needed. In figure 5.24 the simulation function is seen.

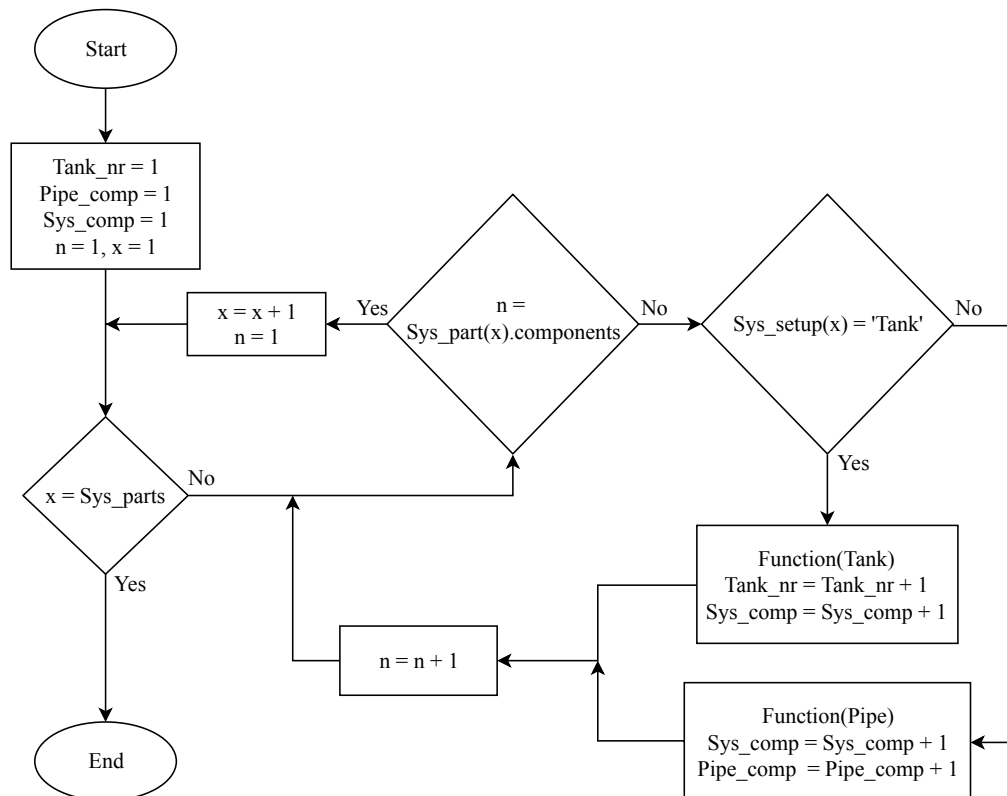


Figure 5.24: Simulation function.

The simulation function is given input of flow, concentrate and actuator for pipes and tanks respectively. Furthermore specifications of system, pipe and tank is given. The basic functionality is an outer and an inner loop. The outer loop iterates through the parts in “Sys\_setup” and the inner loop iterates through the components each part consists of. Iterating through the parts, checking whether the component is a tank or pipe, the respective function is called. The tank function is given tank specifications, current iteration value, flow and actuator input. Furthermore the index number of the tank is given. The iteration value “m” is in the function used to index when logging data. Output flow is found by equation 4.44. The value of  $\bar{Q}$  is set to be the maximum inflow of the adjoining pipe.

$$Q_{out} = u_{pump} \cdot Q_{max\_outflow} \quad (5.29)$$

Where maximum outflow is equal to maximum inflow of the down stream adjoining pipe. Doing so makes it possible to always have an actuator input which ranges from zero to one, which helps minimizing complexity when implementing control on large scale setups where several tanks of various sizes could be present. In figure 5.25 a flow chart of the tank function can be seen.

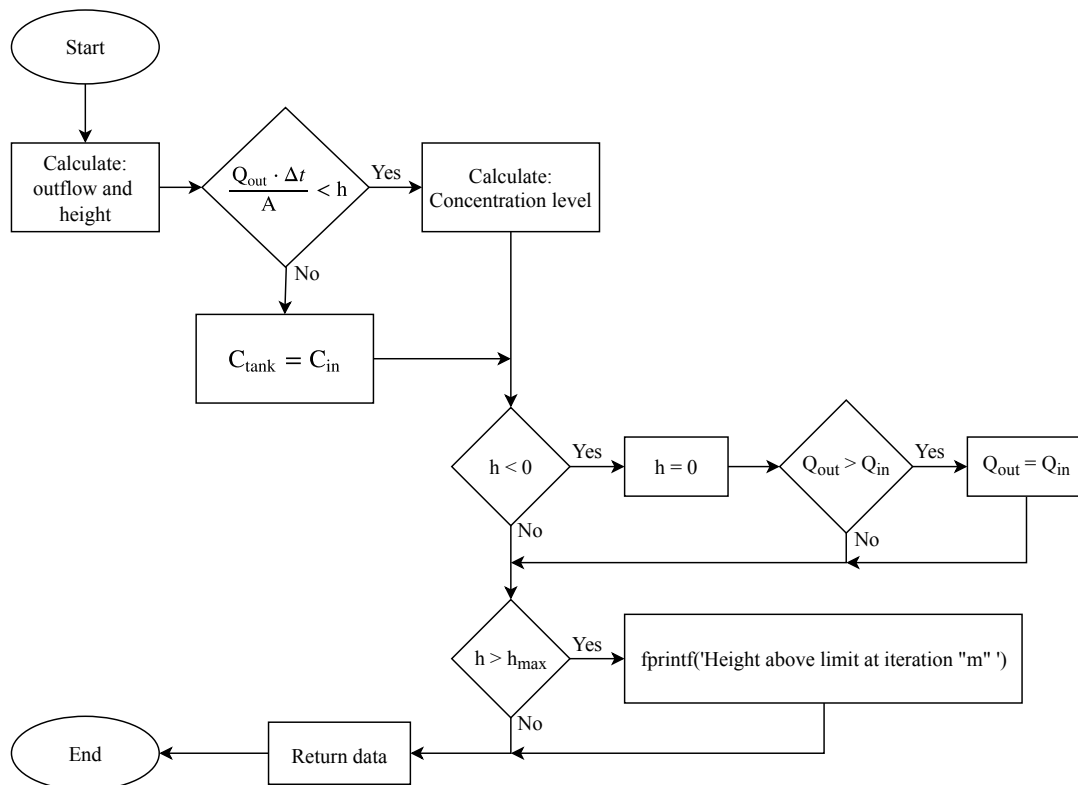


Figure 5.25: Tank function.

The tank function is given inflow, actuator input, “Tank\_nr”, tank specification, iteration value “m”, part index “x” and data stored at index “Sys\_comp”. Iteration and part index is used to fetch previous values of height and concentrate level, used in calculation of new values. Furthermore the value of “Tank\_nr” is used as index in “Tank\_spec”. First when the height and flow has been calculated, the condition mentioned in section 5.4 is checked to avoid oscillating concentrate level in the tank. Secondly, as seen in the flowchart, if the calculated height gives a result below zero the height is set to zero and maximum outflow is set equal to inflow. In the case of concentrate level, if height is less than  $Q_{out} \cdot \Delta t / A$  then the level in the tank is set equal to the inflow level. If the fluid level exceed the

height of the tank a message is printed to the command windows which also contains at which iteration the overflow occurred. Instead of placing a hard limit on tank height, knowing when a tank overflow occurs, and how much the dimension of the tank needs to be adjusted, would be more valuable. In figure 5.26 the pipe function can be seen.

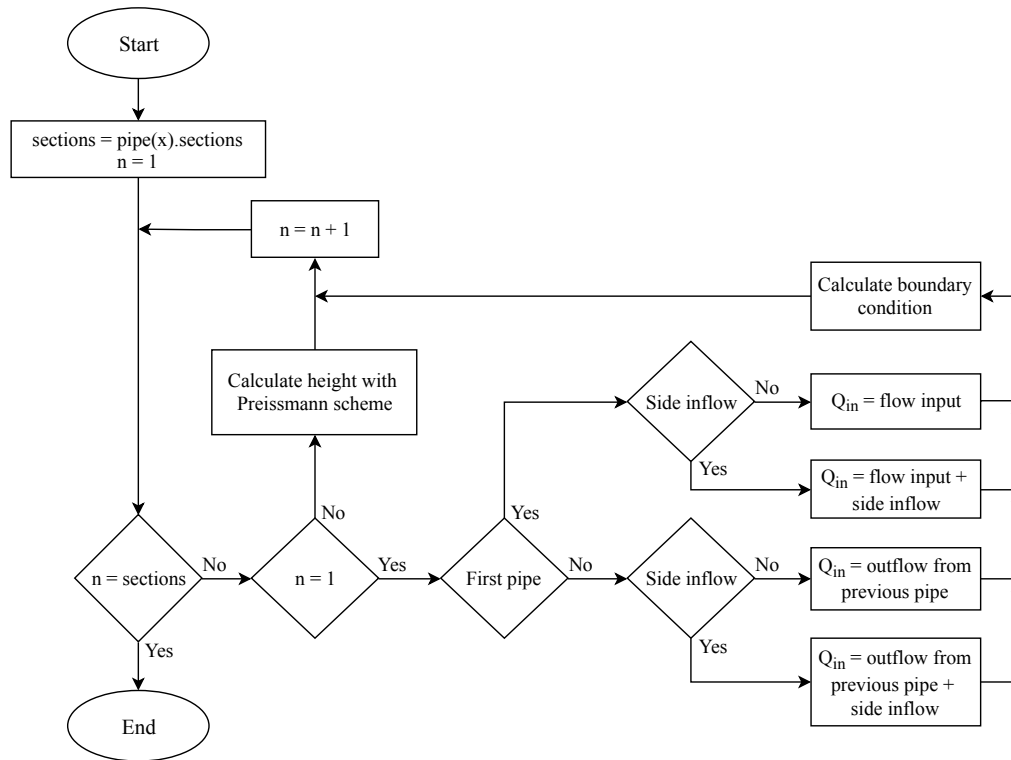


Figure 5.26: Pipe function.

The function is given inflow, pipe\_comp, pipe specifications, iteration value “m”, part index “x” and data stored at index “Sys\_comp”. Once again iteration and part index is used to fetch previous values of height and concentrate level, used in calculation of new values. The value of pipe\_comp is used as index in “pipe\_spec”. The functionality of the function is to iterate through the sections which the pipe consists of. At the first section,  $n = 1$ , it is determined if the pipe is the first in the specific part. Afterwards it is checked if side inflow is present. If the pipe is the first then inflow needs to be given, otherwise the flow out of the previous pipe is set as inflow. When inflow is obtained height can be found from either curve fitted polynomial or lookup table as mentioned in the initialization part of the implementation. For the remaining sections in the pipe the the height is found by the Preissmann scheme. Lastly data is returned to the simulation function. To decided upon which of the, curve fitted polynomial or lookup table, methods should be implemented a test with the pipe setup shown in figure 5.16 is performed for various iterations. Furthermore two values of  $\Delta t$  is tested. A sinusoidal input is given for all tests to increase the computational power needed to solve the Preissmann scheme. The input can be seen in figure 5.27.

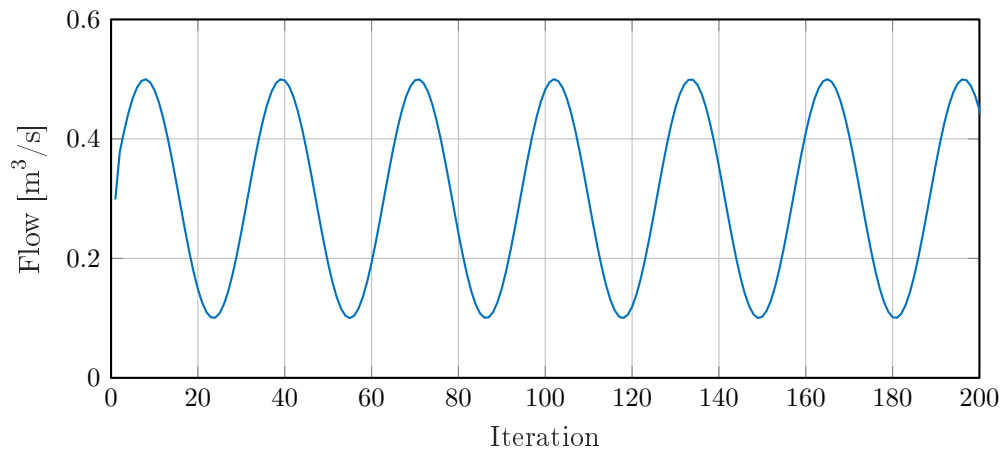


Figure 5.27: Input flow for comparison test of lookup table and curve fitted polynomial.

The results of the computational tests can be seen in table 5.3, 5.4 and 5.5.

$\Delta t$	15 s	20 s
lookup table	4,600 s	4,978 s
Curve fitted polynomial	5,554 s	5,893 s
Difference	20.722 %	18.393 %

Table 5.3: Computation time of 400 iterations

$\Delta t$	15 s	20 s
lookup table	10,073 s	10,574 s
Curve fitted polynomial	11,868 s	11,859 s
Difference	17.817 %	12.153 %

Table 5.4: Computation time of 800 iterations

$\Delta t$	15 s	20 s
lookup table	30,380 s	30,776 s
Curve fitted polynomial	33,247 s	34,194 s
Difference	9.437 %	11.105 %

Table 5.5: Computation time of 2000 iterations

The results are obtained by using the MATLAB function “tic-toc” on the main simulation loop shown in figure 5.23. Clearly the lookup table is preferable both in accuracy and computational speed. For this reason it is implemented as the solution to obtain fluid height border condition from inflow of the pipe.

## Result





## 6.1 Linearization

To be able to obtain a MPC control algorithm the system needs to be transform into state space form. In this section it will be elaborated how this is obtained.

The continuity equation from section 4.1 and the equation to describe the flow in a pipe knowing the height is used:

$$\frac{\partial A(x, t)}{\partial t} + \frac{\partial Q(x, t)}{\partial x} = 0 \quad (6.1)$$

$$Q = f(h) = \left( 0.46 - 0.5 \cdot \cos\left(\pi \frac{h}{d}\right) + 0.04 \cdot \cos\left(2\pi \frac{h}{d}\right) \right) Q_f \quad (6.2)$$

To be able to implement control in this project, some form of measurement is needed from the pipe. Because it is needed to get information about the condition in the pipe to be able to control it. Therefore it is assumed that it is possible to measure the height of the wastewater in the pipe.

1

In the state space model it is desired to have the states as heights of the wastewater. Therefore, equation 6.1, is expanded to the following:

$$\frac{\partial A(h)}{\partial h} \frac{\partial h(x, t)}{\partial t} + \frac{\partial Q(h)}{\partial h} \frac{\partial h(x, t)}{\partial x} = 0 \quad (6.3)$$

By applying the Preissmann scheme from section 5.2 equation 5.5 and equation 5.6 on the partial derivate of h in terms of time and position, the following is obtained:

$$\begin{aligned} & \frac{\partial A(x, t)}{\partial h} \left( \frac{1}{2} \frac{h_{j+1}^{i+1} - h_{j+1}^i}{\Delta t} + \frac{1}{2} \frac{h_j^{i+1} - h_j^i}{\Delta t} \right) + \\ & \frac{\partial Q(x, t)}{\partial h} \left( \theta \frac{h_{j+1}^{i+1} - h_j^{i+1}}{\Delta x} + (1 - \theta) \frac{h_{j+1}^i - h_j^i}{\Delta x} \right) = 0 \end{aligned} \quad (6.4)$$

---

<sup>1</sup>Fixme Note: Ved ikke om det skal stå her (det skal det vist ikke). Somewhere in the report you need to put some words on how you get information above  $x(k|k)$ . If you should measure it, it means that you should have level measurements along the pipe which is a bit realistic. Therefore, ideas to avoid this must be described somewhere (though you don't need to build a method.)

Where the derivate of Q given h can be found by taking the derivate of equation 6.2 with respect to h, and the the derivate of A can be found by taking the derivate of equation the following equation with the respect to h:

$$A = \frac{d^2}{4} \cdot \text{acos} \left( \frac{\frac{d}{2} - h}{\frac{d}{2}} \right) - \sqrt{h \cdot (d - h)} \cdot \left( \frac{d}{2} - h \right) \quad (6.5)$$

Equation 6.4 can be written on matrix form as:

$$\begin{aligned} & \left[ \underbrace{\frac{1}{2\Delta t} \frac{\partial A}{\partial h} - \frac{\theta}{\Delta x} \frac{\partial Q}{\partial h}}_a \quad \underbrace{\frac{1}{2\Delta t} \frac{\partial A}{\partial h} + \frac{\theta}{\Delta x} \frac{\partial Q}{\partial h}}_b \right] \begin{bmatrix} h_{j+1}^{i+1} \\ h_{j+1}^j \end{bmatrix} = \\ & - \left[ \underbrace{\frac{-1}{2\Delta t} \frac{\partial A}{\partial h} - \frac{(1-\theta)}{\Delta x} \frac{\partial Q}{\partial h}}_c \quad \underbrace{\frac{-1}{2\Delta t} \frac{\partial A}{\partial h} + \frac{\theta}{\Delta x} \frac{\partial Q}{\partial h}}_d \right] \begin{bmatrix} h_j^i \\ h_{j+1}^i \end{bmatrix} \end{aligned} \quad (6.6)$$

This equation can be written on state space form, where the heights are the states of the state space system and a, b, c, and d are the parameters in the system matrix and the input vector. As the equations are discretized a discretized state space model is needed:

$$x(k+1) = Ax(k) + Bu(k) + B_d d \quad (6.7)$$

Where A is the system matrix, x is the state of the system, B is the input vector, u is the input,  $B_d$  is the input disturbance vector and d is the disturbance. By utilizing equation 6.6 the following can be written:

$$\begin{aligned} & \underbrace{\begin{bmatrix} 1 & 0 & 0 & \cdots & 0 \\ 0 & b_1 & 0 & \cdots & 0 \\ 0 & a_1 & b_2 & \cdots & \vdots \\ \vdots & \vdots & \ddots & \ddots & 0 \\ 0 & 0 & 0 & a_{m-1} & b_m \end{bmatrix}}_{\xi} \underbrace{\begin{bmatrix} h_0^{i+1} \\ h_1^{i+1} \\ h_2^{i+1} \\ \vdots \\ h_m^{i+1} \end{bmatrix}}_{x(k+1)} = \underbrace{\begin{bmatrix} 0 & 0 & 0 & \cdots & 0 \\ c_0 & d_1 & 0 & \cdots & 0 \\ 0 & c_1 & d_2 & \cdots & 0 \\ \vdots & \vdots & \ddots & \ddots & \vdots \\ 0 & 0 & 0 & c_{m-1} & d_m \end{bmatrix}}_A \underbrace{\begin{bmatrix} h_0^i \\ h_1^i \\ h_2^i \\ \vdots \\ h_m^i \end{bmatrix}}_{x(k)} + \\ & \underbrace{\begin{bmatrix} 1 \\ -a_0 \\ 0 \\ \vdots \\ 0 \end{bmatrix}}_B h_0^{i+1} + \underbrace{\begin{bmatrix} \frac{dh}{dQ} \\ 0 \\ 0 \\ \vdots \\ 0 \end{bmatrix}}_{B_d} d_0^{i+1} \end{aligned} \quad (6.8)$$

<sup>2</sup> Where m denotes the pipe sections. To obtain a state space form  $\xi$  needs to be inversed, thereby obtaining the following equation:

$$x(k+1) = \xi^{-1}(Ax(k) + Bu(k) + B_d d(k)) \quad (6.9)$$

---

<sup>2</sup>FiXme Note: Subscript til forstyrrelsen, hvad skal der står der?

A verification has been conducted to investigate if the linear model creates a similar response as the nonlinear model for small signal values. Therefore, a test has been conducted on the sewer network setup where the specification for the pipes are shown in figure 5.16 and the specification for the tank placed after the first pipe is seen in 6.1

Component number	2
Size [ $m^3$ ]	90
Height [m]	10
Area [ $m^2$ ]	9

Table 6.1: The tank specification for comparing the nonlinear model with the linear model.

Furthermore in the table 6.2 the system setup is shown.

Type	Component	Sections
Pipe	1	35
Tank	1	1
Pipe	18	227
Total	20	263

Table 6.2: The system setup.

It can be seen that the setup consist of 19 pipes and one tank. The input to the pipes after tank is a sinus wave as is shown in figure 6.1.

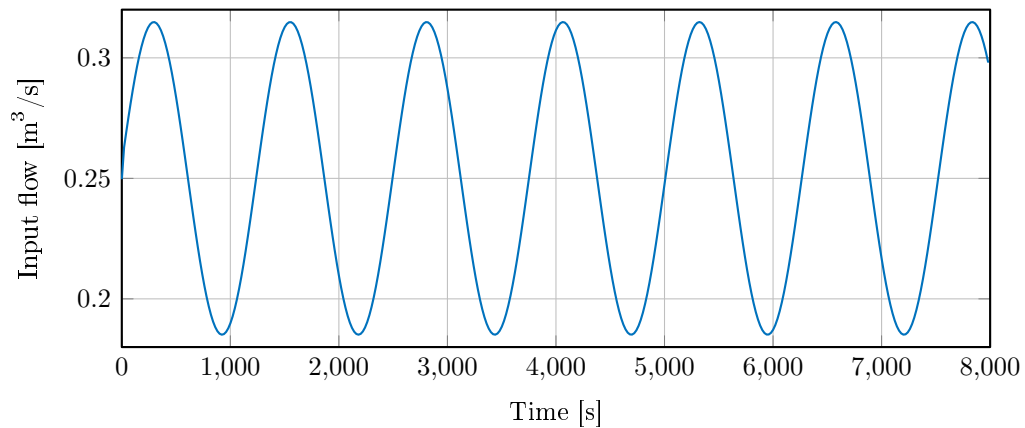


Figure 6.1: Input flow for the simulation.

In figure 6.2 a comparison of the output nonlinear model and the linear model is shown.

<sup>3</sup>FiXme Note: Noget om, hvordan tanken er indsat

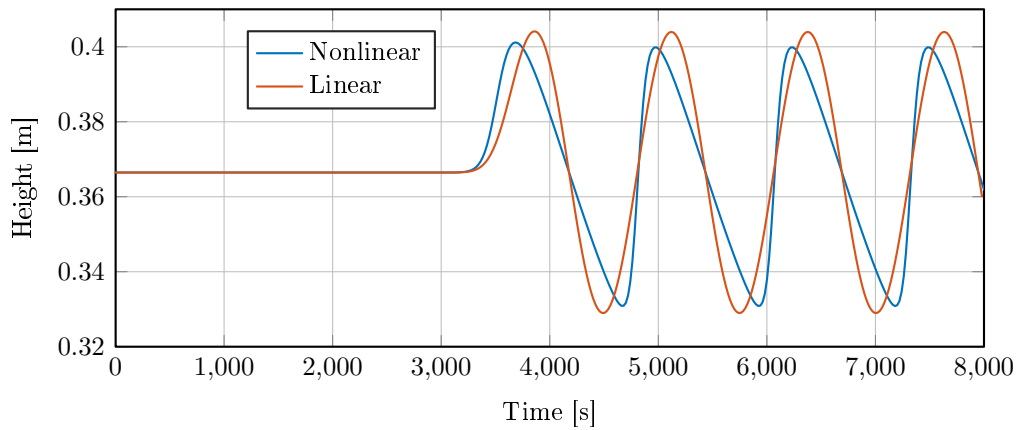


Figure 6.2: Output height for the linear and Preissmann scheme simulation.

The fluctuations of the response of the nonlinear and linear are not identical as the top and bottom of the curves peaks at different times. However, the linear output looks very similar in phase as the input signal shown in figure 6.1 where the nonlinear has a faster response up going, and a slower one down going. It should be noted, that each time the response for both the models crosses the linearization point, they cross the same point. Hence it can be verified that the two models follows a similar pattern. It can be concluded that the plot of the nonlinear and linear responses are very similar, and therefore the linear model will be used to construct the MPC controller.

## 6.2 Model predictive control

In this section, the design of the controller is elaborated. First the control problem thereafter Model predictive controller (MPC) is elaborated followed by the design of the MPC controller and ending with the implementation and results from the simulation.

The simulation covered in chapter 5 is to be controlled with respect to the problems elaborated in section 1.4 and stated here.

1. Flow variations due to large industries and natural phenomenon
2. Concentration variations due to large industries and natural phenomenon
  - a) Chloride variations
  - b) Phosphor variations
  - c) Nitrogen variations
  - d) Organic matter variations

From the problem statement, it is stated that flow and concentration variations must be kept to a minimum without causing any overflow in the sewer. To achieve this, tanks are used. These are placed in the sewer network to find locations where they are able to hold back disturbance that will otherwise cause flow and concentration variations into the WWTP. However, the output of these tanks must be controlled in a way where overflow in the tank is prohibited. Therefore the controller must control the output of these tanks in an optimal manner to keep the input variations to the WWTP at a minimum and still be controlled according to some constraints.

To obtain such an optimal behavior MPC is chosen as stated in section 1.4. MPC solves a optimizations problem at each time instant,  $k$ , where the main point is to compute a control vector,  $u$  that is feed to the system.

An MPC algorithm consists of:

**Cost function** or control objective,  $\mathcal{J}$ , is an algorithm measuring e.g. the difference between future outputs and a reference while at the same time instant recognizing that any control action is costly for the system. Therefore the price is measured in the cost function over the prediction horizon,  $H_p$ . This function is therefore minimized with the respect to the future control vector to keep the cost minimized. Furthermore, only the first control input from the vector is used in each time instant thus this optimization is process is calculated at each time step where a new control input is calculated [Ruscio, 2001].

**Constraints** is unique advantages of MPC. Constraints can be applied to the process variables e.g. constraints can be set on the states of the system not allowing them to go below a certain value or above. Constraints are usually written as inequality constraint  $Ax \leq b$  where the constraint is subject to the optimization problem [Ruscio, 2001].

**Prediction model** is a model that is able to predict future system behavior. The model describes the input output behavior of the system. The model will mainly be used to predict the output of the system over the prediction horizon [Ruscio, 2001].

For MPC to optimize the system a cost function must be written to penalize variations of the flow output  $Q(k+i|k)$  and the concentration output  $C(k+i|k)$ . Where  $k$  defines the prediction time and  $i$  is a value going from 1 to  $H_p$ . The cost function for flow and concentration is:

$$\begin{aligned} \mathcal{J} = & \sum_{i=1}^{H_p-1} \|Q(k+i|k)C_1(k+i|k) - Q(k+i-1|k)C_1(k+i-1|k)\|_{\mathcal{Q}(i)}^2 \\ & + \sum_{i=1}^{H_p-1} \|Q(k+i|k)C_2(k+i|k) - Q(k+i-1|k)C_2(k+i-1|k)\|_{\mathcal{Q}(i)}^2 \\ & + \sum_{i=1}^{H_p-1} \|Q(k+i|k)C_3(k+i|k) - Q(k+i-1|k)C_3(k+i-1|k)\|_{\mathcal{Q}(i)}^2 \\ & + \sum_{i=1}^{H_p-1} \|Q(k+i|k)C_4(k+i|k) - Q(k+i-1|k)C_4(k+i-1|k)\|_{\mathcal{Q}(i)}^2 \\ & + \sum_{i=1}^{H_p-1} \|Q(k+i|k) - Q(k+i-1|k)\|_{\mathcal{Q}(i)}^2 \end{aligned} \quad (6.10)$$

<sup>4</sup> Where  $\mathcal{J}$  is the cost function that needs to be minimized,  $Q$  is the flow,  $C$  is the concentration and  $\mathcal{Q}$  is a weighting parameter. The concentrations  $C_1, C_2, C_3$  and  $C_4$  are respectively chloride, phosphor nitrogen and organic matter levels in the wastewater. However, It has been chosen to only look at flow variation in the simulation and thereby excluding concentrations from the cost function and retention time in the tank<sup>5</sup>. This has been done to limit the control problem and ease the computation, to begin with. Thereby

<sup>4</sup>FiXme Note: skal skrives så alle 4 koncentrationer er med, samt en for flow og et eller andet sted afgrænsning for liggetid i tank

<sup>5</sup>FiXme Note: enten skal vi fra vælge os den noget før eller os skal vi have fundet på en cost function til liggetid

the cost function has been rewritten to:

$$\mathcal{J} = \sum_{i=1}^{H_p-1} \|\hat{y}(k+i|k) - \hat{y}(k+i-1|k)\|_{\mathcal{Q}(i)}^2 \quad (6.11)$$

$$\begin{aligned} \text{s.t.} \quad & \hat{x}(k+i+1) = A\hat{x}(k+i|k) + B\hat{u}(k+i|k) + B_d\hat{d}(k+i|k) \\ & \hat{y}(k+i) = C\hat{x}(k+i|k) \\ & x_{min} \leq x \leq x_{max} \\ & u_{min} \leq u \leq u_{max} \end{aligned} \quad (6.12)$$

Where  $\mathcal{Q}$  has been replaced with the output  $y$  as it can be measured directly from the state space system. The hat denotes a small signal value and not an estimate for  $y$ . This notation is used throughout the chapter. Where  $y$  corresponds to the height of the wastewater in the channel. It is the same to minimize height difference as the flow, due to both describe the variation in the output of the sewer. Furthermore, the cost function is subject to constraints for the states and control input. Both the states and the control input have a lower and upper constraint corresponding respectively to the bottom of the pipe and the top of the pipe and respectively to the minimum and maximum input to the pump. In order for the controller to minimize the variations in the output, it must be able to predict future events from ~~knowing~~ the current state. Therefore, by iterating the linear model, shown in section 6.1, up to the prediction horizon the controller is able to predict future states [Maciejowski, 2002].

By using the state equation recursively the state ~~equation~~ can be predicted up to the prediction horizon as shown in equation 6.13:

$$\begin{aligned} \hat{x}(k+1|k) &= A\hat{x}(k|k) + B\hat{u}(k|k) + B_d\hat{d}(k|k) \\ \hat{x}(k+2|k) &= A\hat{x}(k+1|k) + B\hat{u}(k+1|k) + B_d\hat{d}(k+1|k) \\ &= A^2\hat{x}(k|k) + AB\hat{u}(k|k) + AB_d\hat{d}(k|k) + B\hat{u}(k+1|k) \\ &\quad + B_d\hat{d}(k+1|k) \\ &\vdots \\ \hat{x}(k+H_p|k) &= A\hat{x}(k+H_p-1|k) + B\hat{u}(k+H_p-1|k) + B_d\hat{d}(k+H_p-1|k) \\ &= A^{H_p}\hat{x}(k|k) + A^{H_p-1}B\hat{u}(k|k) + \dots + B\hat{u}(k+H_p-1|k) \\ &\quad + A^{H_p-1}B_d\hat{d}(k|k) + \dots + B_d\hat{d}(k+H_p-1|k) \end{aligned} \quad (6.13)$$

Here the first equation  $\hat{x}(k+1|k)$  is inserted into the second and this is iterated up to the prediction horizon. This can be setup as prediction vectors and matrices denoted by

$\mathcal{X}, \mathcal{A}, \mathcal{B}, \mathcal{U}, \mathcal{B}_d$  and  $\mathcal{D}$ :

$$\underbrace{\begin{bmatrix} \hat{x}(k+1|k) \\ \hat{x}(k+2|k) \\ \vdots \\ \hat{x}(k+H_p|k) \end{bmatrix}}_{\mathcal{X}} = \underbrace{\begin{bmatrix} A \\ A^2 \\ \vdots \\ A^{H_p} \end{bmatrix}}_{\mathcal{A}} \hat{x}(k|k) + \underbrace{\begin{bmatrix} B & 0 & \cdots & 0 \\ AB & B & \cdots & 0 \\ \vdots & \vdots & \ddots & \vdots \\ A^{H_p-1}B & A^{H_p-2}B & \cdots & B \end{bmatrix}}_{\mathcal{B}} \underbrace{\begin{bmatrix} \hat{u}(k|k) \\ \hat{u}(k+1|k) \\ \vdots \\ \hat{u}(k+H_p-1|k) \end{bmatrix}}_{\mathcal{U}} + \underbrace{\begin{bmatrix} B_d & 0 & \cdots & 0 \\ AB_d & B_d & \cdots & 0 \\ \vdots & \vdots & \ddots & \vdots \\ A^{H_p-1}B_d & A^{H_p-2}B_d & \cdots & B_d \end{bmatrix}}_{\mathcal{B}_d} \underbrace{\begin{bmatrix} \hat{d}(k|k) \\ \hat{d}(k+1|k) \\ \vdots \\ \hat{d}(k+H_p-1|k) \end{bmatrix}}_{\mathcal{D}} \quad (6.14)$$

Where  $\mathcal{X}$  is the predicted state vector for the entire prediction horizon.  $\mathcal{A}$  is the state matrix up to the prediction horizon.  $x(k|k)$  is the initial state and is used to predict the whole prediction horizon,  $\mathcal{B}$  is the input matrix for the prediction horizon,  $\mathcal{U}$  is the predicted input vector, which consists of all the predicted inputs from the current timestep until  $(k+H_p-1)$ .  $\mathcal{B}_d$  is the disturbance matrix for the prediction horizon and  $\mathcal{D}$  is the disturbance vector.

This iteration process is also done for the output equation:

$$\hat{\mathcal{Y}}(k) = \underbrace{\begin{bmatrix} \hat{y}(k+1|k) \\ \hat{y}(k+2|k) \\ \vdots \\ \hat{y}(k+H_p-1|k) \end{bmatrix}}_{\mathcal{Y}} = \underbrace{\begin{bmatrix} C & 0 & \cdots & 0 \\ 0 & C & \cdots & 0 \\ \vdots & \vdots & \ddots & 0 \\ 0 & 0 & 0 & C \end{bmatrix}}_{\mathcal{C}} \underbrace{\begin{bmatrix} \hat{x}(k+1|k) \\ \hat{x}(k+2|k) \\ \vdots \\ \hat{x}(k+H_p|k) \end{bmatrix}}_{\mathcal{X}} \quad (6.15)$$

Where  $\mathcal{C}$  is a diagonal matrix with the output matrix  $C$ . By inserting the predicted state equation 6.14, into the predicted output equation 6.15 the following is achieved:

$$\hat{\mathcal{Y}}(k) = \mathcal{C}\mathcal{A}\hat{x}(k) + \mathcal{C}\mathcal{B}\hat{\mathcal{U}}(k) + \mathcal{C}\mathcal{B}_d\hat{\mathcal{D}}(k) \quad (6.16)$$

By using the following notation on equation 6.16:

$$\psi = \mathcal{C}\mathcal{A} \quad \gamma = \mathcal{C}\mathcal{B} \quad \Theta = \mathcal{C}\mathcal{B}_d \quad (6.17)$$

The predicted output equation can be rewritten as:

$$\hat{\mathcal{Y}}(k) = \psi\hat{x}(k) + \gamma\hat{\mathcal{U}}(k) + \Theta\hat{\mathcal{D}}(k) \quad (6.18)$$

To be able to use the cost function, equation 6.11, it has to be rewritten so the predicted output equation is used. Thereby, replacing the output  $y$  with the predicted output  $\hat{y}$  hence the following is obtained:

$$\mathcal{J} = \|\hat{\mathcal{Y}}(k) - \hat{\mathcal{Y}}(k-1)\|_{\mathcal{Q}(i)}^2 \quad (6.19)$$

Where the difference between  $\hat{\mathcal{Y}}(k)$  and  $\hat{\mathcal{Y}}(k-1)$  can be expressed as:

$$\Delta\hat{\mathcal{Y}}(k) = \hat{\mathcal{Y}}(k) - \hat{\mathcal{Y}}(k-1) \quad (6.20)$$

Thereby the following cost function is achieved:

$$J = \Delta\hat{\mathcal{Y}}(k)^T \cdot Q \cdot \Delta\hat{\mathcal{Y}}(k) \quad (6.21)$$

To be able to write the cost function as quadratic and linear terms of the predicted output  $\Delta\mathcal{U}$ , equation 6.18 is therefore inserted into equation 6.19 and thereby the following is obtained:

$$\mathcal{J} = (\psi\Delta\hat{x}(k) + \gamma\Delta\hat{\mathcal{U}}(k) + \Theta\Delta\hat{\mathcal{D}}(k))^T \cdot Q \cdot (\psi\Delta\hat{x}(k) + \gamma\Delta\hat{\mathcal{U}}(k) + \Theta\Delta\hat{\mathcal{D}}(k)) \quad (6.22)$$

The term on the right hand side of equation 6.22 is equal to:

$$\begin{aligned} & (\psi\Delta\hat{x}(k) + \gamma\Delta\hat{\mathcal{U}}(k) + \Theta\Delta\hat{\mathcal{D}}(k))^T \cdot Q \cdot (\psi\Delta\hat{x}(k) + \gamma\Delta\hat{\mathcal{U}}(k) + \Theta\Delta\hat{\mathcal{D}}(k)) = \\ & \Delta\hat{x}(k)^T \psi^T Q \psi \Delta\hat{x}(k) + \underbrace{\Delta\hat{x}(k)^T \psi^T Q \gamma \Delta\hat{\mathcal{U}}(k)}_{\text{Linear}} + \Delta\hat{x}(k)^T \psi^T Q \Theta \Delta\hat{\mathcal{D}}(k) \\ & \underbrace{\Delta\hat{\mathcal{U}}(k)^T \gamma^T Q \psi \Delta\hat{x}(k)}_{\text{Linear}} + \underbrace{\Delta\hat{\mathcal{U}}(k)^T \gamma^T Q \gamma \Delta\hat{\mathcal{U}}(k)}_{\text{Quadratic}} + \underbrace{\Delta\hat{\mathcal{U}}(k)^T \gamma^T Q \Theta \Delta\hat{\mathcal{D}}(k)}_{\text{Linear}} \\ & \Delta\hat{\mathcal{D}}(k)^T \Theta^T Q \psi \Delta\hat{x}(k) + \underbrace{\Delta\hat{\mathcal{D}}(k)^T \Theta^T Q \gamma \Delta\hat{\mathcal{U}}(k)}_{\text{Linear}} + \Delta\hat{\mathcal{D}}(k)^T \Theta^T Q \Theta \Delta\hat{\mathcal{D}}(k) \end{aligned} \quad (6.23)$$

Here the quadratic and linear terms of  $\Delta\mathcal{U}$  are denoted respectively, the remaining terms are the constants and these are not denoted in the equation, however, they will be referred to in the following equations as,  $c$ . The quadratic variables are collected in:

$$\mathcal{H} = \gamma^T Q \gamma \quad (6.24)$$

And the linear variables are collected in:

$$\mathcal{G} = 2\Delta\hat{x}(k)^T \psi^T Q \gamma + 2\Delta\hat{\mathcal{D}}(k)^T \Theta^T Q \gamma \quad (6.25)$$

Thereby inserting these expressions in equation 6.23 the final cost function is obtained:

$$\min_{\Delta\mathcal{U}(k)} \mathcal{J}(\Delta\mathcal{U}(k)) = \min_{\Delta\mathcal{U}(k)} \Delta\mathcal{U}(k)^T \mathcal{H} \Delta\mathcal{U}(k) + \mathcal{G} \Delta\mathcal{U}(k) + c \quad (6.26)$$



### 6.2.1 Constraints

In order to apply the constraints, shown in equation 6.11 for the states, to the optimization problem in equation 6.26 the constraints must be reformulated so they are a constraint of the controller input  $\Delta\mathcal{U}$ , therefore it is required to reformulate the inequalities constraints.

The constraints applied to the states are upper and lower bound to the channel and the tank. This will not allow the simulation to overfill the channel or the tank, or to have a negative height in either of the two. In the following equation the constraint for the states are shown:

$$x_{min} \leq \mathcal{X}(k) \leq x_{max} \quad (6.27)$$

Where  $x_{min}$  and  $x_{max}$  are respectively lower and upper bound. As the constraint needs to be for small signal value and as the constraint is for full signal values the operating point needs to be subtracted from the lower and upper bounds thereby transforming the constraint into small signals:

$$x_{min} - \bar{x} \leq \hat{\mathcal{X}}(k) \leq x_{max} - \bar{x} \quad (6.28)$$

To reformulated the constraint the predicted state equation 6.14 is inserted instead of the state vector.

$$x_{min} - \bar{x} \leq \mathcal{A}\hat{x}(k) + \mathcal{B}\hat{\mathcal{U}}(k) + \mathcal{B}\hat{\mathcal{D}}(k) \leq x_{max} - \bar{x} \quad (6.29)$$

However, to make the constraint depend on  $\Delta\mathcal{U}$  the difference between the current time step and the previous time step,  $\mathcal{U}(k) = v\mathcal{U}(k-1) + W\Delta\mathcal{U}(k)$ , where  $v$  is a vector and  $W$  is a matrix on the form:

$$v = \begin{bmatrix} v(k+1|k) \\ v(k+2|k) \\ \vdots \\ v(k+H_p|k) \end{bmatrix} = \begin{bmatrix} 1 \\ 1 \\ \vdots \\ 1 \end{bmatrix} \quad (6.30)$$

$$W = \begin{bmatrix} w_{1,1} & w_{1,2} & w_{1,3} & w_{1,H_p} \\ w_{2,1} & w_{2,2} & w_{2,3} & w_{2,H_p} \\ w_{3,1} & \vdots & \ddots & w_{3,H_p} \\ w_{H_p,1} & w_{H_p,2} & \cdots & w_{H_p,H_p} \end{bmatrix} = \begin{bmatrix} 1 & 0 & 0 & 0 \\ 1 & 1 & 0 & 0 \\ 1 & \vdots & \ddots & 0 \\ 1 & 1 & \cdots & 1 \end{bmatrix} \quad (6.31)$$

Now the constraint is set up as a constraint on the input signal. In addition, the constraint has to be setup as equality constraints, therefore, it is divided into two constraints:

$$\underbrace{BW}_{\Lambda} \Delta\hat{\mathcal{U}}(k) \leq \underbrace{x_{max} - \bar{x} - \mathcal{A}\hat{x}(k) - \mathcal{B}\hat{u}(k-1) - \mathcal{B}\hat{\mathcal{D}}(k)}_{\Gamma_1} \quad (6.32)$$

$$\underbrace{\mathcal{B}W}_{\Lambda} \Delta \hat{\mathcal{U}}(k) \leq \underbrace{-x_{min} + \bar{x} + \mathcal{A}\hat{x}(k) + \mathcal{B}\hat{u}(k-1) + \mathcal{B}\hat{\mathcal{D}}(k)}_{\Gamma_2} \quad (6.33)$$

Constraints are also applied on the controller output. The reason for these constraints is to not allow the controller to produce a higher output than what the pipe after the tank is able to transport. The constraint for the controller output is construct in the same way as for the states in the system. Below the constraint for the controller output is shown:

$$u_{min} \leq \mathcal{U}(k) \leq u_{max} \quad (6.34)$$

The constraint needs to be written for small signal values, and needs to depend on  $\Delta \mathcal{U}$ :

$$u_{min} - \bar{u} \leq v\hat{u}(k-1) + W\Delta \hat{\mathcal{U}}(k) \leq u_{max} - \bar{u} \quad (6.35)$$

The constraint is split up into lower and upper bound for the signal, the upper bound is:

$$\begin{aligned} v\hat{u}(k-1) + W\Delta \hat{\mathcal{U}}(k) &\leq u_{max} - \bar{u} \\ W\Delta \hat{\mathcal{U}}(k) &\leq \underbrace{u_{max} - \bar{u} - v\hat{u}(k-1)}_{\Gamma_3} \end{aligned} \quad (6.36)$$

And the lower bound:

$$\begin{aligned} u_{min} - \bar{u} &\leq v\hat{u}(k-1) + W\Delta \hat{\mathcal{U}}(k) \\ -W\Delta \hat{\mathcal{U}}(k) &\leq \underbrace{\hat{u}(k-1) - u_{min} + \bar{u}}_{\Gamma_4} \end{aligned} \quad (6.37)$$

The constraints can be setup on the standard inequality constraint form and thereby be included in the algorithm for the MPC implementation.

$$\begin{bmatrix} \Lambda \\ -\Lambda \\ W \\ -W \end{bmatrix} \Delta \mathcal{U} \leq \begin{bmatrix} \Gamma_{1.max} \\ \Gamma_{2.min} \\ \Gamma_{3.max} \\ \Gamma_{4.min} \end{bmatrix} \quad (6.38)$$

In the following section the implementation of the cost function and constraints, shown in this section, in MATLAB will be elaborated

### 6.2.2 Implementation of MPC

In this section the implementation of MPC in MATLAB will be elaborated.

The cost function in equation 6.26 is a quadratic problem. In order to solve this minimization problem and find a global minimum quadratic programming (QP) is used. In MATLAB there well develop solvers for QP problems, in this project the quadprog function has been chosen. Quadprog solves the minimization problem subject to constraints to the specified convex cost function. The model used for the predictive model is the one covered in section 6.1. Furthermore, the constraints for the cost explained in the previous section will also be included.

In figure 6.3 an illustration of a MPC controller is shown.

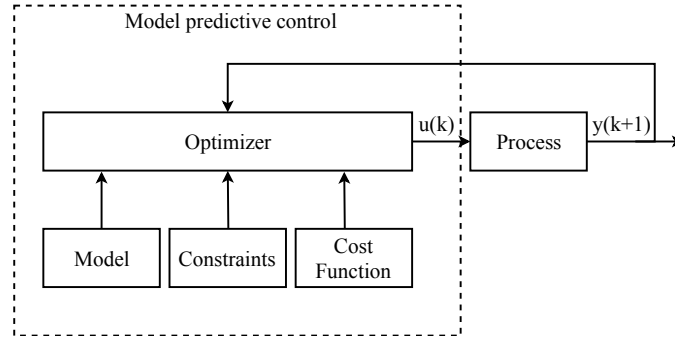


Figure 6.3: Diagram of an MPC controller

Here it is illustrated that the model, constraint and cost function will be used in the optimizer to generate an control output, that will be used in the process, which in this case is the nonlinear model. The output  $y(k+1)$  is the output height at the end of the last pipe in the sewer network. At each time step the current value of the output is feedback to the MPC controller. Here the MPC will at each iteration calculate up to  $H_p$  control inputs, as it calculates for future disturbances, however, only the first element of this  $u$  vector will be used to control the process. Thereafter a new measurement will be taken and a new controller output will be calculated and this will iterate for the entire simulation.

In determining the length of the prediction horizon several considerations were taken into account. As illustration in figure 1.5 a daily flow from the households is shown. Here the flow is illustrated for working days and in the weekend. Thereby by knowing the flow pattern for households the MPC would be able to include this knowledge in the prediction model. Thus an ideal prediction horizon would be 24 hours, as it would be able to see the disturbance across a whole day.

However, as the households are not the only disturbance in this setup this is not entirely true. Because the disturbance coming from the larger industry e.g. the bottling plant and the brewery are stochastic in a way, where it is unknown when the wastewater from the plants is coming and the periodicity between the outlets are unknown. Furthermore, the amount of wastewater coming from the plants are also different from time to time. Therefore, it would not be preferable to place the tank next to the industry as it would not be able to predict the disturbance. Thus the tank needs to be placed in a distance away from the industry, where it would be able to use the disturbance in the prediction model by knowing the disturbance coming from the industry by having a measurement of it. The time it takes the wastewater to leave the industry and to arrive at the tank would then decide the length of the prediction horizon.

However, in the implementation of the MPC, it was discovered that the prediction horizon was restricted. Because when it was set to high, above 20, the quadratic matrix  $\mathcal{H}$ , equation 6.24, was not semi-positive definite, as in the eigenvalues of it was negative,

hence the quadratic problem was not convex. The reason for this problem is, that in the linearized model, some of the elements in matrices are very small and therefore, when the system is predicted, as shown in equation 6.14, the elements would be even smaller, thus causing the  $\mathcal{H}$  matrix to have an extremely small negative eigenvalue. Therefore, several tests were conducted to find a prediction horizon that did not result in a negative eigenvalue. It was found that a prediction horizon of 20, where the lowest eigenvalue of  $\mathcal{H}$  was zero. However, this restricts the length of the pipe after the tank, because if the pipe is too long the MPC will not be able to predict all the way down to the output of it. Therefore, in the simulation of the MPC controller, this must be kept in mind.



## Results

In this subsection the results obtained from the testing of the MPC controller will be covered. Two simulation will conducted, one where the constraints are neglected and therefore minimized without any restriction and another simulation where the constraints included.

The pipe and tank setup for the simulation includes two pipes and one tank, where the tank is placed in the middle of the pipes. The specification for both pipes and the tank can be seen in tabular 6.3 and 6.4 respectively.

Pipe number	Length [m]	Sections	Dx [m]	Ib	d [m]	$\theta$	Qf [ $m^3/s$ ]
1	100	5	20	0,003	0,9	0,65	0,97
2	100	5	20	0,003	0,9	0,65	0,97

Table 6.3: The pipe specification for the simulation.

Size [ $m^3$ ]	90
Height [m]	10
Area [ $m^2$ ]	9
Q_out_max [ $m^3/s$ ]	0,97

Table 6.4: Tank specification for the simulation.

In the first simulation the MPC controller is minimizing the output variations of the tank without any constraints included. The input signal in the first pipe is shown in figure 6.4.

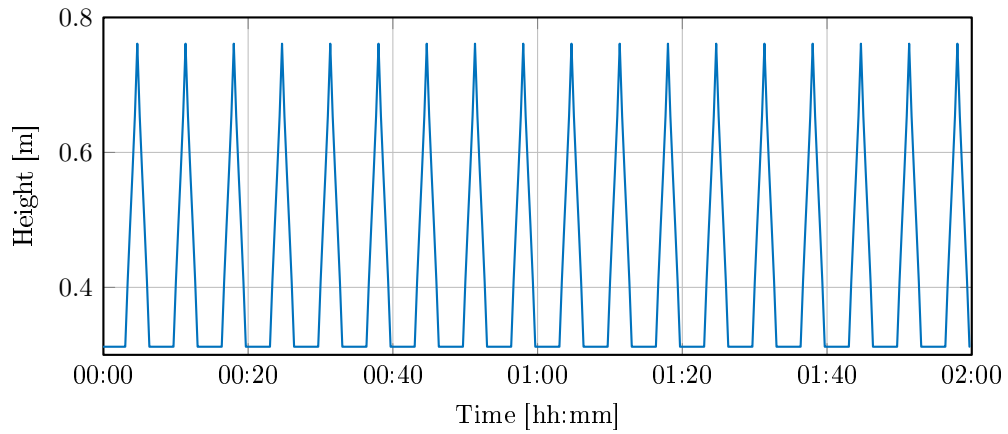


Figure 6.4: The input to the first pipe.

Here there is a constant input of  $0,2 \text{ m}^3/\text{s}$ , which results in a height of 0,31 meters in the pipe. On top of the input a disturbance signal is added. This is done to see if the MPC is able to keep the flow variations out of the tank to a minimum. This signal is a upper triangular signal which goes from the constant input up to  $0,9 \text{ m}^3/\text{s}$  which is equal to a height of 0,75 meters in the pipe. The time between each disturbance signal is 200 seconds and the period of the triangle signal is 100 seconds. This simulation conducted is for two hours where  $\Delta t$  is 20 seconds. In figure 6.5 the output of the the last pipe is shown.

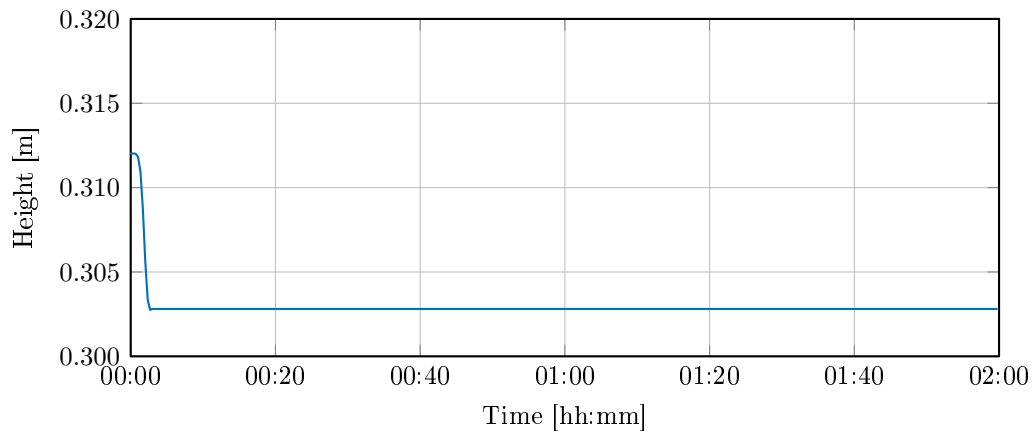


Figure 6.5: The output of the last pipe.

Here it can be seen that the MPC controller is able to minimize the disturbance coming from the first pipe as the output is constant. At the beginning the height of the output is a bit higher, this is due to that the tank holds wastewater at the beginning of the simulation. After it is emptied the height falls down to a constant level. In figure 6.6 the height in the tank can be seen.

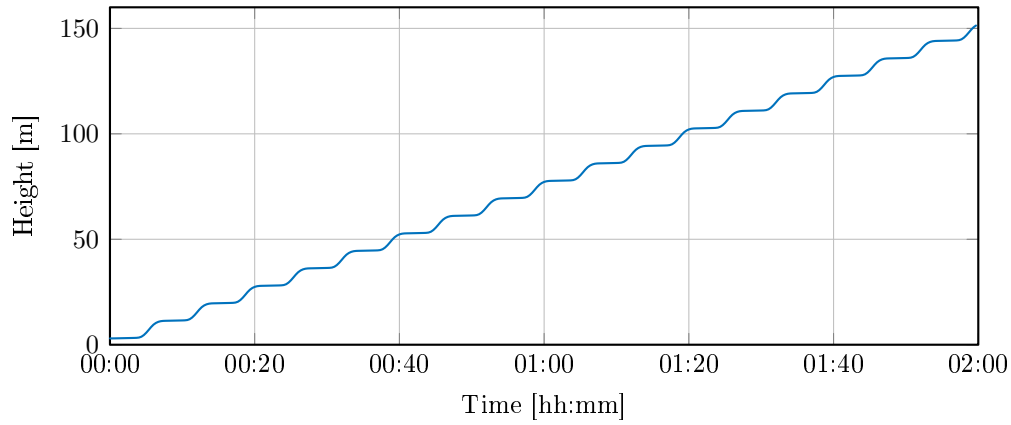


Figure 6.6: The height in the tank.

As expected the tank would be overfilled, as the disturbance coming from the first pipe is much higher than the output of the second. However, the cost function does what is expected, as it keeps a steady output of the tank and has no knowledge about the limitations of the tank and therefore overfills it. In the second simulation the same input is applied to the first pipe, where the constraints shown in equation 6.2.1 is utilized. In this simulation only constraints regarding the tank and the control input to the pump have constraints in this system setup. The reason for not having constraints on the heights in the second pipe is, it should be sufficient to have on the control input to the pump, as it will only allow inputs between 0 to 1, where the constant is multiplied on the maximum flow that the second pipe can transfer and thereby not allowing flows higher than that. Furthermore, the constraints for the tank goes from 0 to the maximum height it, which is 10 meters in this simulation, as seen in table 6.4. The reason for not have constraints on the first pipe is, as it is impossible for the MPC controller to regulate the height in that part. In figure 6.7 the height of the tank is shown from the second simulation.

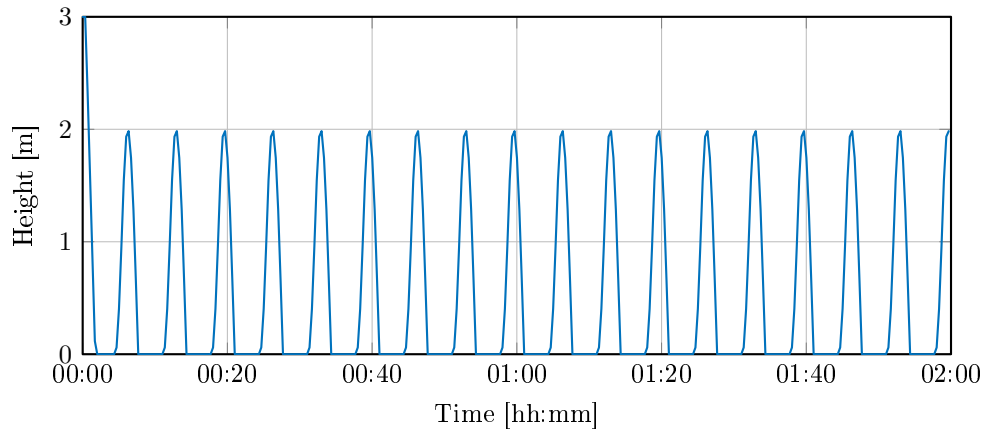


Figure 6.7: The height in the tank for the second simulation.

It can be seen that the tank does not get overfilled any more, thereby is within the constraints for the tank. At the beginning the tank is emptied again due to it was initials with wastewater in it. Hereafter the tank is filled up to 2 meters and then emptied again. In figure 6.8 the output of the second pipe is shown.

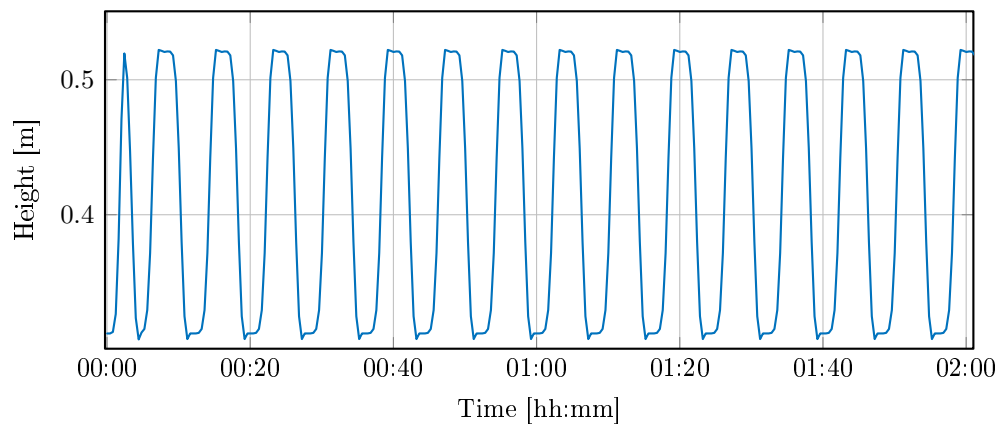



Figure 6.8: The output of the last pipe.

It is clear from the figure that the output is not even close to be constant. It fluctuates between two values, the constant input, approximately 0,31 meters, and 0,51 meters. In the top and bottom of the curve, it can be seen that the curve levels off. The bottom is due to the tank is empty and therefore, the input, that goes into the tank from the first pipe, goes right into the second pipe without storing any wastewater in the tank. When the top levels off the tank starts to be filled up and as it goes down the tank is emptied. It was discovered that the reason for the top is due to constraints on the upper bound for the input, this however is not a wanted feature. It was desired to get a constant output or a minimum of variations in the output, which is not achieved. Through several tries of changing the parameters of the constraints, e.g. lessen the controller constraint a solution was not found, in every case the output looked similar to the one shown in figure 6.8. 





# Results 7

In this chapter, the results of the simulation model will be shown.

The goal of this simulation is to simulate a daily flow in the northern part of Fredericia, where the disturbance can be seen on the input to the WWTP. To do so the simulation model explained in chapter 5 is utilized. The pump station, illustrated with the blue solid circle in figure 2.1, is not included in this simulation, as it will smooth the flow from that station down to the WWTP, thus there will not be any variation in the flow into the WWTP. To generate the disturbances from the residential and industrial zones, shown in figure 2.1, the flow profiles in appendix A.3 is used. These disturbance models are not simulated from the zones into the main sewer line but are directly added on the main sewer line, therefore the results are expected to have higher peaks, as these models are not attenuated, as they would have been if they were simulated from the zones. It has been chosen to only use the disturbance from the brewery and bottling plant, as the data from the refinery is not accessible. The disturbance from the brewery and bottling plant is shown in figure 2.4. The pipe specifications for this simulation can be seen in table 7.1.

Component number	Length [m]	Sections	Dx [m]	Ib	d [m]	$\theta$	$Q_f$ [ $m^3/s$ ]
1	700	35	20	0,003	0,9	0,65	0,972
3	303	15	20,2	0,003	0,9	0,65	0,972
4	27	1	13,5	0,003	1	0,65	1,284
5	155	8	19,4	0,0041	1	0,65	1,50
6	295	14	21	0,0122	0,8	0,65	1,438
7	318	15	21,2	0,0053	0,9	0,65	1,293
8	110	5	22	0,0036	0,9	0,65	1,066
9	38	2	19	0,0024	1	0,65	1,149
10	665	30	22,2	0,003	1	0,65	1,284
11	155	7	22,1	0,0008	1	0,65	0,663
12	955	47	20,3	0,0029	1,2	0,65	2,041
13	304	15	20,3	0,003	1,2	0,65	2,076
14	116	5	23,2	0,0021	1,2	0,65	1,737
15	283	12	23,6	0,0017	1,4	0,65	2,346
16	31	2	15,5	0,0019	1,4	0,65	2,480
17	125	6	20,8	0,0021	1,6	0,65	3,707
18	94	4	23,5	0,0013	1,5	0,65	2,461
19	360	18	20	0,0046	1,6	0,65	5,487
20	736	38	19,4	0,0012	1,6	0,65	2,802

Table 7.1: The specification of the pipes for in the simulation.

The tank specification can be seen in table 7.2.

Component number	2
Size [ $m^3$ ]	90
Height [m]	10
Area [ $m^2$ ]	9

Table 7.2: The tank specification for the simulation.

Furthermore, table 7.3 shows the system setup.

Type	Component	Sections
Pipe	1	35
Tank	1	1
Pipe	18	227
Total	20	263

Table 7.3: The system setup.

Where the first component in the simulated sewer network is a pipe followed by a tank and hereafter 18 pipes follows. The first pipe and the tank have been added to the original sewer network shown in figure 2.2. The first pipe goes from the larger industrial area down to the main sewer line showed with a black circle in figure 2.1, where the tank is placed as well. The reason for placing the tank there is, that the idea would have been to smoothen the wastewater coming from the larger industry. Furthermore, the pipe is placed, as the MPC could have used it for prediction, as it would be able to measure the disturbance going into the pipe at the industry, and thereby use it in the predictive model to calculate the most optimal control output to the pump. However, as this is not possible, due to the MPC controller is not able to keep a flow output, where the flow variations are kept to a minimum, and as the prediction horizon is limited due to non-convexity as explained in section 6.2. Therefore in the simulation, the tank will just transfer wastewater from the previous pipe to the pipe after the tank.

Several simulations were conducted to find the most optimal  $\Delta t$  as explained in section 5.2.1. As the pipes are split into different sections and as the average flow height is also different from pipe to pipe, the Courant number variates from pipe to pipe. Thus it is therefore difficult to tune so all pipes have the most optimal Courant number. However, it was found that a  $\Delta t = 20$ , with the given  $\Delta x$  shown in table 7.1, gave the most realistic outcome, as values lower resulted in an output where some distortion was visible.

In figure 7.1 the output of a simulation across two days are shown.

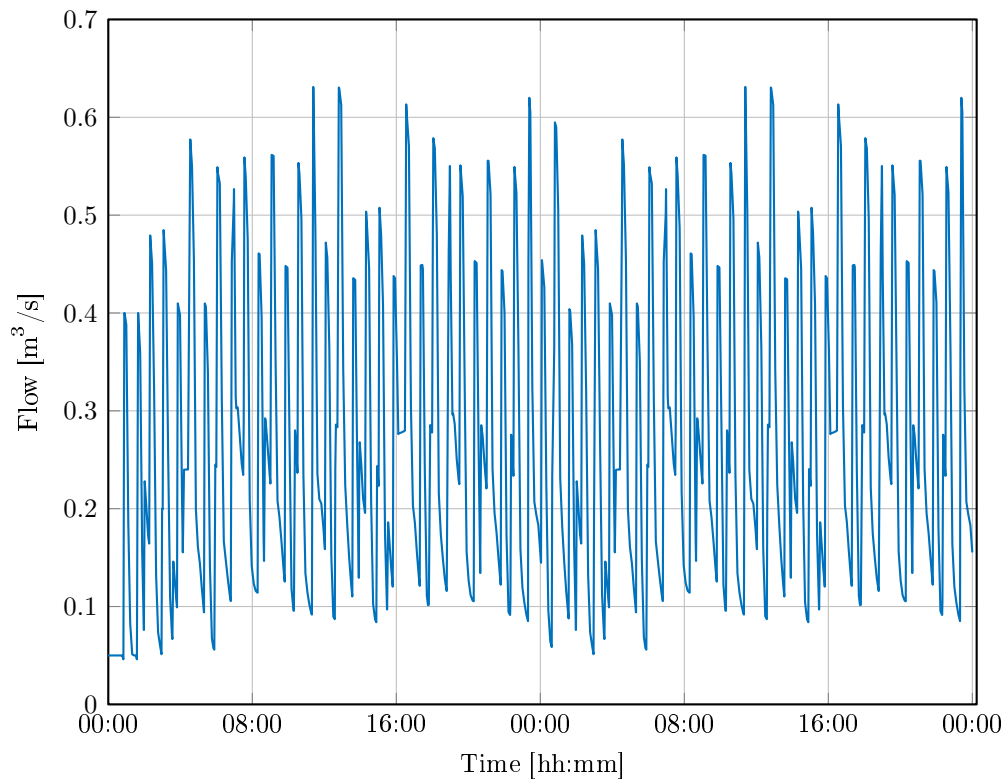


Figure 7.1: Output of the last pipe into the WWTP.

It is clear that flow varies to a great extent as is also shown in figure 2.5 from the WWTP at Fredericia. However, these two can not be directly compared, as the data from Fredericia also includes the wastewater from the southern part of the city. But can give an indication that the simulation corresponds to what is happening in the reality. However, the simulated results in a greater variation of flow than the data obtained from Fredericia. This could be due to the pump, as mention previously, that it smoothen the flow from the northern part of the city and therefore the variations on the figure from Fredericia is due to disturbance coming from the southern part of the city. By taking the mean of the data in figure 2.5 the WWTP have a inflow at  $0,28 \text{ m}^3/\text{s}$  and doing the same to the data in figure 7.1 where the mean is  $0,273 \text{ m}^3/\text{s}$ . As the data from Fredericia is both from the northern and southern part of Fredericia the simulate flow is a bit high compared to that. However, this could be due to the flow profiles from the residential and industrial areas in the simulated results are estimated to be larger than the reality.

In figure 7.2 the concentration at the output for the first eight hours can be seen.

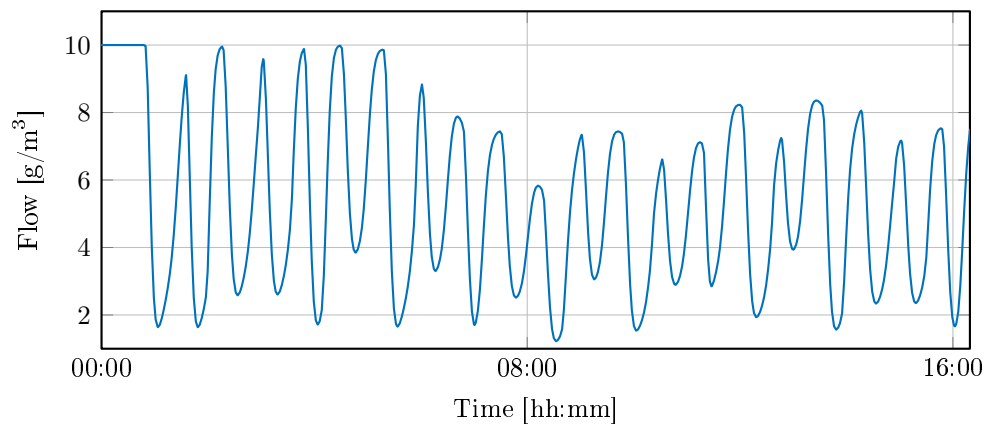


Figure 7.2: Concentration output for the first eight hours of the last pipe into the WWTP.

The disturbance coming from the brewery and bottling plant has a concentration on  $10 \text{ g/m}^3$  where the rest of the wastewater has zero concentration. The concentration from the brewery and bottling plant is therefore attenuated by the wastewater coming from the residential areas.

# Discussion 8

---



# Conclusion 9

---

We made it!





# Bibliography

---

- [AquaEnviro, 2010] AquaEnviro (2010). Fungal problems in wastewater treatment works. Website. Posted 16th June 2010 - <https://www.aquaenviro.co.uk/fungal-problems-in-wastewater-treatment-works/>.
- [College, 2018] College, M. E. C. (2018). Biological components of wastewater. Website. <http://water.me.vccs.edu/courses/ENV149/biological.htm>.
- [Cunge et al., 1980] Cunge, J. A., Holly, F. M., and Verwey, A. (1980). Practical aspects of computational river hydraulics.
- [Dansk-betonforening, 2013] Dansk-betonforening (2013). Betonhåndbogen. Online. Chapter 12.5 <https://www.danskbetonforening.dk/Publikationer/Betonhaandbogen/Den-elektroniske-betonhaandbog>.
- [Eniro, 2018] Eniro (2018). [www.krak.dk](http://www.krak.dk).
- [EPA, 1994] EPA (1994). How wastewater treatment works... the basics. website. <https://www3.epa.gov/npdes/pubs/bastre.pdf>.
- [Eschooltoday, 2017] Eschooltoday (2017). Liquid waste (sewage/wastewater) treatment. Website. <http://eschooltoday.com/pollution/water-pollution/sewage-treatment-process-for-kids.html>.
- [Fredericia-Spildevand, 2018a] Fredericia-Spildevand (2018a). Geographical information systems. A map to describe the length, slope and size of the different sewers in Fredericia. <http://frsp.webgrafkort.dk/Mainpage.aspx>.
- [Fredericia-Spildevand, 2018b] Fredericia-Spildevand (2018b). Summary of company visits. Summary from a meeting with Fredericia Spildevand og Energi A/S can be found in appendix A.1.
- [Hvitved-Jacobsen et al., 2013] Hvitved-Jacobsen, T., Vollertsen, J., and Nielsen, A. H. (2013). *Sewer processes: microbial and chemical process engineering of sewer networks*. CRC press.
- [Institute of hydromechanics, ] Institute of hydromechanics. Concepts, definitions and the diffusion equation. Technical report, Karlsruhe Institute of Technology.
- [Maciejowski, 2002] Maciejowski, J. M. (2002). *Predictive control: with constraints*. Pearson education.
- [Mays, 2001] Mays, L. W. (2001). *Stormwater collection systems design handbook*. McGraw-Hill Professional.
- [Michelsen, 1976] Michelsen, H. (1976). Ikke-stationær strømning i delvis fyldte kloakledninger. Master's thesis, Den kongelige veterinær og landbohøjskole.
- [Nykredit, 2018] Nykredit (2018). Familietyperne. website. website - <https://www.mitnykredit.dk/privat/info/bank/forbrugsoverblik-familietyper.xml>.

- [Rinkesh, 2009] Rinkesh (2009). What is wastewater treatment. website. <https://www.conserve-energy-future.com/process-of-wastewater-treatment.php>.
- [Rossi et al., 2014] Rossi, F., Motta, O., Matrella, S., Proto, A., and Vigliotta, G. (2014). Nitrate removal from wastewater through biological denitrification with oga 24 in a batch reactor. *Water*, 7(1):51–62.
- [Ruscio, 2001] Ruscio, D. D. (2001). Model predictive control and optimization. Lecture notes. Lecture notes on Model Predictive Control.
- [Schlütter, 1999] Schlütter, F. (1999). *Numerical modelling of sediment transport in combined sewer systems*. PhD thesis, The Hydraulics and Coastal Engineering Group, Dept. of Civil Engineering, Aalborg University.
- [Schütze et al., 2011] Schütze, M., Butler, D., and Beck, B. M. (2011). *Modelling, simulation and control of urban wastewater systems*. Springer Science & Business Media.
- [Sjøholm, 2016] Sjøholm, P. (2016). Rensningsanlæg (wastewater plant). Video. [https://www.youtube.com/watch?v=cEQ\\_INO6OlE](https://www.youtube.com/watch?v=cEQ_INO6OlE).
- [Statistics-Denmark, 2018] Statistics-Denmark (2018). Population according to cities in 2017. <https://www.dst.dk/en>.
- [Szymkiewicz, 2010] Szymkiewicz, R. (2010). *Numerical modeling in open channel hydraulics*, volume 83. Springer Science & Business Media.
- [Szymkiewicz, 1998] Szymkiewicz, R. (1998). *Numerical Modeling in Open Channel Hydraulics*. Springer.
- [Vestergaard, 1989] Vestergaard, K. (1989). *Numerical Modelling of Streams: Hydrodynamic models and models for transport and spreading of pollutants*. PhD thesis, Hydraulic & Coastal Engineering Laboratory, Department of Civil Engineering, Aalborg University.
- [Vojtesek et al., ] Vojtesek, J., Dostal, P., and Maslan, M. Modelling and simulation of water tank.

## A.1 Summary of company visits

This appendix contains a summary from a meeting with the Fredericia wastewater department. The summary is in danish.

Virksomheds besøg 19/03/2018

Spildevand der kommer til rensning ved Fredericia rensningsanlæg stammer hovedsageligt fra industrien, 60-65 %. Ved Carlsberg og Arla er der flow målinger. Der er ikke målinger fra beboelse, hverken flow eller koncentrat, dog er der flow målinger ved nogle af pumpe stationer, samt flow og koncentrations målinger ind på rensningsanlægget. Stofmængden er ukendt fra det meste af industrien. Der er biotector ved Carlsberg (TOC) og COD måler ved Arla. Fredericia kunne evt. skaffe flowmålinger til os efter kontakt med industrien. På nuværende tidspunkt regulerer Carlsberg deres spildevand så det har en pH værdi mellem 6 og 9. Carlsberg har også et spare bassin. Arla har to spare bassiner, hvor de også kontrollere deres pH udledning. Shell har deres eget rensningsanlæg. Industrien er typisk gode til at holde en konsistent udledning af flow og koncentrat, der kan dog forekomme uheld. Fordelene ved Fredericia er, at temperaturen på spildevandet i kloakkerne ligger omkring 16-17 grader året rundt. Dette hjælper bakterierne med denitrificering af spildevandet. Bakterierne er mindre aktive med nitrificeringen og denitrificering når temperaturen kommer under 10 grader celsius. Hvilket betyder, at fjernelsen af nitrogen går langsommere.

- Der er problemer i ledningsnettet når der falder kraftig regn, der kan forekommer overløb, derudover gør man rensningsprocessen hurtigere ved kun at føre vandet igennem den mekaniske rensning og derefter udlede det til Lillebælt.
- Der er kul filter på næsten alt for at fjerne lugtgener, såsom dæksler, overtryksventiler og lukkede bassiner.
- Man vil gerne minimere opholdstid i spare bassiner for at undgå produktion af hydrogen sulfid.
- Ved vedligeholdelse af rensningsanlægget lukkes hovedledningen ind til rensningsanlægget, hvor det er muligt at stuve spildevand op i hoved ledning i 3-4 timer i tørvejr.
- Grundvandsindtrængning er forhøjet under regnvejr, samt forhøjet når vandstanden i Lillebælt er over normen.
  - Forhøjet vandstand kan øge klorid indholdet i spildevandet både ved at trænge ind gennem grundvandet, men også ved tilbageløb i overløbsanlæg beliggende ud til Lillebælt. Dette er et problem, da bakterierne fungerer bedst med en konstant mængde af klorid i spildevandet. Variationer i klorid gør, at bakteriernes nedbrydningsproces af de forskellige stoffer i spildevandet er nedsat for en periode. Når indholdet af klorid er konstant igen tilpasser bakterierne sig og deres nedbrydningsproces går tilbage til normal kapacitet.
- Der er ingen forfældning i rensningsanlægget pga. lugtgener.

- Har tidligere udtaget primær slam ved bundfældning, det blev stoppet pga. høj gas udvikling, da dette gav lugtgener.
- Der planlægges igen at udtage primær slam ved en filtreringsproces for at undgå lugtgener.
- Fosfor kommer hovedsageligt fra industri ca. 300-500 kg/døgn under normal drift. Fosfor er nødvendigt da dette indgår i processen til at nedbryde kvælstof.
- Varierende indhold af klorid i spildevandet er et problem for bakterierne, dette er især et problem under 10 mg/l.
- Rensningsanlægget har en kapacitet på 420.000 People Equivalent (PE), PE svarer til 120 COD/døgn eller 0,2 mg/l/døgn for en person.
- Når der er tørvejr er der et typisk flow på 800-1200  $m^3/time$  ind til rensningsanlægget.

Det ideelle scenarie er,

- Konstant flow og koncentrat
- Fast indhold af koncentrat (Klorid bl.a.)
  - Nødvendigvis ikke et lavt indhold

Prioriteringer i forhold til forstyrrelse i styring af ledningsnetværk.

- Små klorid variationer
- Slam/bakterier nok til at kunne omsætte kvælstof
  - Dette reguleres der for i rensningsanlægget.
- Der skal være en hvis mængde kulstof
  - Hvis spildevand flowet er konstant, er dette ikke et problem for rensningsanlægget.
- Små flow variationer
- Lav opholdstid i bassiner

## A.2 Pump information

Information regarding some of the pumps in Fredericia.

In tabluar A.1 information regarding the pumps located in Fredericia can be found. These values have been given by Fredericia.

Location	Pump capacity [ $m^3/s$ ]	Number of pumps	Surface area of the well [ $m^2$ ]	Start/stop level [m]	Wear reduction [%]	Total pumping capacity [ $m^3/s$ ]
Damvej P215	0,0478	2	12.56	0,7/0,37	5-10	0.0956
Thulesvej P217	0,0719	2	12.56	0,59/0,07	25-30	0.1438
Treldevej P218	0,0206	1	7.06	0,67/0,17	25-30	0,0206
Treldevej east P219	0,0214	2	12.56	0,79/0,34	25-30	0,0428
Lillebælts allé P221	0,0138	2	6	1,06/0,7	5-10	0,0276
Benzinvej P254	0,0476	2	12.56	1/0.36	5-10	0,0952
Norgesgade P255	0,350	3	N/A	N/A	N/A	1,05
Vesthavnsvej P256	0,240	5	N/A	N/A	N/A	1,2

Table A.1: Information for the different pumps located in Fredericia

### A.3 Flow profiles

In this appendix the flow profiles for the residential and industrial parts are shown.

The legend in the plots refereces to the figure 2.1 shown in chapter 2.

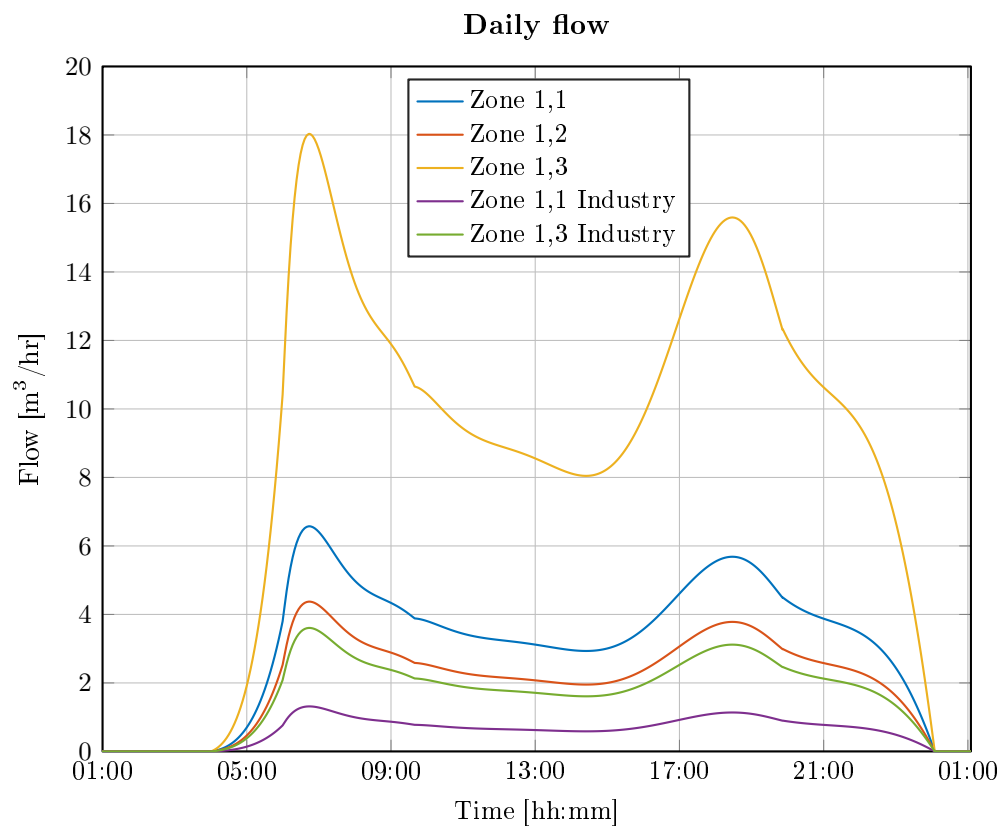


Figure A.1: A daily flow profile zone 1.

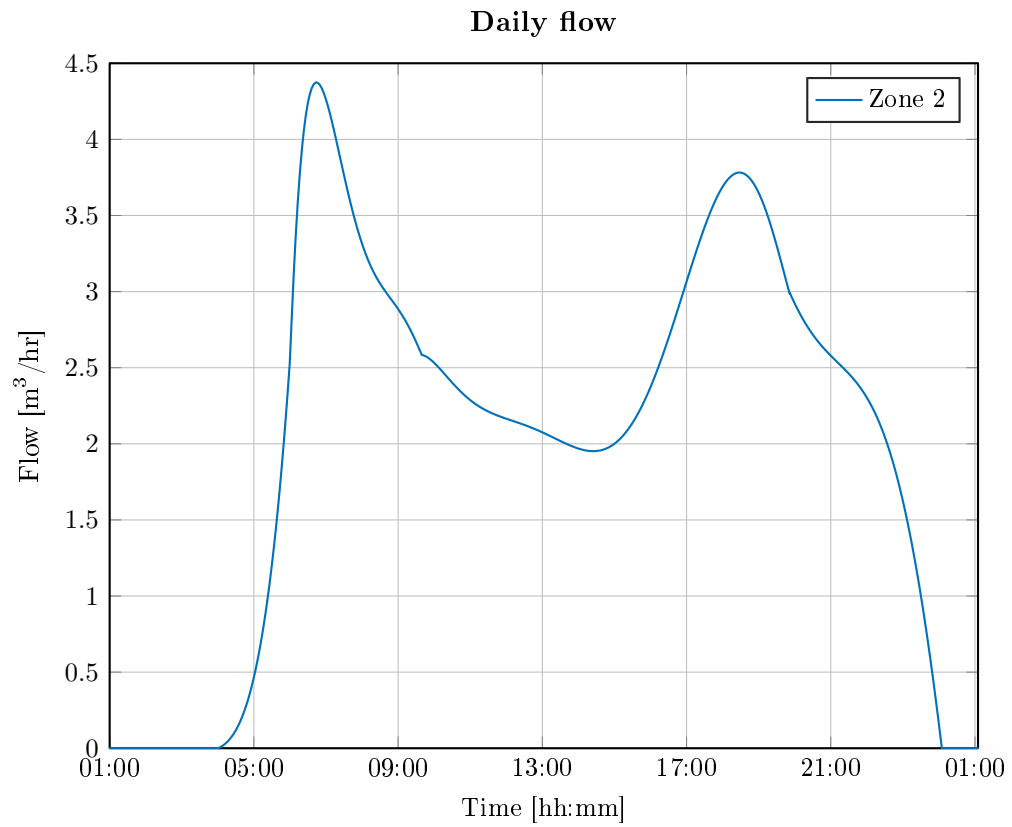


Figure A.2: A daily flow profile for zone 2.

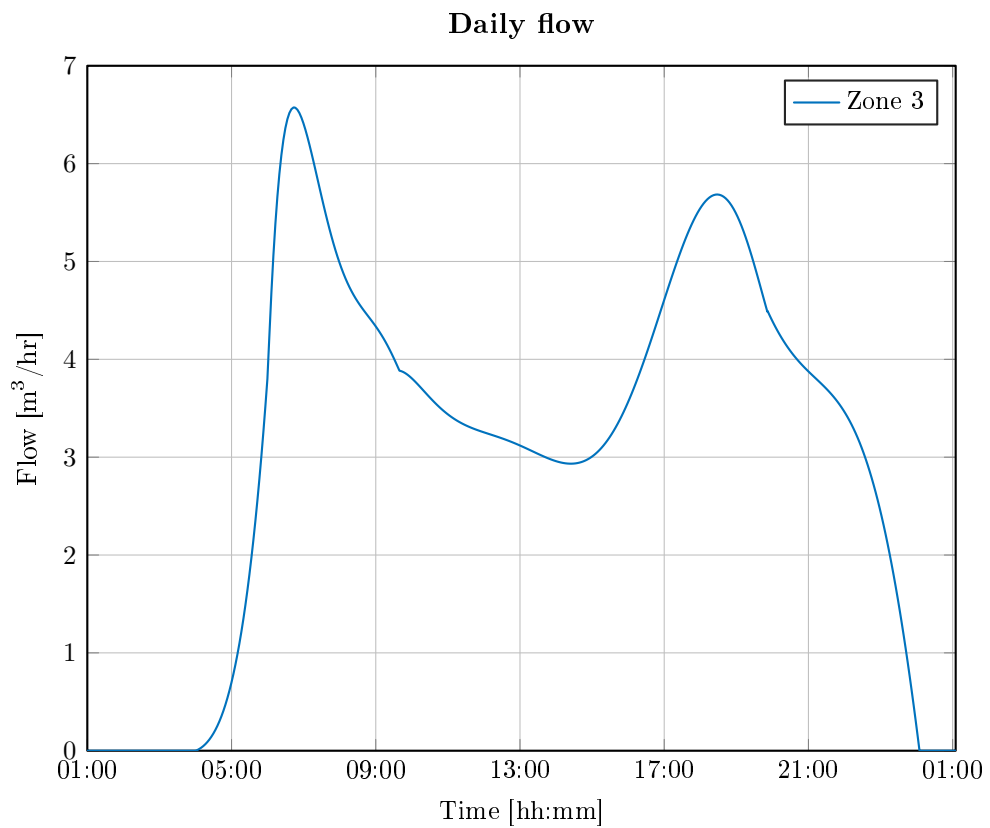


Figure A.3: A daily flow profile for zone 3.

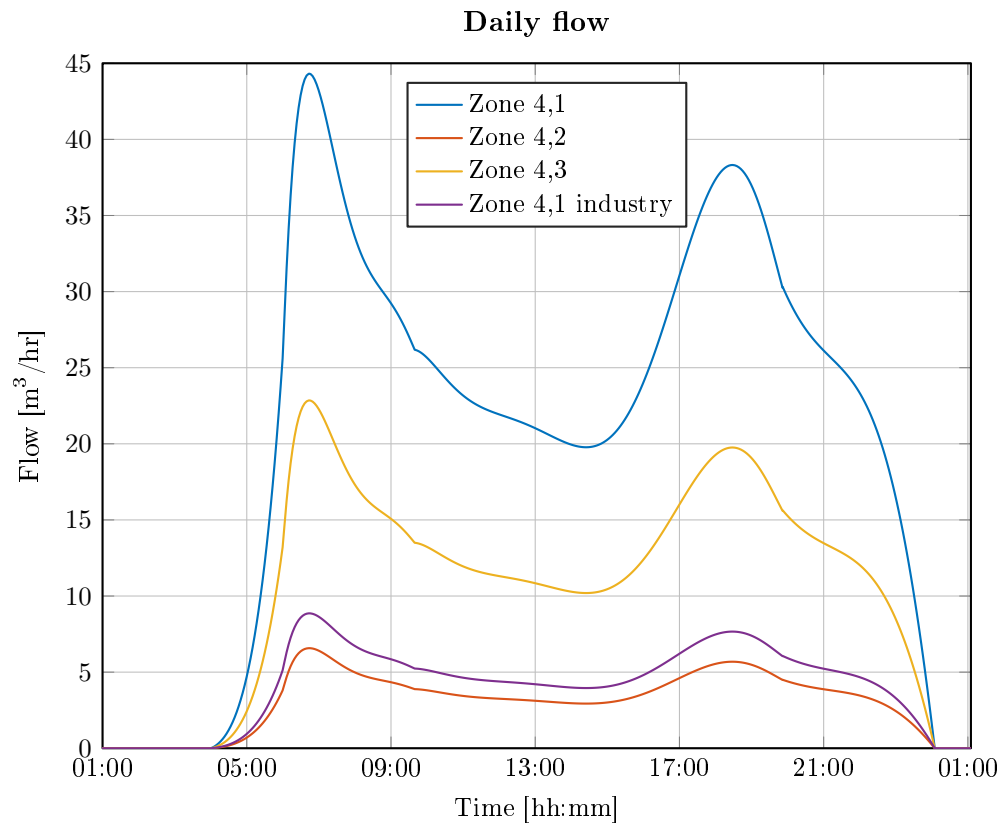


Figure A.4: A daily flow profile for zone 4.

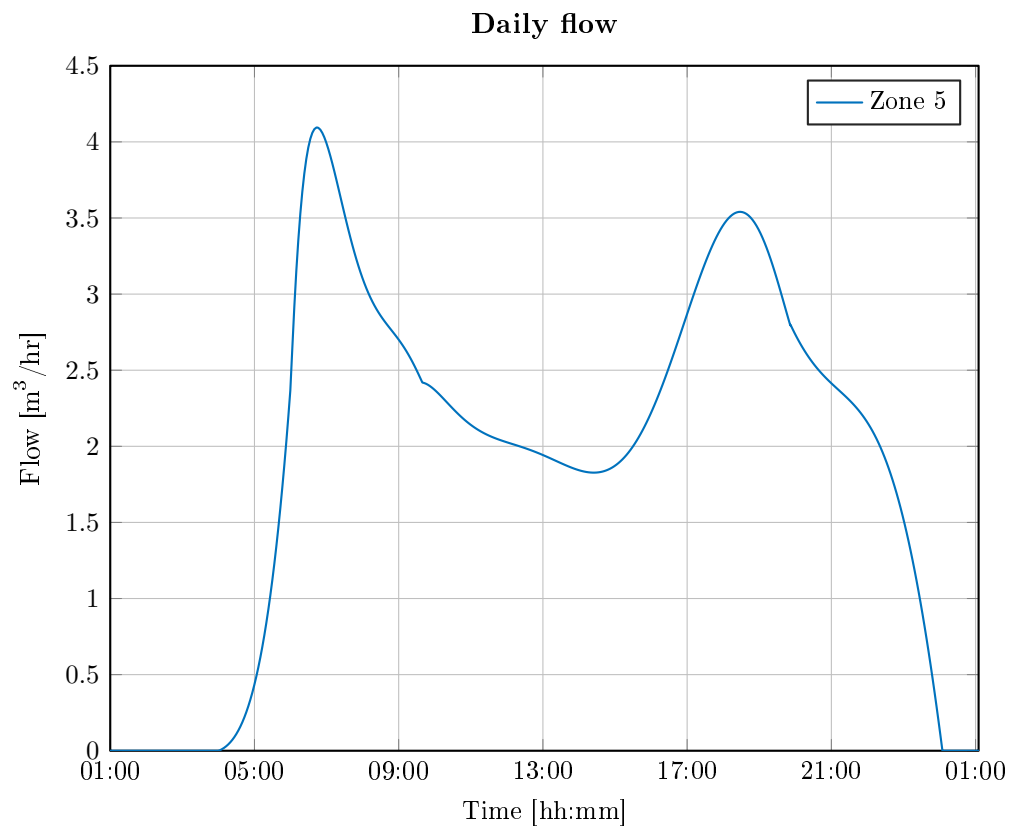


Figure A.5: A daily flow profile for zone 5.



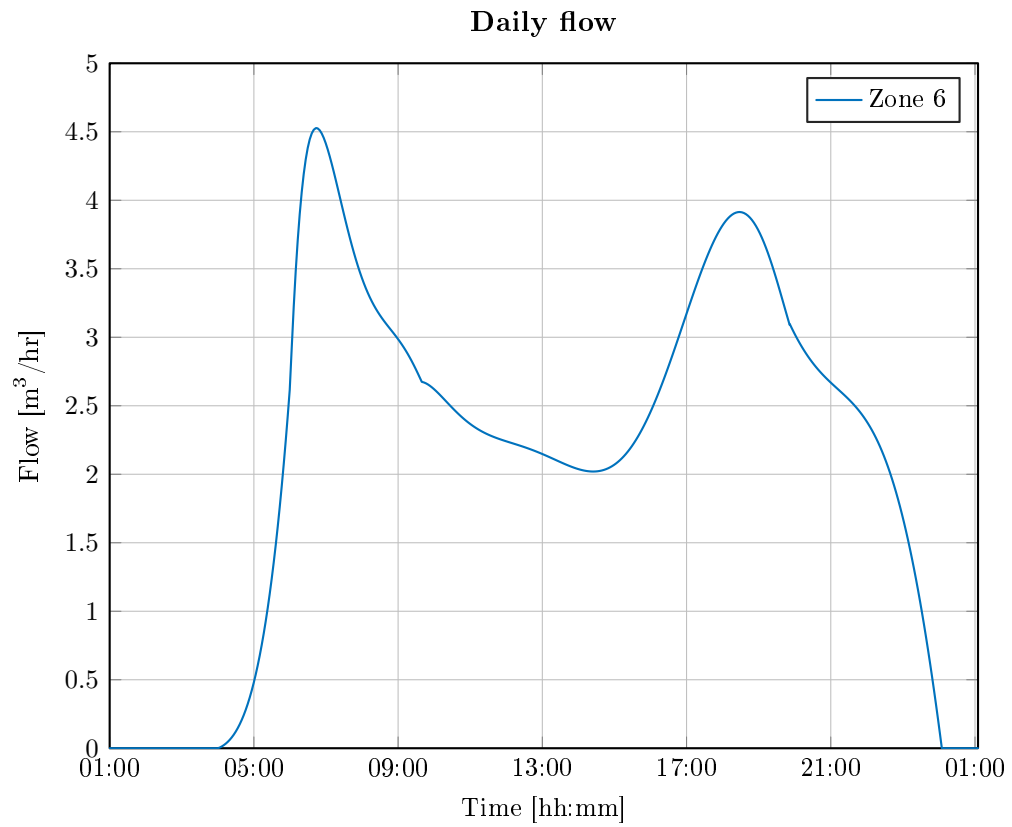


Figure A.6: A daily flow profile for zone 6.

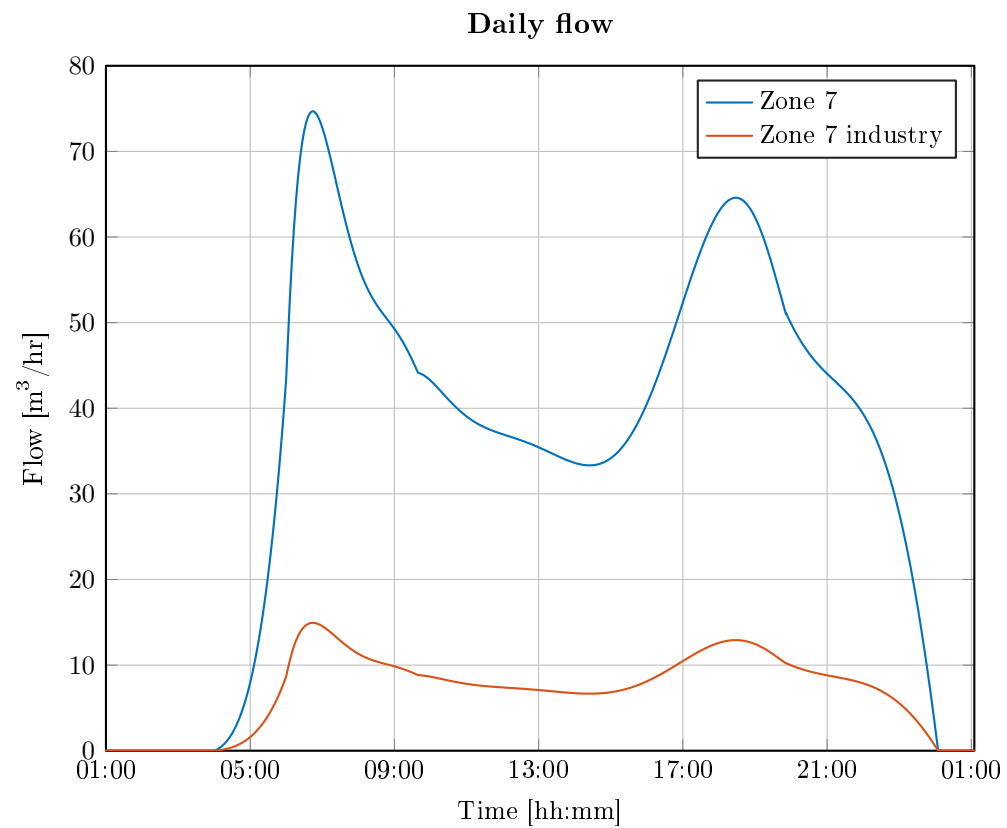


Figure A.7: A daily flow profile for zone 7.

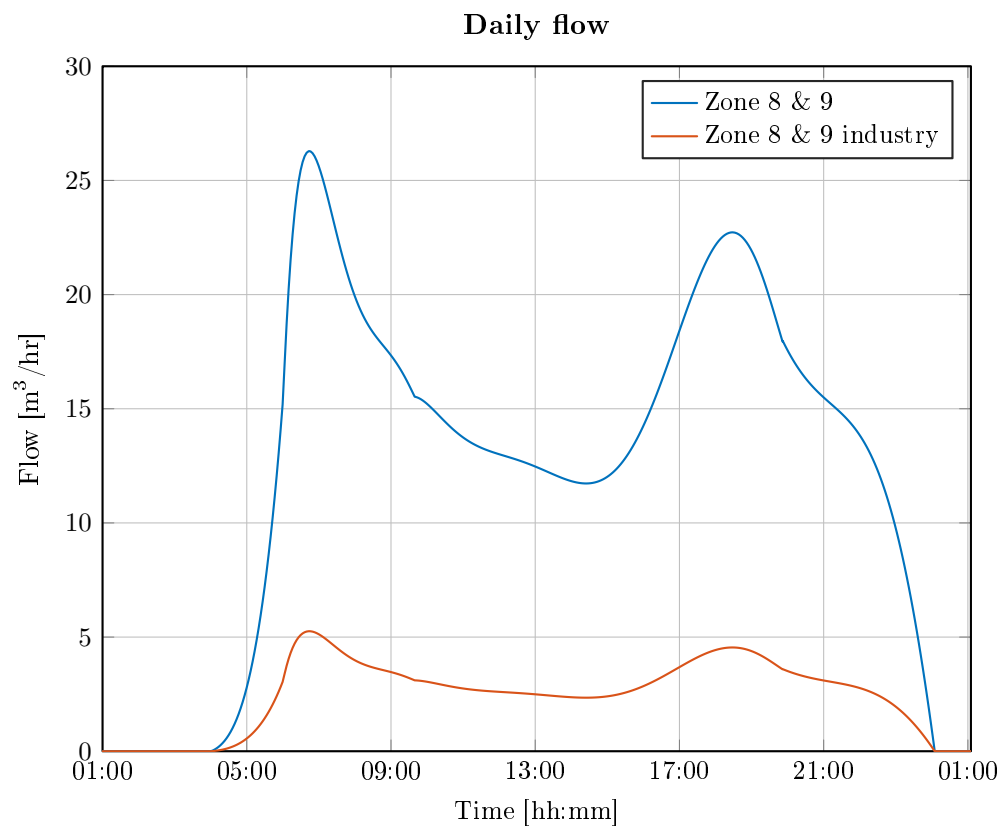


Figure A.8: A daily flow profile for zone 8 and 9.

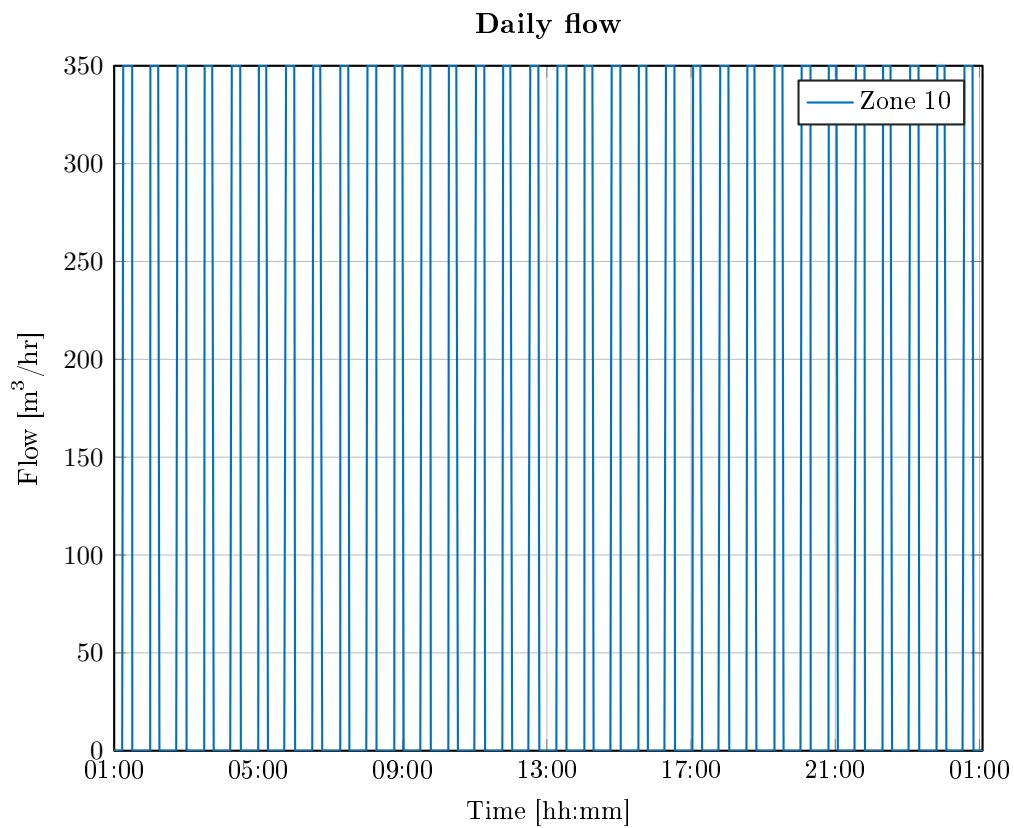


Figure A.9: A daily flow profile for zone 10.

From zone ten a pump is pumping the wastewater to the main sewer line every 30 minutes for a period of 15 minutes. The pump has a pumping capacity of  $0,350 \text{ m}^3/\text{s}$  which have been state by Fredericia and seen in tabel A.1. Therefore the flow profile for this area will be a constant input of  $0,350 \text{ m}^3/\text{s}$  for 15 minutes every 30 minute.

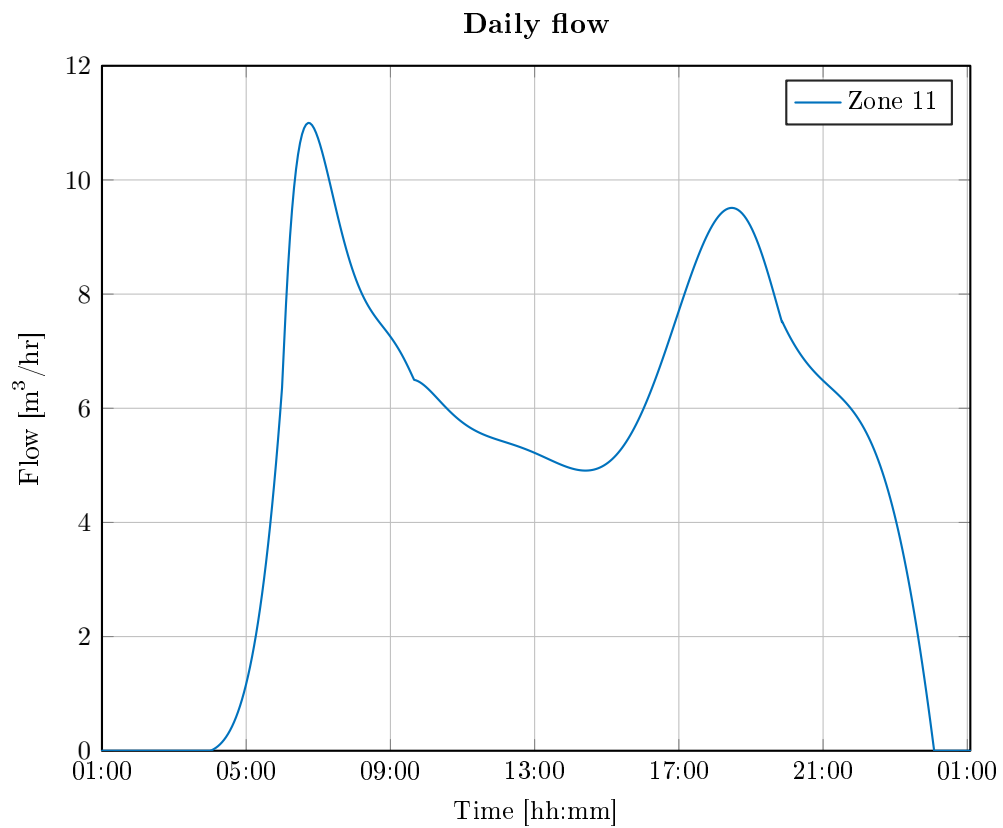


Figure A.10: A daily flow profile for zone 11.

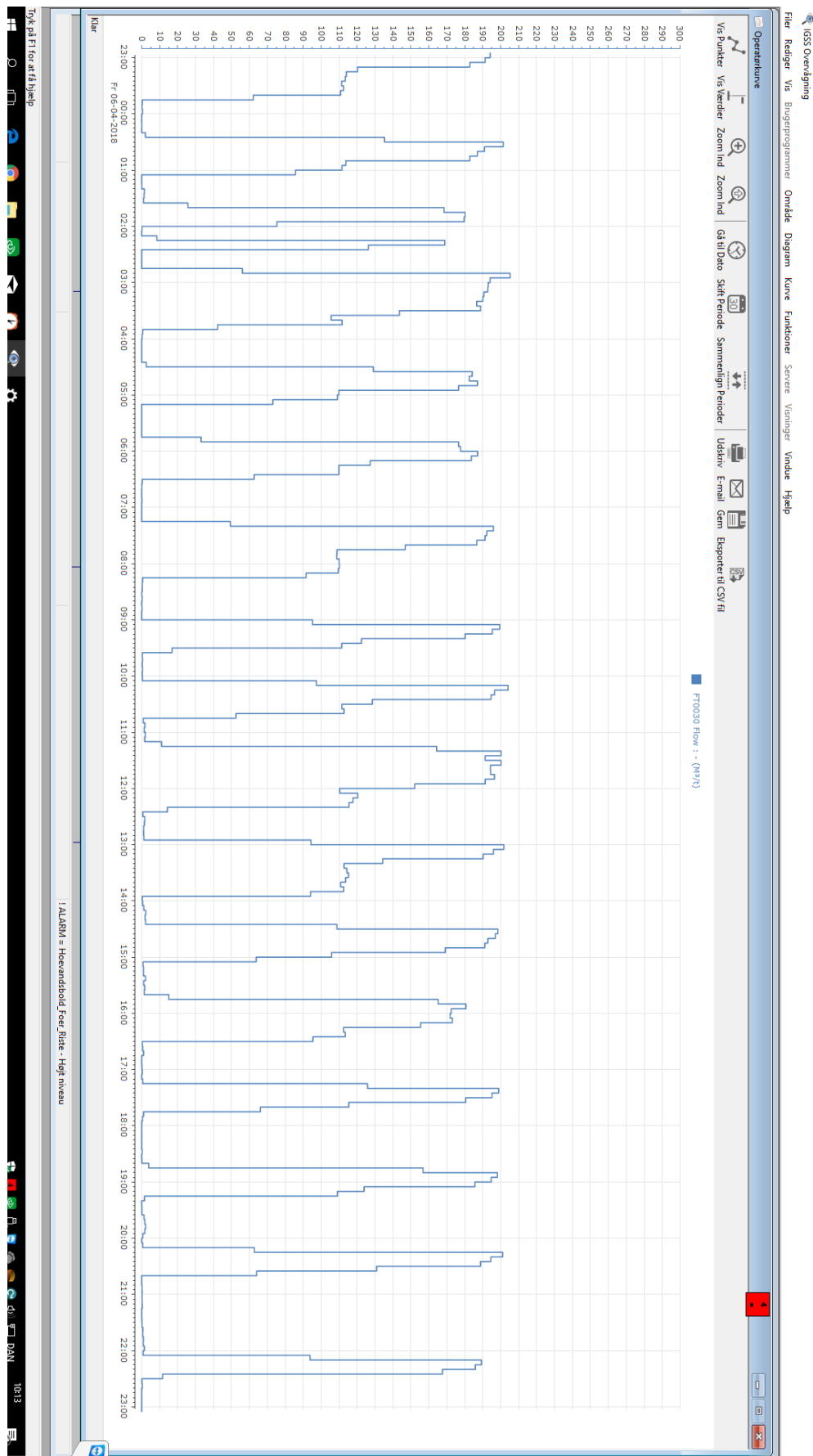


Figure A.11: Daily flow from a brewery and bottling plant in Fredericia.

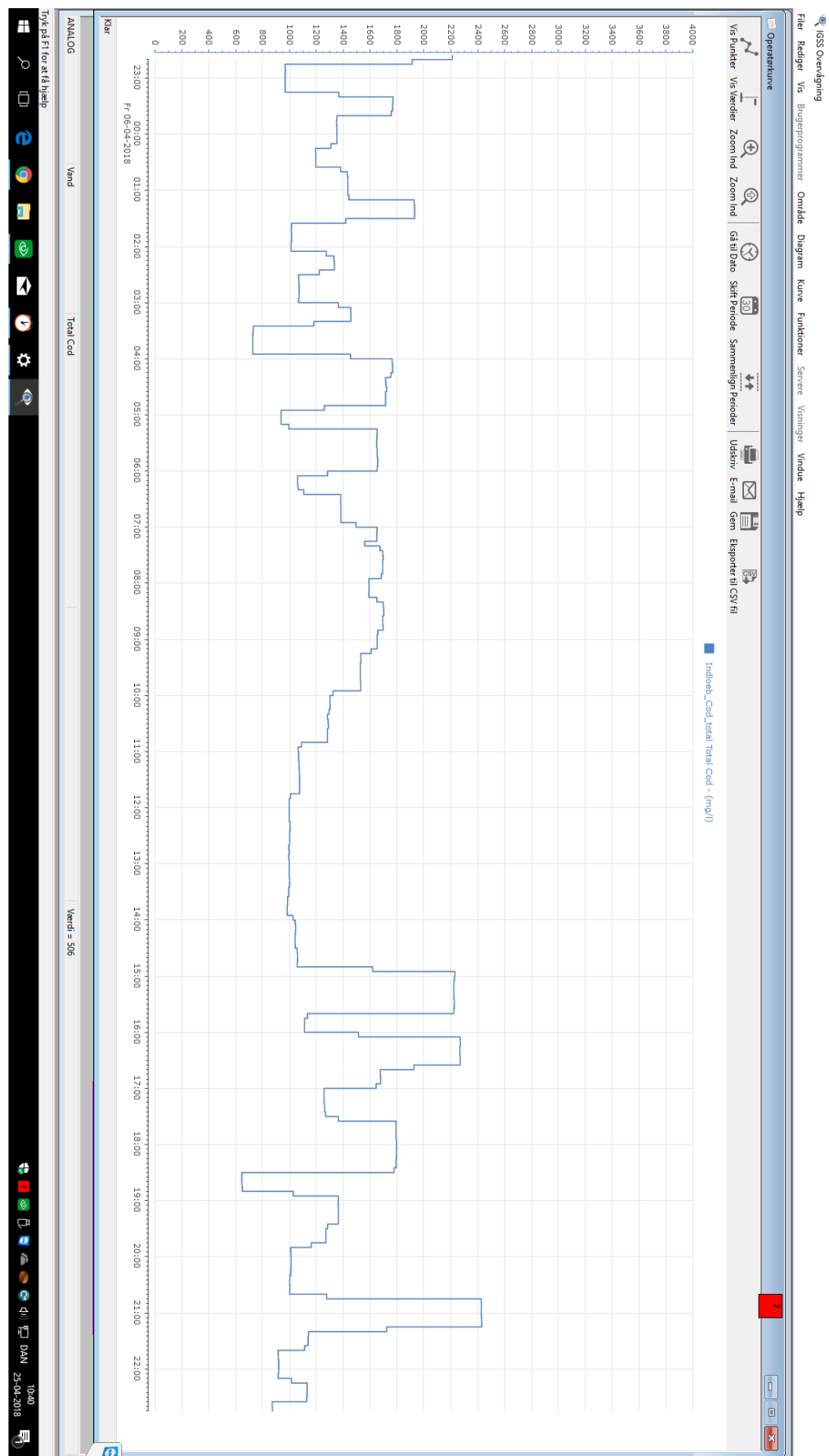


Figure A.12: COD inflow to the WWTP.

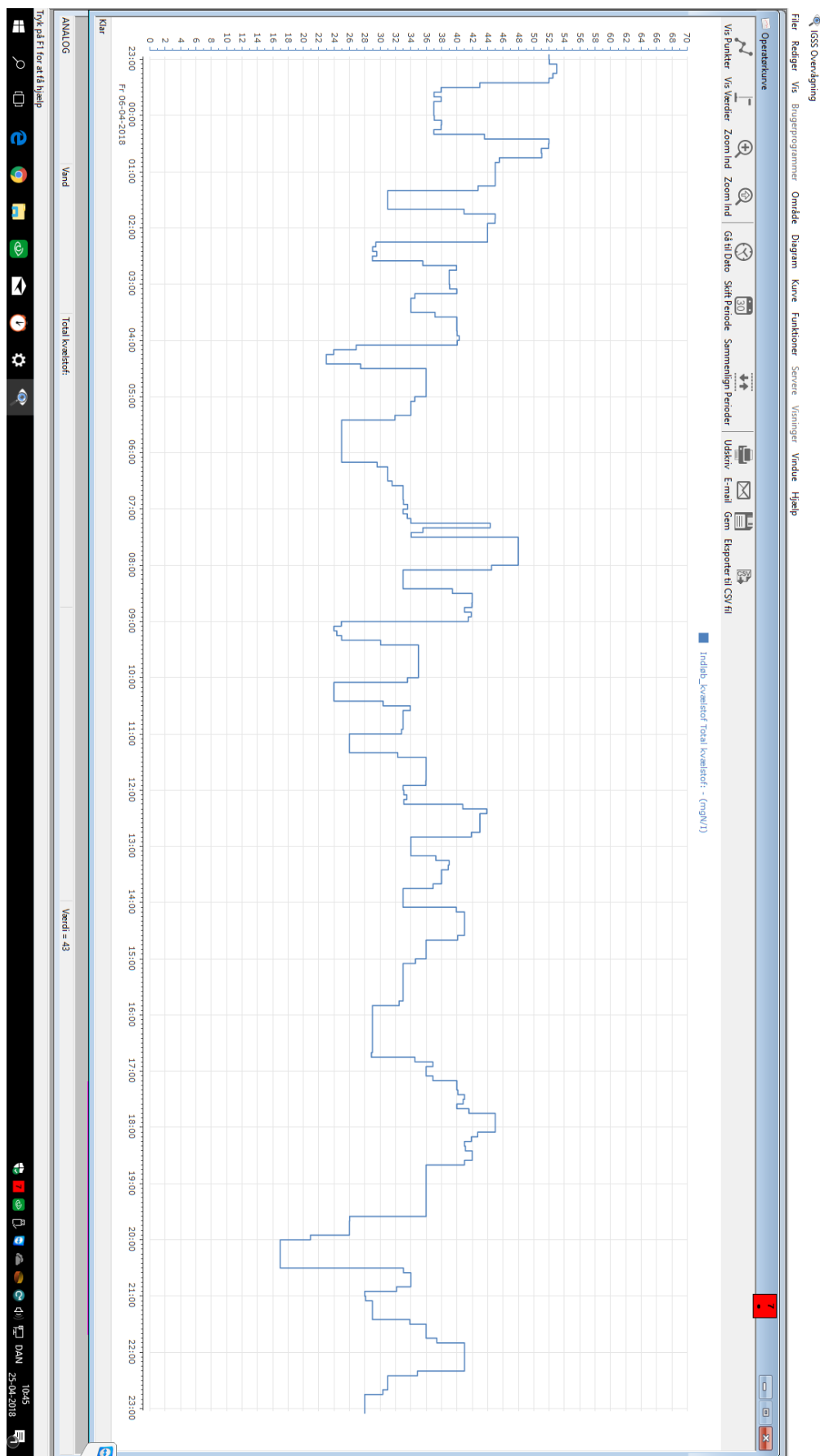


Figure A.13: Fosfor inflow to the WWTP.

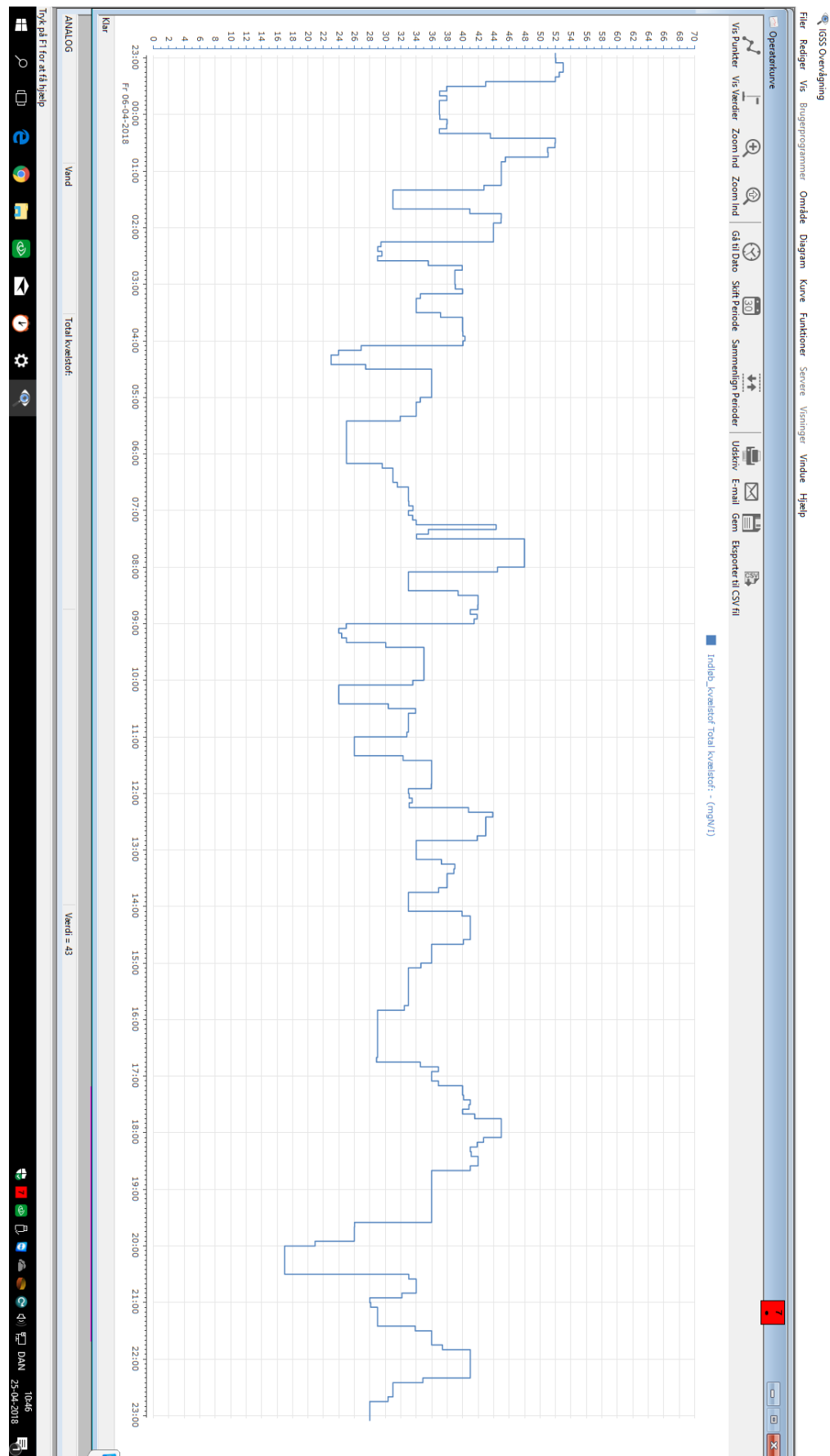


Figure A.14: Nitrogen inflow to the WWTP.

## A.4 Formulas

In this section the equations for calculation the area, water width and flow in a pipe will be shown.

In figure A.15 a illustration a cross view of a circular pipe is shown

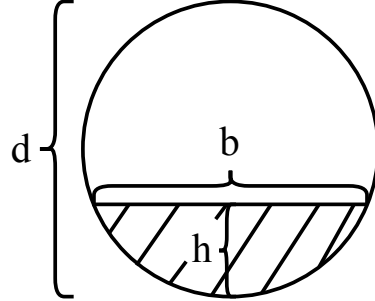


Figure A.15: Cross section view of a circular pipe. Where  $d$  is the diameter,  $b$  is the width of the water in a given height,  $h$  is the height and the crossed section in the bottom illustrates the area of the water in the pipe.

The area of the water in a circular pipe is calculated with the following [Michelsen, 1976]:

$$A = \frac{d^2}{4} \cdot \arccos\left(\frac{\frac{d}{2} - h}{\frac{d}{2}}\right) - \sqrt{h \cdot (d - h)} \cdot \left(\frac{d}{2} - h\right) \quad (\text{A.1})$$

The water width in a pipe to a given height is calculated with the following equation [Michelsen, 1976]:

$$b = 2 \cdot \sqrt{-h + h \cdot d} \quad (\text{A.2})$$

The flow in a filled pipe can be calculated as [Michelsen, 1976]:

$$Q_f = -72 \cdot \left(\frac{d}{4}\right)^{0.635} \pi \cdot \left(\frac{d}{2}\right)^2 \cdot I_e^{0.5} \quad (\text{A.3})$$

Where  $I_e$  is a friction term.

The flow in a pipe given a height can be calculated with the following equation [Michelsen, 1976]:

$$Q = \left(0.46 - 0.5 \cdot \cos\left(\pi \frac{h}{d}\right) + 0.04 \cdot \cos\left(2\pi \frac{h}{d}\right)\right) \cdot Q_f \quad (\text{A.4})$$



## Rettelser

Note: Antal sider . . . . .	iii
Note: Ny tegning og sikkert også caption . . . . .	23
Note: Mangler antagelser . . . . .	29
Note: Skal der står mere om valg af at sætte $I_e = I_b$ . . . . .	40
Note: skal der skrives her, at det er antaget at friction er lig med hældning? . . . .	40
Note: lav hjælpe formeller . . . . .	40
Note: afsnit om de forskellige ligninger til beregning af Areal, $I_e, I_b, Q_f, Q$ . . . . .	42
Note: Ved ikke om det skal stå her (det skal det vist ikke). Somewhere in the report you need to put some words on how you get information above $x(k k)$ . If you should measure it, it means that you should have level measurements along the pipe which is a bit realistic. Therefore, ideas to avoid this must be described somewhere (though you don't need to build a method.) . . . . .	63
Note: Subscribt til forstyrrelsen, hvad skal der står der? . . . . .	64
Note: Noget om, hvordan tanken er indsat . . . . .	65
Note: skal skrives så alle 4 koncentrationer er med, samt en for flow og et eller andet sted afgrænsning for liggetid i tank . . . . .	67
Note: enten skal vi fra vælge os den noget før eller os skal vi have fundet på en cost function til liggetid . . . . .	67